

# Electromagnetic Production of Electron Positron Pairs in Relativistic Heavy Ion Collisions

Inauguraldissertation

zur

Erlangung der Würde eines Doktors der Philosophie

vorgelegt der

Philosophisch-Naturwissenschaftlichen Fakultät  
der Universität Basel

von

Kai Hencken  
aus Deutschland

Basel, 1994

Genehmigt von der Philosophisch–Naturwissenschaftlichen Fakultät  
auf Antrag der  
Herren Professoren Dr. Gerhard Baur und Dr. Dirk Trautmann

Basel, den 31. Mai 1994

Prof. Dr. Hugh Rowell  
Dekan

# Abstract

Various aspects of the electromagnetic production of electron-positron pairs in relativistic heavy-ion collisions are studied. Using the general theory of a fermion field in an external field we show that the  $N$ -pair creation amplitude can be reduced to an antisymmetrised product of the (reduced) one-pair creation amplitudes and the vacuum amplitude. Neglecting all exchange diagrams in the calculation of the total probability we get a Poisson distribution for the  $N$ -pair production probability. The same result can also be found using perturbation theory and the Wick theorem. But we get also some perturbation theory expansions of the individual terms in the reduction then. We show that Feynman boundary conditions are much better suited for this case, whereas the Dirac sea picture only gives this reduction in terms of an infinite series. Then we compare our result with existent ones. Finally the general form of the  $S$  operator in second-order Magnus theory is derived.

We calculate explicitly the impact parameter dependent probability in second-order Born approximation. We start by deriving an analytic form of the matrix element for impact parameter  $b$  zero. Total and differential probabilities are calculated and discussed. A comparison with the results of the double equivalent photon approximation (DEPA) shows the inapplicability of this approximation, as it overestimates the total probability by order of magnitude. A detailed comparison for large invariant masses finally shows that there are discrepancies between both results also in this case.

The calculations are then extended to arbitrary small impact parameter  $b$ . Total probabilities up to impact parameters of several Compton wavelengths are calculated. The results for an extended charge distribution, described by a form factor, as well as for a point charge are given. These calculations are used also to get the total cross sections for this process, which we compare with results found earlier.

Finally we derive the corrections to the one-pair creation amplitude due to higher-order multiple-particle effects. For this calculation we use the result of the second-order Magnus theory, where we neglect the Coulomb rescattering terms. The first of these multiple-particle corrections is calculated for impact parameter  $b$  zero and compared with the lowest-order Born result. Differential probabilities are compared also. Finally this calculation is used to test the deviation of the two-pair production probability from the Poisson distribution.

# Zusammenfassung

Wir untersuchen eine Reihe von Aspekten der elektromagnetischen Erzeugung von Elektron-Positron-Paaren in relativistischen Schwerionenstößen. Mithilfe der allgemeinen Theorie eines Fermionfeldes in einem externen Feld zeigen wir, daß die Amplitude für die Erzeugung von  $N$  Paaren als antisymmetrisiertes Produkt der (reduzierten) Einpaarerzeugungsamplituden und der Vakuumamplitude geschrieben werden kann. Wenn wir alle Exchange-Diagramme bei der Berechnung der totalen Wahrscheinlichkeiten vernachlässigen, erhalten wir eine Poissonverteilung für die  $N$ -Paarerzeugungswahrscheinlichkeit. Das gleiche Ergebnis bekommen wir auch mithilfe der Störungstheorie und des Wick'schen Theorems. Aber dabei erhalten wir außerdem die Entwicklung der einzelnen Terme in einer Störungsreihe. Wir zeigen, daß die Feynmanschen Randbedingungen für diese Reduktion besser geeignet sind als das Dirac-See Bild, wo diese Reduktion nur in Form einer unendlichen Reihe geschrieben werden kann. Schließlich vergleichen wir unsere mit schon existierenden Ergebnissen. Am Ende leiten wir die allgemeine Form des  $S$  Operators in Magnus Theorie in zweiter Ordnung her.

Die  $b$  abhängige Wahrscheinlichkeit wird dann in zweiter Ordnung Born Approximation berechnet. Zuerst berechnen wir dazu analytisch das Matrixelement für Stoßparameter  $b$  null. Sowohl totale als auch differentielle Wahrscheinlichkeiten werden berechnet und diskutiert. Ein Vergleich mit den Ergebnissen der „double equivalent photon approximation“ (DEPA) zeigt, daß diese Näherung hier nicht angewendet werden kann, da sie Ergebnisse liefert, die um mehrere Größenordnungen zu groß sind. Ein genauerer Vergleich für große invariante Massen zeigt schließlich, daß auch in diesem Fall die Ergebnisse nicht übereinstimmen.

Die Rechnungen werden dann auf beliebige kleine Stoßparameter ausgedehnt. Totale Wahrscheinlichkeiten bis zu Stoßparametern von mehreren Comptonwellenlängen werden berechnet. Der Einfluß der endlichen Ladungsausdehnung im Kern wird durch einen Vergleich der Rechnungen mit und ohne Formfaktor untersucht. Außerdem können wir diese Rechnungen für eine Berechnung des totalen Wirkungsquerschnittes verwenden, den wir mit anderen Ergebnissen vergleichen.

Schließlich leiten wir noch Korrekturen zur Einpaarerzeugungsamplitude durch Mehrteilcheneffekte her. Diese werden in Magnustheorie in zweiter Ordnung berechnet, wobei wir außerdem die Coulombstreuung vernachlässigen. Die erste dieser Mehrteilchenkorrekturen wird für Stoßparameter  $b$  null berechnet und mit den Ergebnissen in niedrigster Ordnung Born Approximation verglichen. Differentielle Wahrscheinlichkeiten werden außerdem miteinander verglichen. Schließlich wird diese Rechnung benutzt, um Abweichungen der Wahrscheinlichkeit der Zweipaarerzeugung von der Poissonverteilung zu untersuchen.

# Contents

<b>1</b>	<b>Introduction</b>	<b>1</b>
1.1	Historical overview . . . . .	1
1.2	Overview . . . . .	4
1.3	Heavy ion collisions in external field approximation . . . . .	5
<b>2</b>	<b>General theory of pair creation in an external field</b>	<b>9</b>
2.1	Reduction using Feynman boundary conditions . . . . .	9
2.2	Reduction using perturbation theory . . . . .	13
2.3	Reduction using the Dirac sea picture . . . . .	18
2.4	Comparison with earlier results . . . . .	22
2.5	The $S$ operator in Magnus theory . . . . .	25
<b>3</b>	<b>Calculations for impact parameter zero</b>	<b>31</b>
3.1	The matrix element in second order . . . . .	31
3.2	Analytic calculation of the matrix element . . . . .	33
3.3	Pair production in DEPA . . . . .	38
3.4	The total probability $P_{\text{total}}$ . . . . .	40
3.5	The single-differential probabilities . . . . .	44
3.6	A comparison with DEPA for large invariant mass . . . . .	45
<b>4</b>	<b>Calculations for small impact parameter</b>	<b>51</b>
4.1	Calculation of the $b$ -dependent probability . . . . .	51
4.2	Results for the total probability $P_{\text{total}}(b)$ . . . . .	56
<b>5</b>	<b>Multiple particle corrections to the one-pair creation</b>	<b>63</b>
5.1	One-pair creation in second-order Magnus theory . . . . .	63
5.2	Calculation for impact parameter zero . . . . .	68
5.3	Results for impact parameter $b$ zero . . . . .	70
<b>6</b>	<b>Conclusions and Outlook</b>	<b>81</b>
6.1	Conclusions . . . . .	81
6.2	Outlook . . . . .	83

<b>7</b>	<b>Appendix</b>	<b>85</b>
A.1	Conventions and notations . . . . .	85
A.2	Connection between particle operators . . . . .	87
A.3	Vacuum expectation values and singular functions . . . . .	91
A.4	Coefficients in Magnus theory . . . . .	95
A.5	Two dimensional Feynman integrals . . . . .	96
A.6	Discussion of the form factors . . . . .	102

# Chapter 1

## Introduction

### 1.1 Historical overview

Electron-positron pair creation by the field of a fast moving particle or by high energetic photons in the field of a nucleus has been studied since the beginning of relativistic quantum mechanics. Even the discovery of the positron in the cosmic rays is in principal due to these processes. Soon after the discovery of the positron first calculations were already done, for example, by Landau and Lifshitz [1] (see also [2]) and others [3, 4]. For the calculation of these cross sections already the equivalent photon approximation (EPA) or Weizsäcker-Williams method was used [5, 6]. In its essential part this method uses the observation of Fermi [7] that the field of a fast moving charge is similar in its form to that of real photons. Therefore one replaces the electromagnetic field by a spectrum of “equivalent photons”. An overview of these calculations can be found, for example, in the textbook of Heitler [8]. Later the interest in the electromagnetic processes, especially the two photon physics, was mainly focused upon the collision of two electrons or an electron and a positron, as these types of accelerators were available at that time. Here again the equivalent photon approximation was used successfully for a wide range of processes besides the electron-positron pair production [9, 10]. In these collisions the situation is different from the heavy-ion collisions because of the very small mass of the electron with respect to the produced particles. The electrons and positrons are more easily deflected and they may lose a large portion of their energy in the process also.

With the construction of heavy-ion accelerators interest in the electron-positron production in these collisions has been revived. A variety of methods has been proposed and used in order to calculate cross sections and also impact parameter dependent probabilities.

The calculation can be split into two different types, which differ in the system used for the calculations. Using the target system one incorporates the Coulomb potential of the target into the undisturbed system. The perturbation is only due to the projectile field. This is equivalent to the use of the Furry picture.

A more symmetric situation is given by the use of the center of velocity system, which in the case of symmetric collisions is identical to the center of mass (CM) system. The

undisturbed system is then the free system; the perturbation is due to the field of both ions. This corresponds to the use of the interaction picture.

Calculations of the second kind have been done by Bottcher and Strayer [11] in second-order perturbation theory treating the field of the two heavy ions as an external field and integrating over all impact parameter  $b$  in order to get the cross section. This corresponds to the calculation of Landau and Lifshitz [1] without making any approximations. The integration was done using a Monte Carlo (MC) method. Similar Eby [12, 13] has calculated the cross section also in second-order perturbation theory describing the heavy ions as external lines.

Calculations of the first kind are not symmetric with respect to both ions. But they have the advantage of incorporating the interaction with the target field exactly. Calculations using the multipole decomposition of the Coulomb-Dirac wavefunctions and treating the perturbation of the projectile in first order were done by Becker et al. [14, 15]. Because of the decomposition into multipoles and the difficult calculation of the interaction integrals these calculations are normally restricted to small values of the Lorentz factor  $\gamma$ , up to  $\gamma_L = 10$ . (Here  $\gamma_L$  is the Lorentz factor of the projectile in the target system (lab system); it is connected with the one in the center of velocity system by  $\gamma_L = 2\gamma^2 - 1$ .) Therefore calculations using approximate solutions of the Coulomb-Dirac problem have been used, especially Sommerfeld-Maue functions and Darwin wavefunctions. Calculations were done by Bertulani and Baur [16] and also by Decker, Eichler, and Ionescu [17, 18, 19]. These results have been found to be in good agreement with the exact calculations.

A comparison of the results of both kind of calculations shows that they agree well for large values of  $\gamma$ . This seems to indicate that the total cross section for very high energies is not very sensitive to higher-order Coulomb terms. This can also be understood from the discussion of Bertulani and Baur [16], that for large values of  $\gamma$  mainly fast electrons and positrons are produced with energies in the range between  $m_e < E < \gamma m_e$  in contrast to slow ( $E \approx m_e$ ) and ultrafast ( $E \approx \gamma m_e$ ) pairs.

The treatment of the interaction of the electromagnetic field in these calculations has been either exact or with the help of the EPA. This approximation was found to be in good agreement with the exact calculations for large values of  $\gamma$ .

Recently also the impact parameter dependent probability  $P(b)$  has been calculated. Results are given already in Bertulani and Baur [16]. Using EPA they found that one gets total probabilities in lowest order, which are larger than one and therefore violate unitarity for realistic values of  $\gamma$  and impact parameter as large as the Compton wavelength  $\lambda_c \approx 386$  fm. Most of these calculations are done using EPA or its two photon analogon DEPA. As we will see later explicitly, this approximation can not be used for small impact parameter, smaller than the Compton wavelength of the electron  $\lambda_c$ .

Besides these perturbative calculations also nonperturbative calculations have been done. The interest in nonperturbative calculations is mainly in pair creation with capture, i.e., the process, where the produced electron is not free but is captured by one of the ions. This process is important for the construction of heavy-ion colliders, as it is one of the reactions, which limits the lifetime of the ions in the beam; as the ion changes its charge state in this process, it is no longer kept in the beam.



Nonperturbative calculations indicate that the results of the lowest-order perturbation theory are too small at least for not too large values of  $\gamma$ , therefore higher-order effects seem to be important.

Several different techniques have been used in these nonperturbative calculations. Finite element methods have been employed by Bottcher and Strayer [20, 21] and also by Thiel et al. [22]. These calculations are numerically rather involved and especially for the electron-positron pair creation suffer from numerical difficulties because of the singular behavior of the field of the heavy ions.

Coupled channel calculations have been done mainly by two independent groups in Frankfurt [23] and Giessen [24], but also by Baltz et al. [25, 26, 27]. The calculations use again a decomposition of the target wave functions into multipoles, where the positive and negative continuum have to be discretized in wave packets also. Here again difficulties occur because of the fact, that one is limited to small values of the angular momentum, which is no longer justified for large values of  $\gamma$ . Therefore Baltz et al. try to scale the results of the calculations from lower to higher values of  $\gamma$ .

More recently coupled channel calculations have also been done by Thiel et al. [28]. They use the CM system and therefore solutions of the free Dirac equation for the definition of the channels. They also incorporate multiple-particle production in their models by using a mapping of their fermionic system onto a bosonic system (see [28] for details).

Besides this coherent production of electron-positron pairs also the production of pairs due to bremsstrahlung in central collisions has been calculated [29, 30].

An overview of these calculations can be found in [16] with emphasize more on the nuclear aspects, and [31] with emphasize more on atomic aspects. An overview can also be found in [32], where some of the experimental aspects are discussed also.

The problem of the unitarity violation of the  $b$  dependent probability in lowest order has been studied by several groups [33, 34, 35]. The general idea is to incorporate higher-order processes in order to restore unitarity. All three models agree in some of their results: Two kind of processes are responsible for the restoration of the unitarity. One is the multiple-particle production, i.e., the fact that more than one pair can be produced in one collision. The other is the vacuum amplitude, which is neglected in the lowest-order calculations. This vacuum amplitude appears as a common factor in all  $N$ -pair probabilities and reduces them to values smaller than one. Also all of these authors found an approximate Poisson distribution for the  $N$ -pair creation probability, where the unitarity-violating lowest-order result can be interpreted as the pair multiplicity, i.e., the average number of produced pairs.

In a first model Baur [33] found these results using the sudden approximation, that is, neglecting the time ordering of the  $S$  operator and describing the electron-positron pairs as bosons. Rhoades-Brown and Weneser [34] showed then that both approximations are not really necessary in order to get these results. They found the same results summing a restricted class of Feynman diagrams and also for coupled channel calculations. Finally Best et al. [35, 36] showed how these results can be found very generally in a Dirac sea picture and with the help of the path integral formalism. Their derivation also includes the Coulomb rescattering, which was neglected in the other models.

A different approximation scheme has been proposed by Ionescu [37]. His calculations are also based on the sudden approximation and the bosonic treatment of the pairs. But his model does not allow multiple-particle production but only one-pair creation. Recently there have also been some calculation by Thiel et al. [28]. They incorporate the bosonic treatment of the pairs as a basic principle in their model and therefore get also the Poisson distribution as the three models above.

Experiments to measure the electron-positron pairs are already reporting first results [38, 39] and are also planned in the future at the different heavy-ion colliders (CERN Super Proton Synchrotron (SPS), Relativistic Heavy Ion Collider (RHIC), and the Large Hadron Collider (LHC)) [32, 40].

Finally the electron-positron pair creation is only one of a variety of electromagnetic processes, which have been studied. The DEPA is a good approximation in all of these processes and can be used therefore for the calculation of the total cross sections. Also the impact parameter dependent DEPA has been used [41, 42]. Calculations have been done, for example, for the production of the Higgs boson [43]-[48], of mesons and heavy quarks [42, 48], of  $W^-$  and  $Z$ -bosons [49], of supersymmetric particles [50], and nonstandard leptons [51].

## 1.2 Overview

This work is arranged in the following form: In Chap. 2 we discuss the general theory of pair creation in an external field. This will be done for various models. First we find the reduction of the  $N$ -pair creation amplitude using Feynman boundary conditions (Sec. 2.1). This can be used in order to derive the approximate Poisson distribution for the total  $N$ -pair probabilities. The same reduction is then found again using perturbation theory and the Wick theorem (Sec. 2.2), where we also get some perturbation theory expressions for the reduced one-pair creation amplitude and the vacuum amplitude. Finally we show how this result can also be found in the Dirac sea picture (Sec. 2.3). The results are then discussed and compared with other existent models in Sec. 2.4. As we will need it later in Chap. 5, we derive the general form of the  $S$  operator in second-order Magnus theory in Sec. 2.5.

In Chap. 3 we start with explicit calculations of the impact parameter dependent probabilities. We begin in Chap. 3 with the calculation for  $b$  zero. We find an analytic form for the matrix element in second-order Born approximation, which is then used for the calculation of the probability. Total as well as differential probabilities are discussed in Sec. 3.4 and Sec. 3.5. A comparison with the double equivalent photon approximation (DEPA) is made for total probabilities as well as for large invariant masses.

This calculation for impact parameter zero is then extended in Chap. 4 to arbitrary small impact parameter  $b$ . Total probabilities and also the total cross section are calculated; the later is also compared with other calculations.

In Chap. 5 we extend the calculation for impact parameter zero into a different direction. Based on the general theory of Chap. 2 we derive the higher-order multiple-particle

corrections to the one-pair production in second-order Magnus theory. The lowest of these corrections is calculated explicitly and compared with the results of the lowest-order Born approximation. We test also the applicability of the Poisson distribution with an explicit calculation of the two-pair probability in lowest order.

Finally in Chap. 6 the results are summarized and also an outlook is given. Some of the conventions and notations used throughout this work have been summarised in App. A.1.

### 1.3 Heavy ion collisions in external field approximation

Throughout our calculations, we will treat the electromagnetic field of the heavy ions as an external field. For this we have to use the semiclassical approximation (SCA) in order to get a classical trajectory for the movement of the ions. This is also necessary in order to define impact parameter dependent probabilities. The use of the SCA has been studied in atomic processes in heavy-ion collisions [31], and it has been found that it is applicable, if the energy lost in the reaction is much smaller than the kinetic energy and also if the deflection angle of the ions is small. Both conditions are fulfilled in our case. The typical energies, that are needed for the production of an electron-positron pair, are of the order of the rest mass of the electron and therefore in the range of some MeV, whereas the kinetic energy is given by  $M(\gamma - 1)$  and is therefore in the range of GeV to TeV. The deflection angle can be calculated from the momentum transfer in the collision. The momentum transfer due to the Coulomb scattering of the ions is given by [52]:

$$\Delta p = \frac{2Z^2\alpha}{b} \quad (1.1)$$

and the deflection angle therefore is approximately  $\Theta \approx \Delta p/p$

$$\Theta \approx \frac{2Z^2\alpha}{M\gamma b}. \quad (1.2)$$

If one uses  $b = R = 7$  fm and, for example,  $\gamma = 100$  in a Pb–Pb collision, we get an angle of about some mrad. Therefore the influence of the Rutherford bending can be neglected also in relativistic collisions. The advantage of this “straight line approximation” is that we can calculate the electromagnetic potential explicitly in this case.

The electromagnetic current of a point particle is given by its current as

$$\square A^\mu(x) = j^\mu(x). \quad (1.3)$$

In terms of the Fourier transform

$$A^\mu(x) = \int \frac{d^4q}{(2\pi)^4} \exp(-iqx) A^\mu(q), \quad (1.4)$$

$$j^\mu(x) = \int \frac{d^4q}{(2\pi)^4} \exp(-iqx) j^\mu(q), \quad (1.5)$$

we get

$$A_\mu(q) = -\frac{1}{q^2}j_\mu(q). \quad (1.6)$$

The current of a point particle moving along a straight line at distance  $\vec{r}$  from the origin is given by

$$j^\mu(x) = Zeu^\mu/u^0\delta^3(\vec{x} - \vec{v}t - \vec{r}) \quad (1.7)$$

with four velocity  $u^\mu = (\gamma, \gamma\vec{v})$ . The Fourier transform of this is

$$j^\mu(q) = Zeu^\mu \exp(iqr)2\pi\delta(qu). \quad (1.8)$$

The electromagnetic field of the particle therefore is

$$A^\mu(q) = -2\pi Z_{(1,2)}eu^\mu \frac{1}{q^2}\delta(qu) \exp(iqr). \quad (1.9)$$

Please note that the  $r$  dependence comes from the exponential only.

In the calculations we will need also a form factor in order to describe the extended charge distribution of the heavy ions. The form factor changes the electromagnetic potential to

$$A^\mu(q) = -2\pi Z_{(1,2)}eu^\mu \frac{F(q^2)}{q^2}\delta(qu) \exp(iqr). \quad (1.10)$$

The form factors, we use throughout the calculations, are the dipole form factor

$$F_{\text{dipole}}(q^2) = \frac{\Lambda^2}{\Lambda^2 - q^2} \quad (1.11)$$

and a form factor, which is the linear combination of two dipole form factors

$$F_{\text{double}}(q^2) = c_1 \frac{\Lambda_1^2}{\Lambda_1^2 - q^2} + c_2 \frac{\Lambda_2^2}{\Lambda_2^2 - q^2}, \quad (1.12)$$

called by us the “double dipole form factor”.

In Appendix A.6 we show how to choose the parameters in these form factors. The dipole form factor is that of a Yukawa charge distribution, which is surely not very realistic. On the other hand the probabilities are normally not very sensitive to the detailed form of the form factor, and we can treat the matrix element analytically using the form factors of Eq. (1.11) and Eq. (1.12).

Throughout our calculations we will restrict ourself always to symmetric collisions, that is, where both heavy ions are identical ( $Z_1 = Z_2 = Z$ ) and we will always use the CM system, that is, the Lorentz factor of both ions is the same  $\gamma_1 = \gamma_2 = \gamma$ . The definition of the coordinate system and the impact parameter  $b$  is given in Fig. 1.1.

The field produced by both ions is then

$$A_\mu(q) = -2\pi e \frac{F(q^2)}{q^2} \left[ Zu_\mu^{(1)}\delta(qu^{(1)}) \exp(iqb/2) + Zu_\mu^{(2)}\delta(qu^{(2)}) \exp(-iqb/2) \right], \quad (1.13)$$

Figure 1.1: *Definition of the coordinate system and the impact parameter  $b$  in a symmetric heavy-ion collision.*

where the four-velocities are given by  $u^{(1)} = (\gamma, 0, 0, \gamma\beta)$  and  $u^{(2)} = (\gamma, 0, 0, -\gamma\beta)$ .

We will neglect also the interaction of the electrons and positrons among each other. This is normally a good approximation, as the effective coupling constant  $Z\alpha$  between the ions and the fermions is much larger than the coupling constant  $\alpha$  between the fermions. Also, as we will see later, the total number of produced particles is not very large, therefore the smallness of this coupling constant is not compensated by a large number of particles.

Because of these assumptions our many particle system is essentially a system of non-interacting fermions in an external field. For such a system the  $S$  operator is known to be of the form

$$S = \mathcal{T} \exp \left\{ -i \int_{-\infty}^{+\infty} H_I(t) dt \right\} = \mathcal{T} \exp \left\{ \int d^4x : \bar{\Psi}(x) [-ie \mathcal{A}(x)] \Psi(x) : \right\}, \quad (1.14)$$

where  $H_I$  is the Hamiltonian in the interaction picture. This form of the  $S$  operator is the starting point for our calculations.

In the discussion of the general theory we will assume that the external field vanishes asymptotically in order to have free systems there. Even though this is not the case in a strict sense, this presents no difficulties here, as most of the particles are produced with intermediate energies and therefore are not in the neighborhood of the ions asymptotically. This is of course different in a calculation of pair production with capture, were the field of one of the ions is essentially needed for the bound state of the electron.

In Chap. 2 we will need the connection between creation and annihilation operators at those asymptotic boundaries. As we use the interaction picture throughout this work, the connection in this picture are discussed in App. A.2.



# Chapter 2

## General theory of pair creation in an external field

In this chapter we are going to study the general theory of a fermion field interacting with an external field, especially the multiple-pair production. The main result will be that the  $N$ -pair creation amplitude can be reduced to an antisymmetrised product of  $N$  reduced one-pair amplitudes and the vacuum amplitude. This result will be found using three different ways.

The general theory of a fermion interacting with an external electromagnetic field is rather old and has been developed already with the beginning of QED. It has been developed especially by Feynman [53] and Schwinger [54]. An overview can also be found in [55, 56, 57]. The connection of the creation and annihilation operators at the asymptotic boundaries, which we need in this chapter, has also been summarized in App. A.2.

Although we will discuss only the electromagnetic pair production, the general theory can also be applied to other pair production processes in an external field, for example, pair creation due to bremsstrahlung [29, 30].

### 2.1 Reduction using Feynman boundary conditions

The amplitude for the  $N$ -pair creation is given with the help of the  $S$  operator of Eq. (1.14) as

$$S_{fi} = \langle f | S | i \rangle. \quad (2.1)$$

As we want to calculate pair creation, the initial state is the vacuum state  $|0\rangle$  and the final state a  $N$ -pair state given by

$$|f\rangle = b_{k_1}^+ d_{l_1}^+ \cdots b_{k_N}^+ d_{l_N}^+ |0\rangle, \quad (2.2)$$

where  $k_i$  denotes the electron quantum numbers, for example, momentum and spin,  $l_i$  the same for the positrons. The  $S$  matrix is therefore

$$S_N := S(k_1, l_1 \cdots, k_N, l_N) = \langle 0 | d_{l_N} b_{k_N} \cdots d_{l_1} b_{k_1} S | 0 \rangle. \quad (2.3)$$

As described in App. A.2 the creation and annihilation operators at  $t \rightarrow \pm\infty$  are connected with each other through a linear transformation. Using retarded boundary conditions this means that the creation and annihilation operators for electrons and positrons at  $t \rightarrow \infty$  are connected through an unitary matrix with those at  $t \rightarrow -\infty$ . In the interaction picture this transformation is expressed as (Eq. (A.26))

$$b_p S = \sum_{i>0} a_{pi} S b_i + \sum_{j<0} a_{pj} S d_j^+, \quad (2.4a)$$

$$d_q S = \sum_{i>0} a_{qi}^* S b_i^+ + \sum_{j<0} a_{qj}^* S d_j. \quad (2.4b)$$

The main idea is now not to use these boundary conditions but Feynman boundary conditions instead. These are of a mixed retarded and advanced type. With these the electron creation operators for  $t \rightarrow \infty$  are connected with the electron creation operators for  $t \rightarrow -\infty$  and the positron annihilation operators for  $t \rightarrow \infty$ . This corresponds to the Stückelberg-Feynman interpretation of electrons moving forward, positrons moving backwards in time. Again in the interaction picture this is written as (Eq. (A.34))

$$b_p S = \sum_{q>0} s_{pq}^{++} S b_q + \sum_{q'<0} s_{pq'}^{+-} d_{q'}^+ S. \quad (2.5)$$

It has been shown already by Feynman that these boundary conditions are completely equivalent to the retarded ones, but that they are better suited for QED [53].

Similar relations exist also for all other creation and annihilation operators; Eq. (2.5) is the only relation we will need in the following. Applying it to  $b_{k_1}$  we get for  $S_N$ :

$$S_N = \langle 0 | d_{l_N} b_{k_N} \cdots b_{k_2} d_{l_1} \left[ \sum_{q_1>0} s_{k_1 q_1}^{++} S b_{q_1} + \sum_{q'_1<0} s_{k_1 q'_1}^{+-} d_{q'_1}^+ S \right] | 0 \rangle. \quad (2.6)$$

The  $b_{q_1}$  operator annihilates the vacuum state, therefore we drop this term:

$$S_N = \langle 0 | d_{l_N} b_{k_N} \cdots b_{k_2} d_{l_1} \sum_{q'_1<0} s_{k_1 q'_1}^{+-} d_{q'_1}^+ S | 0 \rangle \quad (2.7)$$

$$= \sum_{q'_1<0} s_{k_1 q'_1}^{+-} \langle 0 | d_{l_N} b_{k_N} \cdots b_{k_2} d_{l_1} d_{q'_1}^+ S | 0 \rangle. \quad (2.8)$$

Using the fact that  $b_{k_2}$  anticommutes with  $d_{l_1}$  and  $d_{q'_1}^+$  we get

$$S_N = \sum_{q'_1<0} s_{k_1 q'_1}^{+-} \langle 0 | d_{l_N} b_{k_N} \cdots d_{l_1} d_{q'_1}^+ b_{k_2} S | 0 \rangle. \quad (2.9)$$

Now one replaces  $b_{k_2}$  using again Eq. (2.5) and then commutes the next  $b_{k_i}$  to the most right. Doing this for all  $b_{k_i}$  we get finally:

$$S_N = \sum_{q'_1 \cdots q'_N < 0} s_{k_1 q'_1}^{+-} \cdots s_{k_N q'_N}^{+-} \langle 0 | d_{l_N} \cdots d_{l_1} d_{q'_1}^+ \cdots d_{q'_N}^+ S | 0 \rangle. \quad (2.10)$$



The vacuum expectation value can be calculated easily using the anticommutation relations

$$\{d_{l_i}, d_{q'_j}^+\} = \delta_{l_i, q'_j} \quad (2.11)$$

in order to move  $d_{q'_1}^+$  to the left, until it reaches the left side, where it annihilates the vacuum. Doing this for all creation operators we see that we get a nonvanishing result only, if every  $q'_i$  is equal to some  $l_j$ , and the overall sign of the vacuum expectation value is equal to the signum of the permutation to arrange  $l_1 \cdots l_N$  in the same sequence as the corresponding  $q'_1 \cdots q'_N$ . We get

$$\langle 0 | d_{l_N} \cdots d_{l_1} d_{q'_1}^+ \cdots d_{q'_N}^+ S | 0 \rangle = \langle 0 | S | 0 \rangle \sum_{\sigma} \text{sgn}(\sigma) \delta(l_{\sigma(1)}, q'_1) \cdots \delta(l_{\sigma(N)}, q'_N) \quad (2.12)$$

and therefore for  $S_N$ :

$$S_N(k_1, l_1, \cdots, k_N, l_N) = \langle 0 | S | 0 \rangle \sum_{\sigma} \text{sgn}(\sigma) s_{k_1 l_{\sigma(1)}}^{+-} \cdots s_{k_N l_{\sigma(N)}}^{+-}, \quad (2.13)$$

where the sum consists of  $N!$  terms. This can also be written formally as

$$S_N = \langle 0 | S | 0 \rangle \det [s_{k_i l_j}^{+-}]. \quad (2.14)$$

This is the main result, which we will need. The  $N$ -pair creation amplitude can be written as an antisymmetrised product of the  $s_{kl}^{+-}$  times the vacuum amplitude. It is easy to see that the  $s_{kl}^{+-}$  are just the one-pair creation amplitudes divided by the vacuum amplitude. In the following we will call this amplitude the “reduced” amplitude.

Normally the vacuum amplitude does not show up in calculations as it is often of magnitude one, for example, for time independent systems. In our case the external fields are explicit time dependent, therefore the vacuum amplitude can not be neglected. This can be understood easily, if one notices that the vacuum amplitude is the amplitude for the “no pair creation process”, that is, the probability amplitude for the vacuum to remain the vacuum. As pair creation does occur, this probability must be smaller than one and therefore the amplitude has to be of magnitude less than one. Also we see here that the vacuum amplitude appears as a factor in all  $N$ -pair amplitudes and therefore reduces all these amplitudes by the same factor.

From this we can get easily an approximate Poisson distribution for the total  $N$ -pair probability, which has also been found by earlier calculations. For this we need the absolute value squared of  $S_N$ . As  $S_N$  consists of  $N!$  terms, we get a total of  $(N!)^2$  terms. In most of these terms we have the product coming from two different permutations. Normally the produced electrons and positrons are correlated to some extent with each other. If we therefore assume that terms, where two different permutations appear, are much smaller than those with the same permutation and can therefore be neglected, we get only  $N!$  terms:

$$P(N) \approx |\langle 0 | S | 0 \rangle|^2 \sum_{\sigma} |s_{k_1 l_{\sigma(1)}}^{+-}|^2 \cdots |s_{k_N l_{\sigma(N)}}^{+-}|^2. \quad (2.15)$$

Summing or integrating now over all states we get for the total probability

$$P_{\text{total}}(N) \approx \frac{1}{(N!)^2} |\langle 0 | S | 0 \rangle|^2 \sum_{k_1, l_1, \dots, k_N, l_N} \sum_{\sigma} \left| s_{k_1 l_{\sigma(1)}}^{+-} \right|^2 \cdots \left| s_{k_N l_{\sigma(N)}}^{+-} \right|^2, \quad (2.16)$$

where the factor  $1/(N!)^2$  has been introduced in order to correct for the multiple summation over electrons and positrons. As every term in the sum over  $\sigma$  gives the same result, we get

$$\begin{aligned} P_{\text{total}}(N) &\approx \frac{1}{N!} |\langle 0 | S | 0 \rangle|^2 \sum_{k_1, l_1} \left| s_{k_1 l_1}^{+-} \right|^2 \cdots \sum_{k_N, l_N} \left| s_{k_N l_N}^{+-} \right|^2 \\ &= \frac{1}{N!} |\langle 0 | S | 0 \rangle|^2 \left[ \sum_{k, l} \left| s_{kl}^{+-} \right|^2 \right]^N \\ &= P(0) \frac{[P_{\text{total}}^R]^N}{N!}, \end{aligned} \quad (2.17)$$

with  $P(0)$  the “no pair” probability and  $P_{\text{total}}^R = \sum_{k, l} \left| s_{kl}^{+-} \right|^2$  the total reduced one-pair probability. This is just a Poisson distribution, and  $P(0)$  can be calculated using the fact that the sum over all  $N$  has to be 1:

$$P(0) \sum_N \frac{[P_{\text{total}}^R]^N}{N!} = P(0) \exp [P_{\text{total}}^R] = 1. \quad (2.18)$$

From this we finally get

$$P_{\text{total}}(N) = \exp [-P_{\text{total}}^R] \frac{[P_{\text{total}}^R]^N}{N!}. \quad (2.19)$$

The unitarity violating reduced probability can therefore be interpreted as the pair multiplicity, that is, the average number of produced pairs:

$$\langle N \rangle = \sum_N N P_{\text{total}}(N) = P_{\text{total}}^R. \quad (2.20)$$

The only approximation that was necessary in order to get this result was the neglect of all “exchange terms” in the calculation of the probability. We will show later that at least for the two-pair creation this neglect seems to be justified.

Therefore for the calculation of the  $N$ -pair creation probability it suffices to calculate the reduced one-pair creation probability. All other probabilities are given then by the Poisson distribution. If one wants to go beyond the Poisson distribution, it suffices to calculate the reduced one-pair creation amplitude and the vacuum amplitude.

This derivation is rather simple, but it is not useful for explicit calculations. Especially the nature of the processes contributing to the reduced pair creation amplitude as well as the vacuum amplitude remains unexplained. Therefore we will derive the same result in the next section using the perturbation-theory expansion of the  $S$  operator together with the Wick theorem.

## 2.2 Reduction using perturbation theory

In this section we use the field operator  $\Psi(x)$  directly instead of the creation and annihilation operators as in the previous section, that is, we are going to calculate

$$S_N(y_1, \dots, y_N, y'_1, \dots, y'_N) = \langle f | S | i \rangle, \quad (2.21)$$

where the initial state is again the vacuum  $|0\rangle$ , and the final state is

$$|f\rangle = \bar{\Psi}^{(+)}(y_N)\Psi^{(-)}(y'_N) \cdots \bar{\Psi}^{(+)}(y_1)\Psi^{(-)}(y'_1) |0\rangle. \quad (2.22)$$

Here we have made use of the frequency parts of the field operators for electrons and positrons. The electron coordinates are  $y_i$ , the positron coordinates  $y'_i$  and the time coordinate is the same for all coordinates and assumed to go to  $\infty$ .  $S_N$  gives the probability amplitude in occupation number space to get electrons finally at  $y_i$  and positrons at  $y'_i$ . We rewrite the final state a little bit by introducing normal ordering of the field operators:

$$\langle f | = \langle 0 | : \bar{\Psi}(y'_1)\Psi(y_1) \cdots \bar{\Psi}(y'_N)\Psi(y_N) : , \quad (2.23)$$

where we can use the whole field operators instead of the frequency parts, as the normal ordering together with the vacuum state guarantees that only the appropriate part of each field operator contributes. Throughout the calculation in this section the Dirac indices will be suppressed. In the final form we arrange the operators in the appropriate form, which is not always possible at intermediate steps, but generally Dirac indices can be looked at, as if they are incorporated into the coordinates.

Using the form of the  $S$  matrix from Eq. (1.14) we get

$$\begin{aligned} S(y_1, \dots, y_N, y'_1, \dots, y'_N) = \\ \langle 0 | : \bar{\Psi}(y'_1)\Psi(y_1) \cdots \bar{\Psi}(y'_N)\Psi(y_N) : \mathcal{T} \exp \left\{ \int d^4x : \bar{\Psi}(x)[-ie \not{A}(x)]\Psi(x) : \right\} |0\rangle. \end{aligned} \quad (2.24)$$

As the time, when we detect electrons and positrons, is  $\infty$ , the time ordering can be extended to the whole expression.

We will now use the Wick theorem in the following form [58], where  $O_i$  is an arbitrary fermionic operator:

$$\begin{aligned} \langle 0 | \mathcal{T} O_1 \cdots O_M |0\rangle = \\ \sum_{j, (j \neq i)} \text{sgn}(\pi(j, i)) \langle 0 | \mathcal{T} O_j O_i |0\rangle \langle 0 | \mathcal{T} O_1 \cdots \widehat{O}_j \cdots \widehat{O}_i \cdots O_M |0\rangle. \end{aligned} \quad (2.25)$$

Here  $i$  is a fixed index,  $\pi(j, i)$  is the permutation to put  $O_j$  and  $O_i$  to the left of all other operators, and the hat in the vacuum expectation value means that these operators have been removed from the expression. In our case the  $O_i$  are either  $\bar{\Psi}$  or  $\Psi$  and we can use the fact that

$$\langle 0 | \mathcal{T} \Psi(x)\Psi(y) |0\rangle = \langle 0 | \mathcal{T} \bar{\Psi}(x)\bar{\Psi}(y) |0\rangle = 0 \quad (2.26)$$

and

$$\langle 0 | \mathcal{T} \Psi(x) \bar{\Psi}(y) | 0 \rangle = i S_F(x - y), \quad (2.27)$$

where  $S_F$  is the usual Feynman propagator. As we have also normal-ordered products, the sum over  $j$  in this case also excludes those operators, which are in the same normal-ordered product as the  $O_i$ .

In a first step we apply Eq. (2.25) to  $\Psi(y_N)$  in the expansion of  $S_N$ :

$$\begin{aligned} I_M &:= \int dx_1 \cdots dx_M \langle 0 | \mathcal{T} : \bar{\Psi}(y'_1) \Psi(y_1) \cdots \bar{\Psi}(y'_N) \Psi(y_N) : \\ &\quad \times : \bar{\Psi}(x_1) [-ie \mathcal{A}(x_1)] \Psi(x_1) : \cdots : \bar{\Psi}(x_M) [-ie \mathcal{A}(x_M)] \Psi(x_M) : | 0 \rangle \\ &= \int dx_1 \cdots dx_M \sum_{i=1}^M \langle 0 | \mathcal{T} \Psi(y_N) \bar{\Psi}(x_i) | 0 \rangle [-ie \mathcal{A}(x_i)] \\ &\quad \times \langle 0 | \mathcal{T} : \bar{\Psi}(y'_1) \Psi(y_1) \cdots \bar{\Psi}(y'_N) : \Psi(x_i) : (1) : \cdots : (\widehat{i}) : \cdots : (M) : | 0 \rangle \\ &= M \int dz_1 dx_1 \cdots dx_{M-1} S_F(y_N - z_1) e \mathcal{A}(z_1) \\ &\quad \times \langle 0 | \mathcal{T} : \bar{\Psi}(y'_1) \Psi(y_1) \cdots \bar{\Psi}(y'_N) : \Psi(z_1) : (1) : \cdots : (M-1) : | 0 \rangle, \end{aligned} \quad (2.28)$$

where we have used the fact that each term in the sum is identical after an even permutation and a renumbering of the variables  $x_i$ . This integral is just one term in the expansion of the exponential in  $S$  and applying this reduction to every term we get

$$\begin{aligned} S_N &= \int dz_1 S_F(y_N - z_1) e \mathcal{A}(z_1) \langle 0 | \mathcal{T} : \bar{\Psi}(y'_1) \Psi(y_1) \cdots \bar{\Psi}(y'_N) : \Psi(z_1) \\ &\quad \times \exp \left\{ \int dx : \bar{\Psi}(x) [-ie \mathcal{A}(x)] \Psi(x) : \right\} | 0 \rangle. \end{aligned} \quad (2.29)$$

In a next step we apply the Wick theorem to  $\Psi(z_1)$  and get similar as in the previous case for the integral

$$\begin{aligned} I'_M &:= \int dx_1 \cdots dx_M \langle 0 | \mathcal{T} : \bar{\Psi}(y'_1) \Psi(y_1) \cdots \bar{\Psi}(y'_N) : \Psi(z_1) : (1) : \cdots : (M) : | 0 \rangle \\ &= \sum_{i=1}^N -i S_F(z_1 - y'_i) \int dx_1 \cdots dx_M \\ &\quad \times \langle 0 | \mathcal{T} : \bar{\Psi}(y'_1) \Psi(y_1) \cdots \widehat{\bar{\Psi}(y'_i)} \Psi(y_i) \cdots \bar{\Psi}(y'_N) : : (1) : \cdots : (M) : | 0 \rangle \\ &\quad + M \int dz_2 dx_1 \cdots dx_{M-1} S_F(z_1 - z_2) e \mathcal{A}(z_2) \\ &\quad \times \langle 0 | \mathcal{T} : \bar{\Psi}(y'_1) \Psi(y_1) \cdots \bar{\Psi}(y'_N) : \Psi(z_2) : (1) : \cdots : (M-1) : | 0 \rangle, \end{aligned} \quad (2.30)$$

which is again a term in the expansion of  $S_N$ , so that our amplitude is

$$\begin{aligned} S_N &= \sum_{i=1}^N -i \int dz_1 S_F(y_N - z_1) e \mathcal{A}(z_1) S_F(z_1 - y'_i) \\ &\quad \times \langle 0 | \mathcal{T} : \bar{\Psi}(y'_1) \Psi(y_1) \cdots \widehat{\bar{\Psi}(y'_i)} \Psi(y_i) \cdots \bar{\Psi}(y'_N) : \end{aligned}$$

$$\begin{aligned}
& \times \exp \left\{ \int dx : \bar{\Psi}(x) [-ie \mathcal{A}(x)] \Psi(x) : \right\} |0\rangle \\
& + \int dz_1 dz_2 S_F(y_N - z_1) e \mathcal{A}(z_1) S_F(z_1 - z_2) e \mathcal{A}(z_2) \\
& \times \langle 0 | \mathcal{T} : \bar{\Psi}(y'_1) \Psi(y_1) \cdots \bar{\Psi}(y'_N) : \Psi(z_2) \exp \left\{ \int dx : \bar{\Psi}(x) [-ie \mathcal{A}(x)] \Psi(x) : \right\} |0\rangle .
\end{aligned} \tag{2.31}$$

The vacuum expectation value in the first term is just the  $(N-1)$ -pair creation amplitude, that is,

$$\begin{aligned}
S_N &= \sum_{i=1}^N (-i) \int dz_1 S_F(y_N - z_1) e \mathcal{A}(z_1) S_F(z_1 - y'_i) \\
& \times \text{sgn}(\sigma) S_{N-1}(y_1, \cdots, y_{N-1}, y'_1, \cdots, \widehat{y'_i}, \cdots, y'_N) \\
& + \int dz_1 dz_2 S_F(y_N - z_1) e \mathcal{A}(z_1) S_F(z_1 - z_2) e \mathcal{A}(z_2) \\
& \times \langle 0 | \mathcal{T} : \bar{\Psi}(y'_1) \Psi(y_1) \cdots \bar{\Psi}(y'_N) : \Psi(z_2) \exp \left\{ \int dx : \bar{\Psi}(x) [-ie \mathcal{A}(x)] \Psi(x) : \right\} |0\rangle ,
\end{aligned} \tag{2.32}$$

where  $\sigma$  is the permutation to rearrange the  $\bar{\Psi}(y'_j)$  and  $\Psi(y_j)$  to the standard form. We can use Eq. (2.30) again for the vacuum expectation value in the second term. Doing this recursively and assuming that the series, we get, converges we finally get

$$\begin{aligned}
S_N &= \sum_{i=1}^N \text{sgn}(\sigma) S_{N-1}(y_1, \cdots, y_{N-1}, y'_1, \cdots, \widehat{y'_i}, \cdots, y'_N) \\
& \times (-i) \left[ \int dz_1 S_F(y_N - z_1) e \mathcal{A}(z_1) S_F(z_1 - y'_i) \right. \\
& + \int dz_1 dz_2 S_F(y_N - z_1) e \mathcal{A}(z_1) S_F(z_1 - z_2) e \mathcal{A}(z_2) S_F(z_2 - y'_i) \\
& \left. + \cdots \right].
\end{aligned} \tag{2.33}$$

The infinite series is just the normal perturbation theory expansion for the pair creation without any disconnected parts. We identify it with the reduced one-pair creation amplitude  $S^R(y_N, y'_i)$ . Therefore we have found a way to reduce the  $N$ -pair amplitude to a  $(N-1)$ -pair amplitude. Using recursion we can write for  $S_N$ :

$$S_N(y_1, \cdots, y_N, y'_1, \cdots, y'_N) = S_0 \sum_{\sigma} \text{sgn}(\sigma) S^R(y_1, y'_{\sigma(1)}) \cdots S^R(y_N, y'_{\sigma(N)}) \tag{2.34}$$

with the vacuum amplitude

$$S_0 = \langle 0 | \mathcal{T} \exp \left\{ \int dx : \bar{\Psi}(x) [-ie \mathcal{A}(x)] \Psi(x) : \right\} |0\rangle = \langle 0 | S |0\rangle . \tag{2.35}$$

This is identical to the result of the last section. Therefore we have found an expression for  $S^R$ , that is, for  $s^{+-}$ . It is just the perturbation theory expansion of a fermion interacting an arbitrary number of times with an external field without any disconnected parts.

Finally we want to find also a perturbation theory expression for  $S_0$ . Expanding the exponential we get

$$S_0 = \sum_{M=0}^{\infty} \frac{1}{M!} \tilde{I}_M, \quad (2.36)$$

with  $\tilde{I}_M$  defined as

$$\tilde{I}_M := \int dx_1 \cdots dx_M \langle 0 | \mathcal{T} : \bar{\Psi}(x_1) [-ie \mathcal{A}(x_1)] \Psi(x_1) : \cdots : (M) : | 0 \rangle. \quad (2.37)$$

We are now using the Wick theorem again in order to reduce this expression. Applying it to  $\Psi(x_1)$  we get

$$\begin{aligned} \tilde{I}_M &= (-i)(M-1) \int dx_1 dx_2 \cdots dx_M e \mathcal{A}(x_1) S_F(x_1 - x_2) e \mathcal{A}(x_2) \\ &\quad \times \langle 0 | \mathcal{T} \bar{\Psi}(x_1) \Psi(x_2) : (3) : \cdots : (M) : | 0 \rangle. \end{aligned} \quad (2.38)$$

Similar we get for the following expression

$$\begin{aligned} \tilde{J}_M(x_1, x_2) &:= \int dx_3 \cdots dx_M \langle 0 | \mathcal{T} \bar{\Psi}(x_1) \Psi(x_2) : \bar{\Psi}(x_3) [-ie \mathcal{A}(x_3)] \Psi(x_3) : \cdots : (M) : | 0 \rangle \\ &= -i S_F(x_2 - x_1) \int dx_3 \cdots dx_M \langle 0 | \mathcal{T} : (3) : \cdots : (M) : | 0 \rangle \\ &\quad + (M-2) \int dx_3 dx_4 \cdots dx_M i S_F(x_2 - x_3) [-ie \mathcal{A}(x_3)] \\ &\quad \times \langle 0 | \mathcal{T} \bar{\Psi}(x_1) \Psi(x_3) : (4) : \cdots : (M) : | 0 \rangle. \end{aligned} \quad (2.39)$$

That is,

$$\tilde{I}_M = -i(M-1) \int dx_1 dx_2 e \mathcal{A}(x_1) S_F(x_1 - x_2) e \mathcal{A}(x_2) \tilde{J}_M(x_1, x_2) \quad (2.40)$$

and

$$\tilde{J}_M(x_1, x_2) = -i S_F(x_2 - x_1) \tilde{I}_{M-2} + (M-2) \int dx_3 S_F(x_2 - x_3) e \mathcal{A}(x_3) \tilde{J}_{M-1}(x_1, x_3). \quad (2.41)$$

Using both relations in order to reduce  $\tilde{I}_M$  in terms of  $\tilde{I}_k$  we get

$$\begin{aligned} \tilde{I}_M &= (M-1) C_2 \tilde{I}_{M-2} + (M-1)(M-2) C_3 \tilde{I}_{M-3} + \cdots \\ &\quad + (M-1) \cdots 2 C_{M-1} \tilde{I}_1 + (M-1) \cdots 2 \cdot 1 C_M \tilde{I}_0, \end{aligned} \quad (2.42)$$

with  $C_N$  defined as

$$\begin{aligned} C_N &:= (-1) \int dx_1 \cdots dx_N \\ &\quad \times \text{Tr} [e \mathcal{A}(x_1) S_F(x_1 - x_2) e \mathcal{A}(x_2) \cdots e \mathcal{A}(x_N) S_F(x_N - x_1)], \end{aligned} \quad (2.43)$$

writing explicitly the Dirac indices to get the trace. For ease of writing we define also  $C_0 = C_1 = 0$  and use that  $\tilde{I}_1 = 0$  and  $\tilde{I}_0 = 1$ . With these we can write more compactly

$$\begin{aligned}\tilde{I}_M &= \sum_{k=1}^M C_k \tilde{I}_{M-k} \frac{(M-1)!}{(M-k)!} \\ &= \frac{M!}{M} \sum_{k=1}^M C_k \frac{\tilde{I}_{M-k}}{(M-k)!}.\end{aligned}\quad (2.44)$$

This reduction formula can now be used in order to find an expression for  $S_0$ . For this we write  $\tilde{I}_M$  in a series ordered by the number of  $C_i$ 's (that is, as we will see later, the number of loops) that appear in each term after a complete reduction. We see that the formula above just gives us a recipe, how the next order can be derived from the lower one. Only one term with no  $C_i$  in it exists:

$$\tilde{I}_0^{(0)} = 1, \quad (2.45)$$

giving therefore in zeroth order for  $S_0$ :

$$S_0^{(0)} = 1. \quad (2.46)$$

Using this only nonzero  $\tilde{I}_M^{(0)}$  in Eq. (2.44) we get in first order only a contribution if  $k = M$

$$\tilde{I}_M^{(1)} = \frac{M!}{M} C_M \quad (2.47)$$

and for  $S_0$

$$S_0^{(1)} = \sum_{M=0}^{\infty} \frac{1}{M!} \tilde{I}_M^{(1)} = \sum_{M=1}^{\infty} \frac{C_M}{M}. \quad (2.48)$$

In second order we get

$$\begin{aligned}\tilde{I}_M^{(2)} &= \frac{M!}{M} \sum_{k=1}^M C_k \frac{\tilde{I}_{M-k}^{(1)}}{(M-k)!} = \frac{M!}{M} \sum_{k=1}^M k \frac{C_k}{k} \frac{C_{M-k}}{M-k} \\ &= \frac{M!}{M} \frac{1}{2} \sum_{k=1}^M \left[ k \frac{C_k}{k} \frac{C_{M-k}}{M-k} + (M-k) \frac{C_{M-k}}{M-k} \frac{C_k}{k} \right] = \frac{M!}{2} \sum_{k=1}^M \frac{C_k}{k} \frac{C_{M-k}}{M-k},\end{aligned}\quad (2.49)$$

where we have changed the summation index from  $k$  to  $M-k$  in one step. For  $S_0$  we get

$$S_0^{(2)} = \sum_{M=0}^{\infty} \frac{1}{M!} \tilde{I}_M^{(2)} = \frac{1}{2} \sum_{M=0}^{\infty} \sum_{k=1}^M \frac{C_k}{k} \frac{C_{M-k}}{M-k} = \frac{1}{2} \left[ \sum_{k=1}^{\infty} \frac{C_k}{k} \right] \left[ \sum_{l=1}^{\infty} \frac{C_l}{l} \right] = \frac{1}{2} [S_0^{(1)}]^2. \quad (2.50)$$

Using the same transformations we can express also all higher terms of  $S_0$ , for which we get

$$S_0^{(n)} = \frac{1}{n!} [S_0^{(1)}]^n, \quad (2.51)$$

so that we finally get the vacuum amplitude as

$$S_0 = \exp [S_0^{(1)}] = \exp \left\{ - \sum_{M=2}^{\infty} \frac{1}{M} \int dx_1 \cdots dx_M \right. \\ \left. \times \text{Tr} [e \mathcal{A}(x_1) S_F(x_1 - x_2) \cdots e \mathcal{A}(x_M) S_F(x_M - x_1)] \right\}. \quad (2.52)$$

This is a well known result [54, 55, 56, 59]. Its interpretation is straightforward. The sum in the exponential is just the sum over all single loops, whereas the exponential accounts for the fact that we can have also two or more loops.

With this we have found now perturbation theory expressions for all terms occurring in the reduction formula Eq. (2.34), that is, for the reduced one-pair amplitude and the vacuum amplitude.

A final remark has to be made about the vacuum amplitude  $S_0$ . Already Schwinger found out that the expression for  $S_0$  is not finite due to infinities in the imaginary part of  $S_0^{(1)}$  [54] (see also [57]). But he also mentioned that in the total probabilities we need only the absolute value squared of  $S_0$ , where only the real part of  $S_0^{(1)}$  contributes, which is finite.

## 2.3 Reduction using the Dirac sea picture

The Feynman boundary conditions used in the first section are of a mixed retarded and advanced type. The historically older picture is the Dirac sea picture, which uses only retarded boundary conditions and reinterprets the negative energy states by filling them with electrons; holes in this filled Dirac sea are then interpreted as positrons. In terms of the particle operators this means that negative energy electron annihilation operators are interpreted as positron creation operators, etc.. As already mentioned, both point of views are completely equivalent [53]. Pair creation in the Dirac sea picture has been investigated by Best et al. [35, 36], but he had to neglect some higher-order terms in his derivation in order to get the reduction of the  $N$ -pair amplitudes, whereas we will show that this reduction is also true in the exact case. So our derivation is in principal an extension of his work.

As the calculation is rather complicated, we restrict ourself to the reduction of the one-pair creation amplitude. A generalization of the procedure used here should be possible in principle, but has not been tried by us.

As shown in App. A.2 in the Dirac sea picture the connection between the creation and annihilation operators is written as (see Eq. (A.26))

$$b_p S = \sum_{i>0} a_{pi} S b_i + \sum_{j<0} a_{pj} S d_j^+, \quad (2.53a)$$

$$d_q S = \sum_{i>0} a_{qi}^* S b_i^+ + \sum_{j<0} a_{qj}^* S d_j, \quad (2.53b)$$

$$S b_p^+ = \sum_{i>0} a_{ip} b_i^+ S + \sum_{j<0} a_{jp} d_j S, \quad (2.53c)$$



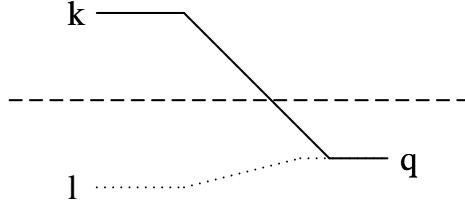


Figure 2.1: Graphical illustration of the first term of the pair creation amplitude (Eq. (2.57)).  $a$  is denoted by a solid line,  $a^*$  by a dotted line.

$$Sd_q^+ = \sum_{i>0} a_{iq}^* b_i S + \sum_{j<0} a_{jq}^* d_j^+ S. \quad (2.53d)$$

The one-pair creation amplitude is as in Eq. (2.3)

$$S_1(k, l) = \langle 0 | d_l b_k S | 0 \rangle. \quad (2.54)$$

Applying Eq. (2.53) for  $b_k$  and  $d_l$  we get

$$S_1 = \langle 0 | S \left( \sum_{p>0} a_{ip}^* b_p^+ + \sum_{q<0} a_{iq}^* d_q \right) \left( \sum_{p'>0} a_{kp'} b_{p'} + \sum_{q'<0} a_{kq'} d_{q'}^+ \right) | 0 \rangle. \quad (2.55)$$

As  $b_{p'} | 0 \rangle = 0$ , we get

$$S_1(k, l) = \sum_{q<0, q'<0} a_{iq}^* a_{kq'} \langle 0 | S d_q d_{q'}^+ | 0 \rangle + \sum_{p>0, q'<0} a_{ip}^* a_{kq'} \langle 0 | S b_p^+ d_{q'}^+ | 0 \rangle. \quad (2.56)$$

Using the anticommutation relations the first vacuum expectation value can be reduced to get

$$S_1(k, l) = \sum_{q<0} a_{iq}^* a_{kq} \langle 0 | S | 0 \rangle + \sum_{p>0, q'<0} a_{ip}^* a_{kq'} \langle 0 | S b_p^+ d_{q'}^+ | 0 \rangle. \quad (2.57)$$

The first term is just of the desired form, i.e., the vacuum amplitude appears as a separate factor. The interpretation of this term is easy (see Fig. 2.1): The state  $q$  of the negative continuum changes with time. Whereas the electron goes from  $q$  to  $k$  in the positive continuum, the remaining hole appears as  $l$  and is interpreted as a positron. The second term is of a different type. As the vacuum expectation value is that of the annihilation of a positron and an electron, we assume that it describes a higher-order process. These higher-order contributions were neglected by Best et al.. But one can use the inverse transformations in Eq. (2.53) in order to go back to the final system again:

$$\begin{aligned} \langle 0 | S b_p^+ d_{q'}^+ | 0 \rangle &= \langle 0 | \left( \sum_{m>0} a_{mp} b_m^+ + \sum_{n<0} a_{np} d_n \right) \\ &\quad \times \left( \sum_{m'>0} a_{m'q'}^* b_{m'} + \sum_{n'<0} a_{n'q'}^* d_{n'}^+ \right) S | 0 \rangle, \end{aligned} \quad (2.58)$$

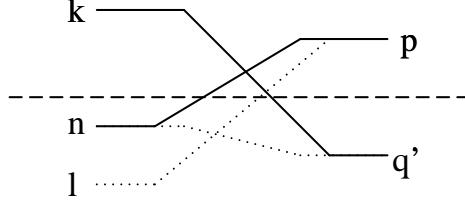


Figure 2.2: Graphical illustration of the second term of the pair creation amplitude (Eq. (2.62)).  $a$  is denoted by a solid line,  $a^*$  by a dotted line.

which can again be simplified

$$\begin{aligned} \langle 0 | S b_p^+ d_{q'}^+ | 0 \rangle &= \sum_{n < 0, n' < 0} a_{np} a_{n'q'}^* \langle 0 | d_n d_{n'}^+ S | 0 \rangle \\ &+ \sum_{n < 0, m' > 0} a_{np} a_{m'q'}^* \langle 0 | d_n b_{m'} S | 0 \rangle \end{aligned} \quad (2.59)$$

$$\begin{aligned} &= \sum_{n < 0} a_{np} a_{nq'}^* \langle 0 | S | 0 \rangle \\ &+ \sum_{n < 0, m' > 0} a_{np} a_{m'q'}^* \langle 0 | d_n b_{m'} S | 0 \rangle. \end{aligned} \quad (2.60)$$

With this we get for the one-pair creation amplitude

$$\begin{aligned} S_1(k, l) &= \sum_{q < 0} a_{lq}^* a_{kq} \langle 0 | S | 0 \rangle + \sum_{p > 0, q' < 0, n < 0} a_{lp}^* a_{kq'} a_{np} a_{nq'}^* \langle 0 | S | 0 \rangle \\ &+ \sum_{p > 0, q' < 0, n < 0, m' > 0} a_{lp}^* a_{kq'} a_{np} a_{m'q'}^* \langle 0 | d_n b_{m'} S | 0 \rangle. \end{aligned} \quad (2.61)$$

The expression  $\langle 0 | d_n b_{m'} S | 0 \rangle$  in the last term is just  $S_1(m', n)$ , therefore we finally get

$$\begin{aligned} S_1(k, l) &= \left[ \sum_{q < 0} a_{lq}^* a_{kq} + \sum_{p > 0, q' < 0, n < 0} a_{lp}^* a_{kq'} a_{np} a_{nq'}^* \right] \langle 0 | S | 0 \rangle \\ &+ \sum_{p > 0, q' < 0, n < 0, m' > 0} a_{lp}^* a_{kq'} a_{np} a_{m'q'}^* S_1(m', n). \end{aligned} \quad (2.62)$$

Therefore we have found a recursive expression for  $S_1$ . Replacing  $S_1$  in it recursively we get higher terms, each of which has the vacuum amplitude as a separate factor. If we assume that the infinite sum that remains after the extraction of the vacuum amplitude converges, we have found the desired result, where the infinite sum is the reduced amplitude.

The interpretation of the first-order term was simple. That of the second term is more complicated. If we make a graphical illustration of this process similar to Fig. 2.1 by drawing again a solid line for  $a$  and a dotted line for  $a^*$ , we get Fig. 2.2. At first sight this process seems to be not allowed, as we have on the right side an electron with positive

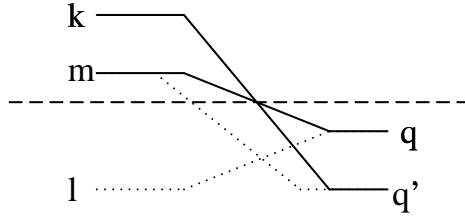


Figure 2.3: Graphical illustration of the alternative form of the second term of the pair creation amplitude (Eq. (2.65)).  $a$  is denoted by a solid line,  $a^*$  by a dotted line.

energy together with its hole. But the positive continuum is not part of the Dirac sea, therefore no electrons do exist there.

Therefore some remarks should be made in order to explain this. First even as this process seems to be impossible in the Dirac sea interpretation, it is not in a charge-conjugate theory, where we have the filled Dirac sea in the positive continuum. Second we are dealing only with asymptotic states, so we should be aware that the filling of this state can also be done in some stage of the time development, whereas we have to interpret everything in terms of the asymptotic states. Finally it is also possible to use the unitarity of  $a$  to rewrite the expressions in a form, where this problem does not occur. For this, we rewrite the second term in Eq. (2.62) with the help of

$$\sum_{n<0} a_{np} a_{nq'}^* = \delta_{pq'} - \sum_{m>0} a_{mp} a_{mq'}^*. \quad (2.63)$$

As  $p$  is from the positive and  $q'$  from the negative continuum, the  $\delta$  function is always zero and we get

$$\sum_{p>0, q'<0, n<0} a_{lp}^* a_{kq'} a_{np} a_{nq'}^* = - \sum_{p>0, q'<0, m>0} a_{lp}^* a_{kq'} a_{mp} a_{mq'}^*. \quad (2.64)$$

Doing now the same with the summation over  $p$ , we finally get

$$\sum_{p>0, q'<0, n<0} a_{lp}^* a_{kq'} a_{np} a_{nq'}^* = \sum_{q<0, q'<0, m>0} a_{lq}^* a_{kq'} a_{mq} a_{mq'}^*. \quad (2.65)$$

The interpretation of this process is much easier (see Fig. 2.3): A negative energy electron at  $q'$  goes to the positive continuum and appears finally as electron  $k$ ; but also the electron at  $q$  goes to the positive continuum, where it would appear as electron  $m$ ; but the hole, that remained from  $q'$ , can now “annihilate” electron  $m$ , whereas the hole remaining from  $q$  finally appears as hole  $l$ .

We see already here that the interpretation of these higher-order diagrams is not easy. The Feynman interpretation with the positrons moving backward in time was much easier because of the fact that this process could be described by one connected line.

The main advantage of the Dirac sea picture is that it can be used in some systems to reduce the many-particle theory back to a single-particle theory. This is the case for processes where multiple-particle effects are not important. But here multiple-particle effects do occur, which are just these higher-order processes. Therefore the first term can be seen as the single-particle contribution to the pair creation, all other diagrams are multiple-particle corrections to it.

We have shown only how the one-pair creation amplitude can be reduced to the reduced amplitude and the vacuum amplitude. This calculation should also be done in principle for the multiple-pair creation processes in order to reproduce the results of the previous two sections. The same relation between the operators in the initial and final system could be used for this. As the explicit calculation gets rather complex and we already know that the Dirac sea picture is equivalent to the Feynman boundary picture, it has not been tried by us.

As in the first section for the reduction using Feynman boundary conditions the results here are not very useful for explicit calculations, as the vacuum amplitude remains again an unexplained factor in the formula. C. Best has given an interpretation of this vacuum amplitude as a determinant over all occupied states in the Dirac sea [36] using the full many-particle theory. On the other hand the recursive formula in Eq. (2.62) may be useful for the calculation of the reduced one-pair amplitudes, as one can use it in order to calculate them in terms of the single-particle amplitudes  $a_{ij}$ .

## 2.4 Comparison with earlier results

The results of especially the first two sections suggest the following picture of the pair production: In the Feynman picture the  $N$ -pair production can be described by two forms of processes (Fig. 2.4).  $N$  positron lines enter the interaction region coming from the future. They interact with the external field an arbitrary number of times, where they may change also their direction in time. Finally they leave the interaction region as electron lines moving into the normal time direction. Besides these processes, which are characterized each by a continuous line coming from and leaving to the future, there are also processes, which consists of closed loops. As they remain entirely inside the interaction region, they are not visible as physical processes. These closed loops form the vacuum amplitude. From this picture it is also clear that the vacuum amplitude is the same for all  $N$ -pair amplitudes and therefore a common factor in all of them. The fact that we are dealing with multiple particles only shows up in the calculation through the antisymmetrisation with respect to all electrons (or equivalent to all positrons).

This means that for a complete calculation of the  $N$ -pair creation probabilities we need to know only the reduced one-pair creation amplitude together with the vacuum amplitude. Both can be calculated in principle using perturbation theory, where the reduced one-pair amplitude is identical to the usual perturbation series result and setting the vacuum amplitude to one, that is, neglecting all diagrams with disconnected parts.

If one neglects the exchange terms in the calculation of the probability, it suffices to

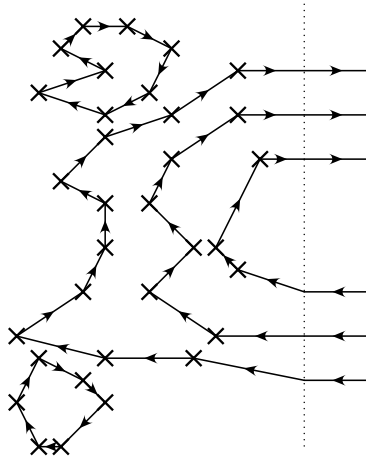


Figure 2.4: *Graphical illustration of the general form of the  $N$ -pair production process. The creation of a pair is described by a connected fermion line entering from and leaving to the future. The vacuum processes are described by all sorts of closed fermion loops. The interaction with the external field is shown as a cross.*

know the reduced one-pair creation probability, as this is the only result needed for the Poisson distribution of the multiple-pair probabilities.

Please note that according to the rules of the Feynman diagrams we have neglected the antisymmetrisation and therefore the Pauli principle for all intermediate states. There is a deeper reason for doing so, which has to do with the connection of the higher-order processes and the occurrence of the vacuum processes through antisymmetrisation. This is, for example, discussed in detail in [56, 59]. Let us look, for example, at a typical higher-order diagram in perturbation theory, where we would expect corrections because of the Pauli principle. In Fig. 2.5 we would expect a deviation as we have two electrons, which are not allowed to be in the same state. (The same is also true for the two positrons.) But it can be shown that the contribution from this process are just canceled by those of the vacuum correction shown in Fig. 2.6, where the electron in the loop and the produced electron are not allowed to be in the same state also. Both processes are connected with each other, as we get one from the other, if we exchange the two electron lines or the two positron lines. This result is of a very general nature, so that the antisymmetrisation of all intermediate particles can be dropped, if we also include the vacuum processes (again without antisymmetrisation).

This shows that the higher-order multiple-particle corrections to the one-pair creation (as in Fig. 2.5) are connected with the vacuum processes. As we have to include the vacuum processes in order to restore unitarity, we should include the corresponding higher-order multiple-particle processes as well. Therefore we think that these processes should be studied in more detail. This even more as we know that the vacuum processes are not neglectable, as they decrease the reduced probabilities larger than one to values less than

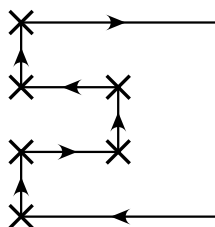


Figure 2.5: One possible higher-order pair creation process, where the Pauli principle is neglected in the intermediate state. Interaction with the external field is shown as a cross.

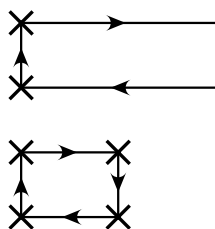


Figure 2.6: Vacuum correction to the one-pair creation connected by an exchange of two lines with the process shown in Fig. 2.5.

one.

The inclusion of these higher-order processes is straightforward in our model. As the Poisson distribution needs only the neglect of the exchange terms, we can include the higher-order terms into the calculation of the reduced probability and use this result then in the Poisson distribution for the multiple-pair probabilities. This procedure is consistent, as it includes automatically the higher-order corrections to the vacuum amplitude. Therefore the calculation changes only the reduced probability used in the Poisson distribution but not the explicit form.

Let us compare this result with the other models [33, 34, 35]: All three models get a Poisson distribution for the multiple-pair creation as well but only based on the summation of a restricted class of diagrams. Studying further these approximations one finds that all of them are essentially “quasi boson” approximations. This means that they have as fundamental processes a pair creation and a pair annihilation process (neglecting at the moment the Coulomb scattering). Combining these processes all previous models assume that only pairs, which have been produced together in a creation process, can be annihilated (see also Fig. 2.7). Therefore the electron and the positron are seen as an unbreakable pair, which behaves more or less like a boson. And for bosons in an external field the Poisson distribution comes out exactly [55]. Even the inclusion of Coulomb scattering in some of these models does not change the “quasi bosonic” nature of them. Our calculation indicates that there are higher-order processes in which electrons and positrons do not

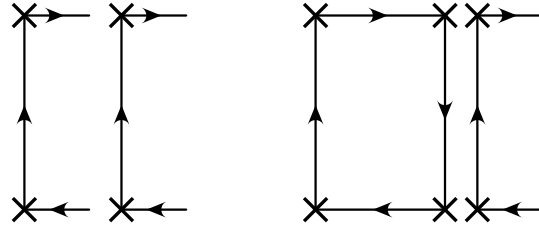


Figure 2.7: Higher-order processes, which are included in the “quasi boson” models: multiple-pair creation and vacuum processes.

behave as “quasi bosons”. These processes are multiple-particle processes in the sense that more than one electron or positron are essentially needed in an intermediate step.

The fact that these are multiple-particle effects also shows the advantage of using the Feynman boundary conditions instead of the retarded boundary conditions used in the Dirac sea picture. In the Feynman picture the production of a pair is described by a continuous fermion line, where the inclusion of multiple-particle effects presents no difficulties. The advantage of the Dirac sea picture is mainly that its particle hole interpretation allows to treat the creation of one electron-positron pair in a single particle formalism. As the higher-order processes need the existence of more than one electron and one hole, this advantage of the Dirac sea picture is no longer existent then.

The other advantage of the Feynman boundary conditions is that the different processes can be separated from each other. Especially the vacuum processes are independent of the reduced pair creation processes. This is not the case in the Dirac sea picture, where vacuum processes and pair creation processes can not be separated in the intermediate steps but only in the final state.

In Chap. 5 we are going to study the processes of the type of Fig. 2.5 in more detail. We will find there that this process is just the lowest-order correction to the one-pair creation, if we neglect Coulomb scattering terms. For this we restrict ourself to second-order Magnus theory. Therefore we will derive now the general form of the  $S$  operator in the next section using this approximation.

## 2.5 The $S$ operator in Magnus theory

The Magnus theory can be seen as an expansion in the interaction time. For large values of  $\gamma$  the interaction time of the two heavy-ion fields is very short, therefore the use of this approximation seems to be justified. Up to second order the  $S$  operator is given by [60, 61]

$$\begin{aligned}
 S &= \mathcal{T} \exp \left[ -i \int_{-\infty}^{+\infty} H_I(t) dt \right] \\
 &\approx \exp \left[ -i \int_{-\infty}^{+\infty} H_I(t) dt + \frac{1}{2} (-i)^2 \int_{-\infty}^{+\infty} dt_2 \int_{-\infty}^{t_2} dt_1 [H_I(t_2), H_I(t_1)] + \dots \right]. \quad (2.66)
 \end{aligned}$$

The commutator of the  $H_I$ 's for  $t_1 < t_2$  is the difference of the time-ordered and the anti-time-ordered product. We rewrite  $S$  as

$$S = \exp \left\{ -i \int_{-\infty}^{+\infty} H_I(t) dt + \frac{1}{4} (-i)^2 \int_{-\infty}^{+\infty} dt_2 \int_{-\infty}^{+\infty} dt_1 \right. \\ \left. \times \mathcal{T} [H_I(t_2) H_I(t_1)] - \mathcal{A} [H_I(t_2) H_I(t_1)] + \dots \right\} \quad (2.67)$$

$$= \exp \left\{ \int d^4x e : \bar{\Psi}(x) [-ie \mathcal{A}(x)] \Psi(x) : \right. \\ \left. + \frac{1}{4} \int d^4x_1 d^4x_2 (\mathcal{T} - \mathcal{A}) : \bar{\Psi}(x_2) [-ie \mathcal{A}(x_2)] \Psi(x_2) : : \bar{\Psi}(x_1) [-ie \mathcal{A}(x_1)] \Psi(x_1) : \right\}. \quad (2.68)$$

Now we use again the Wick theorem in order to put the field operators into normal-ordered form. We use it for the time-ordered and anti-time-ordered products in the form

$$\mathcal{T} AB = : AB : + \langle 0 | \mathcal{T} AB | 0 \rangle = : AB : + \langle \mathcal{T} AB \rangle, \quad (2.69a)$$

$$\mathcal{A} AB = : AB : + \langle 0 | \mathcal{A} AB | 0 \rangle = : AB : + \langle \mathcal{A} AB \rangle. \quad (2.69b)$$

As the first term in  $S$  is in normal-ordered form already, only the second one has to be rearranged. For the time-ordered product we get

$$\mathcal{T} : \bar{\Psi}_2 \Psi_2 : : \bar{\Psi}_1 \Psi_1 : = : \bar{\Psi}_2 \Psi_2 \bar{\Psi}_1 \Psi_1 : + : \Psi_2 \bar{\Psi}_1 : \langle \mathcal{T} \bar{\Psi}_2 \Psi_1 \rangle \\ + : \bar{\Psi}_2 \Psi_1 : \langle \mathcal{T} \Psi_2 \bar{\Psi}_1 \rangle + \langle \mathcal{T} \bar{\Psi}_2 \Psi_1 \rangle \langle \mathcal{T} \Psi_2 \bar{\Psi}_1 \rangle, \quad (2.70)$$

and the same for the anti-time-ordered product by replacing  $\mathcal{T}$  with  $\mathcal{A}$ . We get for  $S$

$$S = \exp \left\{ \int dx [-ie \mathcal{A}(x)_{\alpha\beta}(x)] : \bar{\Psi}_\alpha \Psi_\beta : + \frac{1}{4} \int dx_1 dx_2 [-ie \mathcal{A}(x_2)_{\alpha\beta}] [-ie \mathcal{A}(x_1)_{\gamma\delta}] \right. \\ \times [ : \Psi_\beta(x_2) \bar{\Psi}_\gamma(x_1) : \langle \mathcal{D} \bar{\Psi}_\alpha(x_2) \Psi_\delta(x_1) \rangle + : \bar{\Psi}_\alpha(x_2) \Psi_\delta(x_1) : \langle \mathcal{D} \Psi_\beta(x_2) \bar{\Psi}_\gamma(x_1) \rangle \\ \left. + \langle \mathcal{T} \bar{\Psi}_\alpha(x_2) \Psi_\delta(x_1) \rangle \langle \mathcal{T} \Psi_\beta(x_2) \bar{\Psi}_\gamma(x_1) \rangle - \langle \mathcal{A} \bar{\Psi}_\alpha(x_2) \Psi_\delta(x_1) \rangle \langle \mathcal{A} \Psi_\beta(x_2) \bar{\Psi}_\gamma(x_1) \rangle \right\}. \quad (2.71)$$

The last two terms can be rewritten to give

$$\langle \mathcal{D} \bar{\Psi}_\alpha(x_2) \Psi_\delta(x_1) \rangle \langle \mathcal{T} \Psi_\beta(x_2) \bar{\Psi}_\gamma(x_1) \rangle + \langle \mathcal{A} \bar{\Psi}_\alpha(x_2) \Psi_\delta(x_1) \rangle \langle \mathcal{D} \Psi_\beta(x_2) \bar{\Psi}_\gamma(x_1) \rangle. \quad (2.72)$$

Exchanging the integration of  $dx_1$  and  $dx_2$  we see that the second and the third term of Eq. (2.71) can be combined and also the last two terms, so that we get

$$S = \exp \left\{ \int dx [-ie \mathcal{A}(x)_{\alpha\beta}(x)] : \bar{\Psi}_\alpha \Psi_\beta : + \frac{1}{4} \int dx_1 dx_2 [-ie \mathcal{A}(x_2)_{\alpha\beta}] [-ie \mathcal{A}(x_1)_{\gamma\delta}] \right. \\ \times \left[ 2 : \Psi_\beta(x_2) \bar{\Psi}_\gamma(x_1) : \langle \mathcal{D} \bar{\Psi}_\alpha(x_2) \Psi_\delta(x_1) \rangle \right. \\ \left. + \langle (\mathcal{T} + \mathcal{A}) \Psi_\beta(x_2) \bar{\Psi}_\gamma(x_1) \rangle \langle \mathcal{D} \bar{\Psi}_\alpha(x_2) \Psi_\delta(x_1) \rangle \right] \right\}. \quad (2.73)$$



Now we transform  $S$  into momentum space. For this we need the Fourier transform of the field operator as well as of the vacuum expectation values.

The field operator and its conjugate can be written as (See App. A.1 for this form and the definition of  $d\bar{p}$ )

$$\Psi(x) = \sum_s \int d\bar{p} \left[ b(p, s) u(p, s) \exp(-ipx) + d^+(p, s) v(p, s) \exp(ipx) \right], \quad (2.74a)$$

$$\bar{\Psi}(x) = \sum_s \int d\bar{p} \left[ b^+(p, s) \bar{u}(p, s) \exp(ipx) + d(p, s) \bar{v}(p, s) \exp(-ipx) \right]. \quad (2.74b)$$

As we show in App. A.3, the  $\mathcal{D}$  and the  $\mathcal{T} + \mathcal{A}$  vacuum expectation values are given by

$$\begin{aligned} \langle 0 | \mathcal{D} \Psi(x) \bar{\Psi}(x') | 0 \rangle &= i [S_F(x - x') + S_A(x - x')] \\ &= 2i \int \frac{d^4 p}{(2\pi)^4} (\not{p} + m) \frac{\text{P.P.}}{p^2 - m^2} \exp(-ip(x - x')), \end{aligned} \quad (2.75)$$

where P.P. denotes the principal part of the integral, and

$$\begin{aligned} \langle 0 | (\mathcal{T} + \mathcal{A}) \Psi(x) \bar{\Psi}(x') | 0 \rangle &= i [S_F(x - x') - S_A(x - x')] \\ &= \int d\Gamma(p) (\not{p} + m) \exp(-ip(x - x')) - \int d\Gamma(p) (\not{p} - m) \exp(ip(x - x')), \end{aligned} \quad (2.76)$$

which describes the propagation of on-shell electrons and positrons.

These forms of the vacuum expectation values are put into  $S$  together with the decomposition of the field operators  $\Psi(x)$  and  $\bar{\Psi}(x)$  and using also the Fourier transform of the external field

$$A(x) = \int \frac{d^4 q}{(2\pi)^4} A(q) \exp(-iqx). \quad (2.77)$$

In the following we drop the spin indices assuming that it has been incorporated into  $p$ . With these we rewrite the first term in Eq. (2.73) as

$$\begin{aligned} &\int dx : \bar{\Psi}(x) [-ie \mathcal{A}(x)] \Psi(x) : \\ &= \int dx \int d\bar{p}_1 d\bar{p}_2 \frac{dq}{(2\pi)^4} : \left[ b^+(p_1) \bar{u}(p_1) \exp(ip_1 x) + d(p_1) \bar{v}(p_1) \exp(-ip_1 x) \right] \\ &\quad \times [-ie \mathcal{A}(q)] \exp(-iqx) \left[ b(p_2) u(p_2) \exp(-ip_2 x) + d^+(p_2) v(p_2) \exp(ip_2 x) \right] : \quad (2.78) \\ &= \int d\bar{p}_1 d\bar{p}_2 dq (-ie) \left[ \right. \\ &\quad : b^+(p_1) b(p_2) : \bar{u}(p_1) \mathcal{A}(q) u(p_2) \int \frac{dx}{(2\pi)^4} \exp(ix(p_1 - q - p_2)) \\ &\quad + : b^+(p_1) d^+(p_2) : \bar{u}(p_1) \mathcal{A}(q) v(p_2) \int \frac{dx}{(2\pi)^4} \exp(ix(p_1 - q + p_2)) \\ &\quad \left. + : d(p_1) b(p_2) : \bar{v}(p_1) \mathcal{A}(q) u(p_2) \int \frac{dx}{(2\pi)^4} \exp(ix(-p_1 - q - p_2)) \right] \end{aligned}$$

$$\begin{aligned}
& + : d(p_1)d^+(p_2) : \bar{v}(p_1) \mathcal{A}(q)v(p_2) \int \frac{dx}{(2\pi)^4} \exp(ix(-p_1 - q + p_2)) \Big] \quad (2.79) \\
= & \int d\bar{p}_1 d\bar{p}_2 (-ie) \Big[ \\
& : b^+(p_1)b(p_2) : \bar{u}(p_1) \mathcal{A}(p_1 - p_2)u(p_2) \\
& + : b^+(p_1)d^+(p_2) : \bar{u}(p_1) \mathcal{A}(p_1 + p_2)v(p_2) \\
& + : d(p_1)b(p_2) : \bar{v}(p_1) \mathcal{A}(-p_1 - p_2)u(p_2) \\
& + : d(p_1)d^+(p_2) : \bar{v}(p_1) \mathcal{A}(-p_1 + p_2)v(p_2) \Big], \quad (2.80)
\end{aligned}$$

where we have used the fact that the integration over  $dx$  gives a  $\delta$  function.

The same can also be done with the other terms in Eq. (2.73), where we have to integrate now over two coordinates giving two  $\delta$  functions. We finally get

$$\begin{aligned}
S = & \exp \left\{ -ie \int d\bar{p}_1 d\bar{p}_2 \right. \\
& \times \left[ : b^+(p_1)b(p_2) : \bar{u}(p_1) \mathcal{A}(p_1 - p_2)u(p_2) \right. \\
& + : b^+(p_1)d^+(p_2) : \bar{u}(p_1) \mathcal{A}(p_1 + p_2)v(p_2) \\
& + : d(p_1)b(p_2) : \bar{v}(p_1) \mathcal{A}(-p_1 - p_2)u(p_2) \\
& \left. + : d(p_1)d^+(p_2) : \bar{v}(p_1) \mathcal{A}(-p_1 + p_2)v(p_2) \right] \\
& -ie^2 \int d\bar{p}_1 d\bar{p}_2 \frac{dp}{(2\pi)^4} \\
& \times \left[ : b^+(p_1)b(p_2) : \bar{u}(p_1) \mathcal{A}(p_1 - p) (\not{p} + m) \frac{\text{P.P.}}{p^2 - m^2} \mathcal{A}(p - p_2)u(p_2) \right. \\
& + : b^+(p_1)d^+(p_2) : \bar{u}(p_1) \mathcal{A}(p_1 - p) (\not{p} + m) \frac{\text{P.P.}}{p^2 - m^2} \mathcal{A}(p + p_2)v(p_2) \\
& + : d(p_1)b(p_2) : \bar{v}(p_1) \mathcal{A}(-p_1 - p) (\not{p} + m) \frac{\text{P.P.}}{p^2 - m^2} \mathcal{A}(p - p_2)u(p_2) \\
& \left. + : d(p_1)d^+(p_2) : \bar{v}(p_1) \mathcal{A}(-p_1 - p) (\not{p} + m) \frac{\text{P.P.}}{p^2 - m^2} \mathcal{A}(p + p_2)v(p_2) \right] \\
& + i \frac{e^2}{2} \int \frac{dp}{(2\pi)^4} d\Gamma(p') \text{Tr} \left[ (\not{p}' + m) \mathcal{A}(p' - p) (\not{p}' + m) \frac{\text{P.P.}}{p^2 - m^2} \mathcal{A}(p - p') \right] \\
& \left. - i \frac{e^2}{2} \int \frac{dp}{(2\pi)^4} d\Gamma(p') \text{Tr} \left[ (\not{p}' - m) \mathcal{A}(-p' - p) (\not{p}' + m) \frac{\text{P.P.}}{p^2 - m^2} \mathcal{A}(p + p') \right] \right\}. \quad (2.81)
\end{aligned}$$

The interpretation of the individual terms is straightforward (see Fig. 2.8). Terms of the form  $: b^+b :$  are electron Coulomb scattering terms,  $: dd^+ :$  the corresponding positron scattering terms.  $: b^+d^+ :$  corresponds to pair creation and  $: db :$  to pair annihilation. The

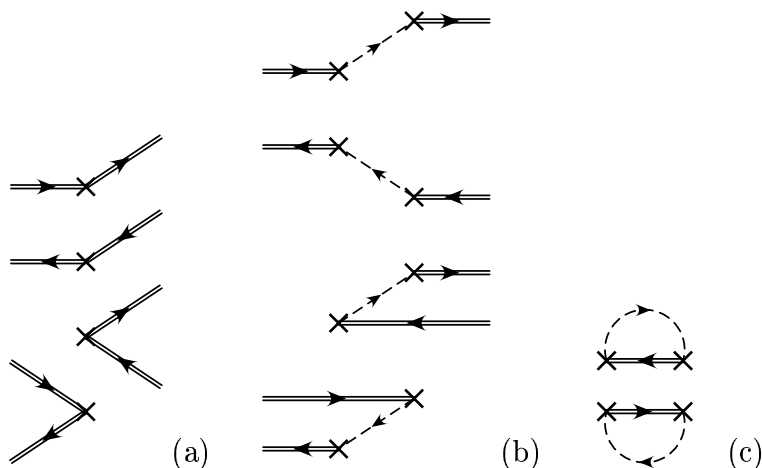


Figure 2.8: Graphical illustration of the processes occurring in first (a) and second order Magnus theory (b and c). Dotted lines denote the propagator, where only the principal part is taken, double lines denote electrons or positrons, which are on-shell. Interaction with the external field is shown as a cross.

last two terms have no operators in them. They correspond to the lowest-order vacuum corrections. As they are only numbers, they commute with all other terms.

The use of the principal-part integrals in the second-order diagrams can be understood easily: Using only the principal part we drop those parts of the propagator, where the particle is on-shell. As these appear as higher-order processes of the first-order Magnus theory, they would be counted twice, and therefore have to be subtracted here.

The Magnus theory can be extended in principle to higher orders also. Here we will use the second order, as this is the lowest order needed in order to get pair creation in heavy-ion collisions.



# Chapter 3

## Calculations for impact parameter zero

We have seen that a calculation of the reduced one-pair creation probability can be used together with the Poisson distribution in order to get the real  $N$ -pair probabilities. Therefore in a first step we are going to calculate the probability in lowest order, which for this process is the second order, and which is identical to the reduced probability in this case. Restricting ourself to impact parameter  $b$  zero allows us to get an analytic form for the matrix element, which we will use to study some of the properties of the pair production at very small  $b$ . As we will see later, the result for  $b$  zero can also be used for small  $b$ , which are of the order of the nuclear radius  $R$  of the heavy ions.

### 3.1 The matrix element in second order

The lowest order, where pair creation is possible, is the second order, as pair creation in first order is not allowed kinematically for “static” electromagnetic field (which the heavy ion fields are in their respective rest frames). Pair creation in second order due to two fast moving particles has been studied for the first time by Landau and Lifshitz [1], see also [2], and in the recent past by Bottcher and Strayer [11], but only total cross sections were calculated, no  $b$  dependent probabilities. The general second-order process is shown

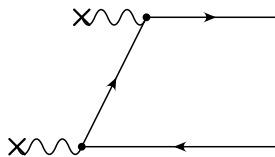


Figure 3.1: *General form of the second-order diagram for pair creation in an external field.*

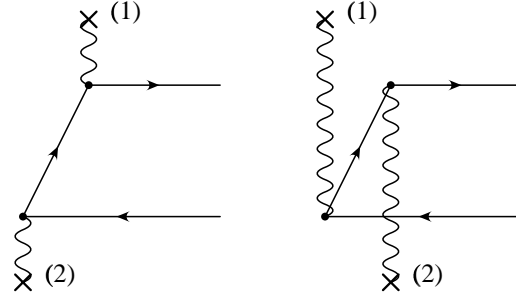


Figure 3.2: The two diagrams contributing to the pair creation in heavy-ion collisions, where (1) and (2) denotes the interaction with the field of ion 1 and 2, respectively.

in Figure 3.1. Its matrix element is

$$\begin{aligned}
 M &= -ie^2 \bar{u}(p_-) \int \frac{d^4 p}{(2\pi)^4} \mathcal{A}(p_- - p) \frac{\not{p} + m}{p^2 - m^2} \mathcal{A}(p_+ + p) v(p_+) \\
 &=: \bar{u}(p_-) \hat{M} v(p_+).
 \end{aligned} \tag{3.1}$$

Here we have introduced the matrix element without Dirac spinors  $\hat{M}$ . From this the unpolarised differential probability to produce an electron with momentum  $p_-$  and a positron with  $p_+$  is given by

$$\begin{aligned}
 P(p_-, p_+) &= \sum_{s_+ s_-} |M|^2 \frac{d^3 p_+ d^3 p_-}{4\epsilon_+ \epsilon_- (2\pi)^6} \\
 &= \text{Tr} \left[ (\not{p}_- + m) \hat{M} (\not{p}_+ - m) \overline{\hat{M}} \right] \frac{d^3 p_+ d^3 p_-}{4\epsilon_+ \epsilon_- (2\pi)^6},
 \end{aligned} \tag{3.2}$$

using the standard method to rewrite the polarisation summation as a trace.

Using the electromagnetic field of Eq. (1.13) there are four possible combinations of the two ions in  $\hat{M}$ , but only two of them are allowed kinematically (see Figure 3.2). Therefore we have

$$\begin{aligned}
 \hat{M} &= -ie^2 \left[ \int \frac{d^4 p}{(2\pi)^4} \mathcal{A}^{(1)}(p_- - p) \frac{\not{p} + m}{p^2 - m^2} \mathcal{A}^{(2)}(p_+ + p) \right. \\
 &\quad \left. + \int \frac{d^4 p}{(2\pi)^4} \mathcal{A}^{(2)}(p_- - p) \frac{\not{p} + m}{p^2 - m^2} \mathcal{A}^{(1)}(p_+ + p) \right] \\
 &= -i \left( \frac{Ze^2}{2\pi} \right)^2 \left[ \not{p}^{(1)} \int d^4 p \frac{\not{p} + m}{(p_- - p)^2 (p^2 - m^2) (p_+ + p)^2} \not{p}^{(2)} \right. \\
 &\quad \times \delta((p_- - p)u^{(1)}) \delta((p_+ + p)u^{(2)}) \exp(-ipb) \exp(i(p_- - p_+)b/2) \\
 &\quad \left. + \not{p}^{(2)} \int d^4 p \frac{\not{p} + m}{(p_- - p)^2 (p^2 - m^2) (p_+ + p)^2} \not{p}^{(1)} \right]
 \end{aligned}$$

$$\times \delta \left( (p_- - p) u^{(2)} \right) \delta \left( (p_+ + p) u^{(1)} \right) \exp(+ipb) \exp(-i(p_- - p_+)b/2) \Big]. \quad (3.3)$$

We now restrict ourself to the case where the impact parameter  $b$  is zero. In  $\hat{M}$   $b$  only occurs in the exponential. As we will see later, this calculation for  $b$  zero is also a good approximation for small  $b$  as long as the impact parameter is not much larger than  $2R$ , where  $R$  is the nuclear radius. This can be understood already here, as we see that  $b$  is multiplied by some momentum  $p_\perp$ . As one knows that mainly small  $p_\perp$  contribute to the total probability, smaller than  $\Lambda$  (of the form factor) and also mainly smaller than  $m_e$ , the case  $b = 0$  can be seen as the first term of an expansion in  $p_\perp b$  and should be good therefore, as long as  $b$  is of the order of the nuclear radius, and should not be too different for  $b$  smaller than the Compton wavelength:  $b < \lambda_c = 1/m_e$ .  $\hat{M}$  for  $b = 0$  is then

$$\begin{aligned} \hat{M} = & -i \left( \frac{Ze^2}{2\pi} \right)^2 \\ & \times \left[ \not{p}^{(1)} \int d^4p \frac{\not{p} + m}{(p_- - p)^2 (p^2 - m^2) (p_+ + p)^2} \not{p}^{(2)} \delta \left( (p_- - p) u^{(1)} \right) \delta \left( (p_+ + p) u^{(2)} \right) \right. \\ & \left. + \not{p}^{(2)} \int d^4p \frac{\not{p} + m}{(p_- - p)^2 (p^2 - m^2) (p_+ + p)^2} \not{p}^{(1)} \delta \left( (p_- - p) u^{(2)} \right) \delta \left( (p_+ + p) u^{(1)} \right) \right]. \end{aligned} \quad (3.4)$$

## 3.2 Analytic calculation of the matrix element

In order to find an analytical form for the matrix element we have to integrate over the internal momentum. First we define

$$\begin{aligned} I_D^{(m,i)} & := \int d^4p \frac{\{m, p_i\}}{(p_- - p)^2 (p^2 - m^2) (p_+ + p)^2} \\ & \times \delta \left( (p_- - p) u^{(1)} \right) \delta \left( (p_+ + p) u^{(2)} \right), \end{aligned} \quad (3.5a)$$

$$\begin{aligned} I_X^{(m,i)} & := \int d^4p \frac{\{m, p_i\}}{(p_- - p)^2 (p^2 - m^2) (p_+ + p)^2} \\ & \times \delta \left( (p_- - p) u^{(2)} \right) \delta \left( (p_+ + p) u^{(1)} \right), \end{aligned} \quad (3.5b)$$

which are the integrals occurring in the “direct” and “exchanged” diagram giving for  $\hat{M}$

$$\hat{M} = -i \left[ \frac{Ze^2}{2\pi} \right]^2 \left[ \not{p}^{(1)} \left( I_D^{(i)} + I_D^{(m)} \right) \not{p}^{(2)} + \not{p}^{(2)} \left( I_X^{(i)} + I_X^{(m)} \right) \not{p}^{(1)} \right]. \quad (3.6)$$

Now we use the two  $\delta$  functions to reduce the four-dimensional integration. The four-velocities  $u^{(1)}$  and  $u^{(2)}$  in the CM system are

$$u^{(1)} = \gamma(1, 0, 0, \beta) =: \gamma w^{(1)}, \quad (3.7a)$$

$$u^{(2)} = \gamma(1, 0, 0, -\beta) =: \gamma w^{(2)}. \quad (3.7b)$$

Evaluating them determines the zero and  $z$  component of the internal momentum. In the case “D” they are

$$\epsilon = \epsilon_D := \frac{1}{2}(\epsilon_- - \epsilon_+) - \frac{1}{2}\beta(p_{-z} + p_{+z}), \quad (3.8a)$$

$$p_z = p_D := \frac{1}{2}(p_{-z} - p_{+z}) - \frac{1}{2\beta}(\epsilon_- + \epsilon_+), \quad (3.8b)$$

and in the case “X”:

$$\epsilon = \epsilon_X := \frac{1}{2}(\epsilon_- - \epsilon_+) + \frac{1}{2}\beta(p_{-z} + p_{+z}), \quad (3.9a)$$

$$p_z = p_X := \frac{1}{2}(p_{-z} - p_{+z}) + \frac{1}{2\beta}(\epsilon_- + \epsilon_+). \quad (3.9b)$$

The only difference between both formulae is the sign between the two terms, which comes from the exchange of  $\beta \leftrightarrow -\beta$  in the four-velocities.

We split now  $p$  into its longitudinal and transverse part defining

$$p_{Dl} := (\epsilon_D, 0, 0, p_D), \quad p_{Xl} := (\epsilon_X, 0, 0, p_X), \quad (3.10)$$

and the same with  $p_-$  and  $p_+$ . The integral  $I_D^{(m,i)}$  is now

$$\begin{aligned} I_D^{(m,i)} &= \frac{1}{2\gamma^2\beta} \int d^2 p_\perp \\ &\times \frac{\{m, p_i\}}{[(p_{-l} - p_{Dl})^2 + (p_{-\perp} - p_\perp)^2] [p_{Dl}^2 + p_\perp^2 - m^2] [(p_{+l} + p_{Dl})^2 + (p_{+\perp} + p_\perp)^2]}, \end{aligned} \quad (3.11)$$

and similar for  $I_X^{(m,i)}$  changing  $p_{Dl}$  to  $p_{Xl}$ . Note that  $p_\perp$  only has spatial components; evaluating the scalar products gives then an extra minus sign. The factor  $\frac{1}{2\gamma^2\beta}$  comes from the evaluation of the  $\delta$  functions.

Examining  $I_D$  and  $I_X$  for  $m, 0$ , and  $z$  we find that the numerator of the integrand does not depend on  $p_\perp$  and therefore we can rewrite them as

$$\begin{aligned} I_D^{(m,0,z)} &= \frac{1}{2\gamma^2\beta} \{m, \epsilon_D, p_D\} \int d^2 p_\perp \\ &\times \frac{1}{[(p_{-l} - p_{Dl})^2 + (p_{-\perp} - p_\perp)^2] [p_{Dl}^2 + p_\perp^2 - m^2] [(p_{+l} + p_{Dl})^2 + (p_{+\perp} + p_\perp)^2]} \end{aligned} \quad (3.12)$$

and the corresponding result for  $I_X^{(m,0,z)}$ . As we show in App. A.5, the integral on the right side is just one of the standard integrals, the scalar three-term integral. Therefore we can



write

$$\begin{aligned} I_D^{(m,0,z)} &= -\frac{1}{2\gamma^2\beta} \{m, \epsilon_D, p_D\} I_3^S(k_{1D}, k_{2D}, m_{0D}^2, m_{1D}^2, m_{2D}^2) \\ &=: -\frac{1}{2\gamma^2\beta} \{m, \epsilon_D, p_D\} I_D^S \end{aligned} \quad (3.13)$$

with

$$\begin{aligned} k_{1D} &= -p_{-\perp}, \\ k_{2D} &= p_{+\perp}, \\ m_{0D}^2 &= m^2 - p_{Dl}^2, \\ m_{1D}^2 &= -(p_{Dl} - p_{-l})^2, \\ m_{2D}^2 &= -(p_{Dl} + p_{+l})^2, \end{aligned} \quad (3.14)$$

and the same for  $I_X^{(m,0,z)}$  by changing the index to “X”.

On the other hand for  $x$  and  $y$  the numerator depends on  $p_{\perp}$ , over which we have to integrate. This integral is the simplest type of a so-called tensor integral, and it is clear that it can be split into two parts:

$$I_D^{(x,y)} = -\frac{1}{2\gamma^2\beta} \left( -p_{-\perp} I_D^1 + p_{+\perp} I_D^2 \right) \quad (3.15)$$

and the corresponding result for  $I_X^{(x,y)}$ .  $I_D^1$  and  $I_D^2$  are again standard Feynman integrals found in App. A.5:

$$I_D^{(1,2)} = I_3^{(1,2)}(k_{1D}, k_{2D}, m_{0D}^2, m_{1D}^2, m_{2D}^2) \quad (3.16)$$

and the corresponding result for  $I_X^{(1,2)}$ .

We finally get

$$\begin{aligned} \hat{M} &= i \frac{2(Z\alpha)^2}{\beta} \left[ \psi^{(1)} (\not{p}_{Dl} + m) \psi^{(2)} I_D^S - \psi^{(1)} \not{p}_{-\perp} \psi^{(2)} I_D^1 + \psi^{(1)} \not{p}_{+\perp} \psi^{(2)} I_D^2 \right. \\ &\quad \left. + \psi^{(2)} (\not{p}_{Xl} + m) \psi^{(1)} I_X^S - \psi^{(2)} \not{p}_{-\perp} \psi^{(1)} I_X^1 + \psi^{(2)} \not{p}_{+\perp} \psi^{(1)} I_X^2 \right]. \end{aligned} \quad (3.17)$$

An alternative form for  $\hat{M}$  can be found by using the properties of the Dirac spinors

$$(\not{p}_+ + m)v(p_+) = 0, \quad (3.18a)$$

$$\bar{u}(p_-)(\not{p}_- - m) = 0. \quad (3.18b)$$

Rewriting them as

$$\not{p}_{+\perp} v(p_+) = -(\not{p}_{+l} + m)v(p_+), \quad (3.19a)$$

$$\bar{u}(p_-) \not{p}_{-\perp} = -\bar{u}(p_-)(\not{p}_{-l} - m), \quad (3.19b)$$

we get

$$\begin{aligned}
\hat{M} = & i \frac{2(Z\alpha)^2}{\beta} \left[ \psi^{(1)}(\not{p}_{Dl} + m) \psi^{(2)} I_D^S \right. \\
& - (\not{p}_{-l} - m) \psi^{(1)} \psi^{(2)} I_D^1 + \psi^{(1)} \psi^{(2)} (\not{p}_{+l} + m) I_D^2 \\
& + \psi^{(2)}(\not{p}_{Xl} + m) \psi^{(1)} I_X^S - (\not{p}_{-l} - m) \psi^{(2)} \psi^{(1)} I_X^1 \\
& \left. + \psi^{(2)} \psi^{(1)} (\not{p}_{+l} + m) I_X^2 \right]. \tag{3.20}
\end{aligned}$$

This form for  $\hat{M}$  has been used to test the correctness of our calculations, as well as its numerical stability.

Let us now come back to the inclusion of the form factor  $F(q^2)$ . It is easy to see that this only changes the form of  $I_D$  to

$$\begin{aligned}
I_D^{(m,i)} = & \frac{1}{2\gamma^2\beta} \int d^2 p_\perp \{m, p_i\} \\
& \times \frac{F((p_- - p)^2) F((p_+ + p)^2)}{(p_- - p)^2 (p^2 - m^2) (p_+ + p)^2} \Big|_{p_l = p_{Dl}} \tag{3.21}
\end{aligned}$$

and similar for  $I_X$  using  $p_{Xl}$  instead of  $p_{Dl}$ .

Here we can use the property of the dipole form factor

$$\frac{F(q^2)}{q^2} = \frac{\Lambda^2}{(\Lambda^2 - q^2)q^2} = \frac{1}{q^2} + \frac{1}{\Lambda^2 - q^2}, \tag{3.22}$$

which allows us to rewrite the integrals as the sum and difference of four integrals of the type, which we have already solved in terms of the elementary Feynman integrals. The scalar and tensor integrals corresponding to (3.13) and (3.16) are

$$\begin{aligned}
I_D^{(S,1,2)} = & I_3^{(S,1,2)}(k_{1D}, k_{2D}, m_{0D}^2, m_{1D}^2, m_{2D}^2) \\
& - I_3^{(S,1,2)}(k_{1D}, k_{2D}, m_{0D}^2, m_{1D}^2 + \Lambda^2, m_{2D}^2) \\
& - I_3^{(S,1,2)}(k_{1D}, k_{2D}, m_{0D}^2, m_{1D}^2, m_{2D}^2 + \Lambda^2) \\
& + I_3^{(S,1,2)}(k_{1D}, k_{2D}, m_{0D}^2, m_{1D}^2 + \Lambda^2, m_{2D}^2 + \Lambda^2), \tag{3.23}
\end{aligned}$$

which we use in formula (3.17) and (3.20) for  $\hat{M}$ .

The same can be done with the double dipole form factor (see also App. A.6)

$$\frac{F(q^2)}{q^2} = \frac{1}{q^2} + c_1 \frac{1}{\Lambda_1^2 - q^2} + c_2 \frac{1}{\Lambda_2^2 - q^2} \tag{3.24}$$

giving a sum total of nine standard Feynman integrals.

$\hat{M}$  is used now in order to calculate the trace  $\text{Tr} \left[ (\not{p}_- + m) \hat{M} (\not{p}_+ - m) \overline{\hat{M}} \right]$ . For this tedious, but straightforward, calculation we have used a symbolic calculation program (FORM [62]).

Some care has been taken in evaluating these long expressions numerically in order to avoid some of the large cancellations, which normally occur in the scalar products. That these cancellations do occur can be shown, e.g., in  $m_{1D}^2$ , where they can be seen very easily:

$$\begin{aligned} m_{1D}^2 &= -(p_{Dl} - p_{-l})^2 = (p_D - p_{-z})^2 - (\epsilon_D - \epsilon_-)^2 \\ &= \frac{1}{4} \frac{1}{\gamma^2 \beta^2} [(\epsilon_- + \epsilon_+) + \beta(p_{-z} + p_{+z})]^2. \end{aligned} \quad (3.25)$$

Here we have used the fact that  $1 - \beta^2 = \gamma^{-2}$ . We see that for large values of  $\gamma$ ,  $m_{1D}^2$  becomes very small, which means that the cancellations in the first expressions are very large.

To avoid these cancellations in the scalar products we did not use the longitudinal parts of the four-vectors directly, but transformed them into light-cone variables. The longitudinal vectors, we have, are  $w^{(1)}$ ,  $w^{(2)}$ ,  $p_{+l}$ ,  $p_{-l}$ ,  $p_{lD}$ , and  $p_{lX}$ , transverse vectors only  $p_{+\perp}$ ,  $p_{-\perp}$ .

For the light cone variables we define a '+' and a '-' component of an arbitrary vector  $v$ :

$$v_{+'} = v_0 + v_z, \quad v_{-'} = v_0 - v_z. \quad (3.26)$$

The scalar product between longitudinal vectors is then

$$(v, w) = \frac{1}{2}(v_{+'} w_{-'} + v_{-'} w_{+'}) \quad (3.27a)$$

$$(v, v) = v_{+'} v_{-'} \quad (3.27b)$$

Generally one of the variables '+', '-' is small, the other large. For example,  $w_{+'}^{(1)} = 1 + \beta$  is large, and  $w_{-'}^{(1)} = 1 - \beta$  is very small, because  $\beta$  is close to one. We calculate it using

$$w_{-'}^{(1)} = 1 - \beta = \frac{(1 - \beta)(1 + \beta)}{(1 + \beta)} = \frac{1}{\gamma^2 w_{+'}^{(1)}}. \quad (3.28)$$

The same can be done with the other vectors, e.g., if  $p_{+z}$ ,  $p_{-z} > 0$ , we calculate  $p_{+',+}$  and  $p_{-',+}$  directly and the other as

$$p_{+',-} = \frac{\epsilon_+^2 - p_{+z}^2}{\epsilon_+ + p_{+z}} = \frac{m^2 + p_{+\perp}^2}{p_{+',+}}, \quad (3.29a)$$

$$p_{-',-} = \frac{\epsilon_-^2 - p_{-z}^2}{\epsilon_- + p_{-z}} = \frac{m^2 + p_{-\perp}^2}{p_{-',+}}. \quad (3.29b)$$

### 3.3 Pair production in DEPA

As described in the introduction the equivalent photon approximation (EPA) or Weizsäcker-Williams method has been used in the past to calculate electromagnetic processes in heavy-ion collisions. It consists of replacing the electromagnetic field of the fast moving ion by a spectrum of real photons. Then one folds the photo cross section with the number of equivalent photons  $N(\omega)$  to get the cross section for the heavy-ion process. In the double equivalent photon approximation (DEPA) one replaces the field of both ions by equivalent photons, then folds with both photon distributions. Normally one uses the total equivalent photon number, the one integrated over all impact parameters [9, 16]. Recently also the  $b$  dependent DEPA has been investigated by Baur and Ferreira Filho [63, 64] and also by Vidović et al. [42]. For an overview of different aspects of the DEPA see also [41]. One of the problems of the DEPA is that, because the virtual photons with  $q^2 \neq 0$  are all replaced by real photons, we have to introduce a cutoff in  $q^2$  to avoid the logarithmic divergence, even though the main contribution comes from that part where  $q^2$  is small. The cutoff can also be interpreted as a cutoff in the impact parameter (in the case of the EPA, where only one ion is replaced by the photon spectrum), or a cutoff in the distance between the ion and the place, where the interaction with the electron or positron takes place. Also contributions coming from scalar photons are neglected. There has been some discussion about the choice of the cutoff. On the one hand the form factor of the ion decreases the number of photons with large  $q^2$ ; on the other hand the matrix element decreases, if the momentum of the internal electron line  $|p|$  is greater than  $m_e$ ; therefore we are not allowed to replace this matrix element with the one for the photo process (see, e.g., the discussion in Section 6 in [9]).

The DEPA gives us, on the one hand, an independent check for the correctness of our results and, on the other hand, a test of the applicability of DEPA in this case, especially to see, if the cutoff is given by the form factor.

For our calculation we use the formula given by Baur and Ferreira Filho [63, 41]. For  $b = 0$  their result is

$$dP(b = 0) = \frac{d\omega_1}{\omega_1} \frac{d\omega_2}{\omega_2} \int d^2\rho N(\omega_1, \rho) N(\omega_2, \rho) \sigma_{\parallel}(\omega_1, \omega_2), \quad (3.30)$$

where  $\sigma_{\parallel}$  is the total cross section for pair production with the two photons with parallel polarisation.  $N(\omega, \rho)$  is the  $\rho$ -dependent equivalent photon number. In the ultrarelativistic limit it is given by

$$N(\omega, \rho) = \frac{Z^2 \alpha}{\pi^2} \frac{\phi(x, \rho)}{\rho^2} \quad (3.31)$$

with  $x := \frac{\omega \rho}{\gamma c}$  and

$$\phi(x, \rho) = \left| \int_0^\infty du u^2 J_1(u) \frac{F\left(-\frac{x^2 + u^2}{\rho^2}\right)}{x^2 + u^2} \right|^2. \quad (3.32)$$

With a dipole form factor (Eq. (1.11)) we are splitting again  $F[-(x^2 + u^2)/\rho^2]/(x^2 + u^2)$

into two parts:

$$\frac{\rho^2 \Lambda^2}{\rho^2 \Lambda^2 + x^2 + u^2} \frac{1}{x^2 + u^2} = \frac{1}{x^2 + u^2} - \frac{1}{\rho^2 \Lambda^2 + x^2 + u^2}, \quad (3.33)$$

rewriting  $\phi$  as

$$\phi(x, \rho) = \left| \int_0^\infty du u^2 J_1(u) \left( \frac{1}{x^2 + u^2} - \frac{1}{\rho^2 \Lambda^2 + x^2 + u^2} \right) \right|^2. \quad (3.34)$$

The integral

$$\int_0^\infty du u^2 J_1(u) \frac{1}{z^2 + u^2} = z K_1(z) \quad (3.35)$$

can be solved analytically giving for  $\phi$  the result for a point source, which is known. Therefore  $\phi(x, \rho)$  is given by

$$\phi(x, \rho) = \left| x K_1(x) - \sqrt{\rho^2 \Lambda^2 + x^2} K_1(\sqrt{\rho^2 \Lambda^2 + x^2}) \right|^2, \quad (3.36)$$

and using the definition of  $x$  we find

$$N(\omega, \rho) = \frac{Z^2 \alpha^2}{\pi^2} \left| \frac{\omega}{\gamma} K_1\left(\frac{\omega}{\gamma} \rho\right) - \left[ \frac{\omega^2}{\gamma^2} + \Lambda^2 \right]^{1/2} K_1\left( \left[ \frac{\omega^2}{\gamma^2} + \Lambda^2 \right]^{1/2} \rho \right) \right|^2. \quad (3.37)$$

The cross section for real photons is [9]

$$\sigma_{\parallel} = \frac{4\pi\alpha^2}{s} \left[ \left( 1 + \frac{4m^2}{s} - \frac{12m^4}{s^2} \right) L - \left( \frac{1}{s} + \frac{6m^2}{s^2} \right) \Delta t \right] \quad (3.38)$$

with

$$\begin{aligned} s &= 4\omega_1\omega_2, \\ \Delta t &= s \left[ 1 - \frac{4m^2}{s} \right]^{1/2}, \\ L &= 2 \ln \left( \frac{\sqrt{s}}{2m} + \left[ \frac{s}{4m^2} - 1 \right]^{1/2} \right). \end{aligned} \quad (3.39)$$

For the total probability we integrate over  $d\omega_1$ ,  $d\omega_2$ , and  $d^2\rho$  using a Monte Carlo (MC) integration routine (VEGAS [65, 66]). The integration variables, we use, are  $\ln \rho$ ,  $\ln \omega_2$ , and  $\ln s$  and the boundaries of the integral have been increased until the result does not change. The accuracy of the MC-integrals is always 1% or better.

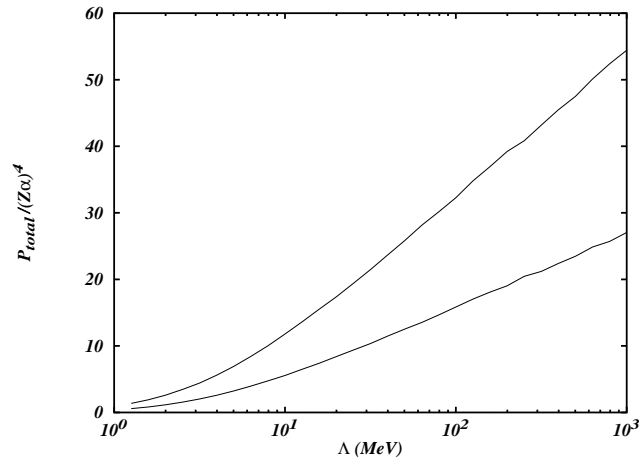


Figure 3.3:  $P_{\text{total}}/(Z\alpha)^4$  for  $b = 0$  as a function of  $\Lambda$  for  $\gamma = 100$  (lower curve) and 3400 (upper curve). The logarithmic increase shows that a form factor is needed, as the result for a point charge seems to diverge.

### 3.4 The total probability $P_{\text{total}}$

The differential probability is now integrated over all six momentum variables. For this we used again the Monte-Carlo integration routine (VEGAS[65, 66]). The integration over one of the angles is trivial, and an integration over five variables remains to be done, for which we used  $t_z$ ,  $t_\perp$ ,  $\phi$ ,  $\eta$ , and  $\chi$ . The momenta of electron and positron expressed in these variables are:

$$\begin{aligned}
 p_{+z} &= [\exp(t_z) - 1] \cos \eta, \\
 p_{-z} &= [\exp(t_z) - 1] \sin \eta, \\
 p_{+\perp} &= [\exp(t_\perp) - 1] \cos \chi(1, 0), \\
 p_{-\perp} &= [\exp(t_\perp) - 1] \sin \chi(\cos \phi, \sin \phi).
 \end{aligned} \tag{3.40}$$

The integration boundaries in  $t_z$  and  $t_\perp$  were incremented, until the MC integral converges. A good estimate for the boundaries is given by  $\ln[\gamma \max(\Lambda, m_e) + 1]$  for  $t_z$  and by  $\ln[\max(\Lambda, m_e) + 1]$  for  $t_\perp$ . The accuracy of the MC integrals was again 1% or better.  $\Lambda$  was chosen according to App. A.6 as  $\Lambda = 83$  MeV for the dipole form factor and similarly for the double dipole form factor. In this section we will only discuss the probability divided by  $(Z\alpha)^4$ , as this is a common factor in our formula.

Figure 3.3 shows the dependence of the total probability on  $\Lambda$  for two different values of  $\gamma$  (100 and 3400). We see that there is a logarithmic dependence on  $\Lambda$ , so that the result seems to be divergent for a point charge. This divergence is, of course, no contradiction to the fact that the total cross section for a point charge

$$\sigma = \int 2\pi b db P(b) \tag{3.41}$$

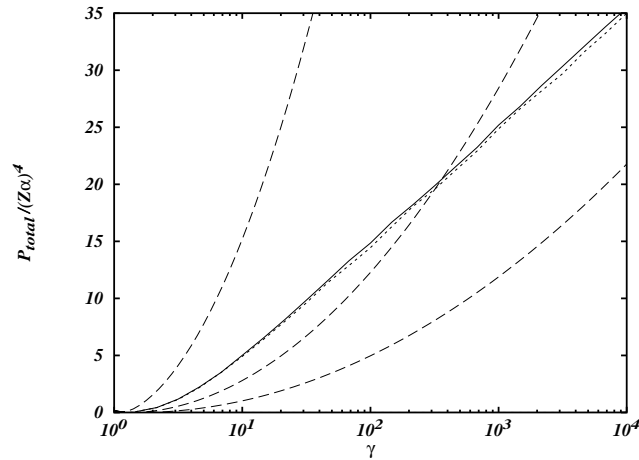


Figure 3.4:  $P_{\text{total}}/(Z\alpha)^4$  for  $b = 0$  as a function of  $\gamma$  for the creation of an electron-positron pair. The solid line is the calculation for a realistic dipole form factor, the dotted line for a realistic double dipole form factor (see App. A.6). The dashed lines are EPA results for impact parameters  $b = 0.5 \lambda_c$ ,  $b = 1.0 \lambda_c$  and  $b = 1.5 \lambda_c$  (from left to right), respectively.

is finite.

Figure 3.4 shows  $P_{\text{total}}/(Z\alpha)^4$  as a function of  $\gamma$ . We use the dipole form factor as well as the double dipole form factor. The difference between both is very small. This confirms our assumption that the detailed form of the form factor is not important, as only small  $q^2$  contribute considerably to the total probability. Together with our calculation we plot also the results of the EPA calculation for different values of the impact parameter  $b$  (Eq. 7.3.10 in [16], where we have neglected the term with  $\bar{f}$ ). One sees that our calculation for  $b = 0$  only increases linearly with  $\ln \gamma$ , whereas the EPA result increases with  $(\ln \gamma)^2$ . Even for  $b \approx \lambda_c$  the EPA result is larger than our result for  $b = 0$ . As the probability should increase with smaller impact parameter, we conclude that the EPA result cannot be used for small impact parameter and that the range, where it is not applicable, even increases slowly for larger values of  $\gamma$ . This result is, of course, well known, therefore Equation 7.3.10 has always been used for impact parameter  $b > \lambda_c$  only.

Also we note that the reduced total probabilities are not very large. Values smaller than 35 have to be multiplied by  $(Z\alpha)^4 < 0.2$ . Therefore the reduced total probability is smaller than seven for realistic parameters, which means that the average number of pairs produced in one collision is less than seven.

Figure 3.5 shows again the total probability, but now together with those for  $\mu$  and  $\tau$  pairs. Their probabilities are much smaller because of the larger mass of the  $\mu$  and the  $\tau$ . Also shown are the results of the DEPA calculation for the heavy ions. As their masses are much larger than  $\Lambda$ , the DEPA is in good agreement with the exact calculation. The deviation at small  $\gamma$  is due to the fact that the DEPA can only be used for relativistic collisions.

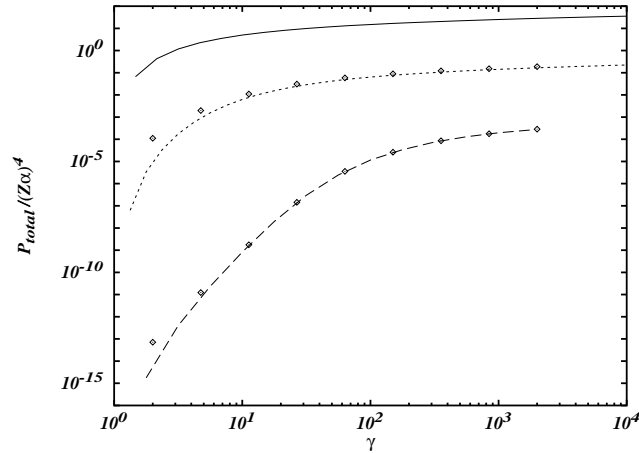


Figure 3.5:  $P_{\text{total}}/(Z\alpha)^4$  for  $b = 0$  as a function of  $\gamma$  for the creation of an electron- (solid),  $\mu^-$  (dotted), and  $\tau$ -pair (dashed). Results of the calculation with a dipole form factor. Also shown are the results of the DEPA calculation for  $\mu^-$  and  $\tau$ -pairs (diamonds), also for a dipole form factor.

	$\gamma$	Ion	$P_{\text{total}}$
AGS	2.35	Au	0.06
CERN SPS	10	Pb	0.63
RHIC	100	Au	1.6
LHC	3400	Pb	3.9

Table 3.1: Predicted values of the reduced probability  $P_{\text{total}}$  for different accelerator parameters.

Finally in Table 3.1 we give our predictions for the total reduced probability for the electron-positron pair production for some heavy-ion accelerators. Using the approximate Poisson distribution we get the real  $N$ -pair production probabilities as shown in Fig. 3.6.

We compare now our calculations with the DEPA result. In Fig. 3.7 we compare both at RHIC-energies ( $\gamma = 100$ ). One sees that DEPA is in good agreement with our calculations, as long as  $\Lambda$  is smaller than  $m_e$ . For larger values the DEPA gets too large and overestimates our results by order of magnitude for realistic  $\Lambda$ 's. Therefore the reduction in  $q^2$  due to the form factors does not suffice, the decrease of the matrix element of the process itself as soon as the internal momentum of the fermion gets larger than  $m_e$  is more important. But even then this decrease alone does not suffice, as the total probability still depends on the form factor.

A more detailed picture is shown on Figure 3.8, where each of the ions now has its own form factor independent of the other, in order to study the influence of the individual



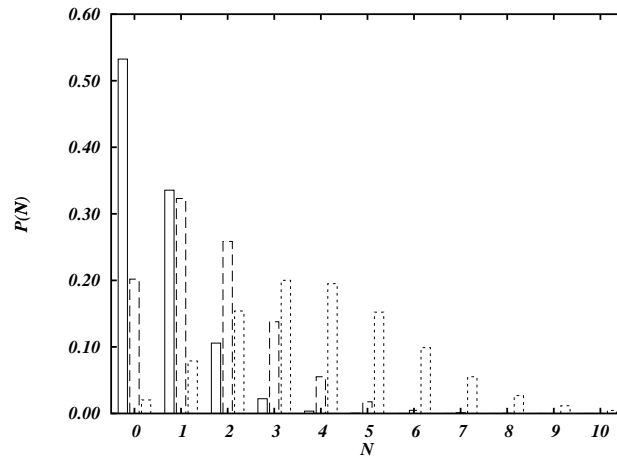


Figure 3.6: Total probabilities for the  $N$ -pair creation based on the Poisson distribution. Solid bars are the results for  $\gamma = 10$  and Pb ions, dashed bars for  $\gamma = 100$  and Au ions, and dotted bars for  $\gamma = 3400$  and Pb ions.

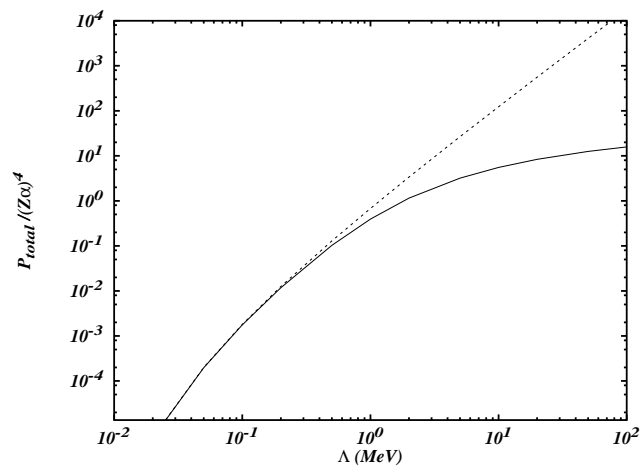


Figure 3.7: A comparison of our calculation (solid) and DEPA (dotted) for  $\gamma = 100$  as a function of the parameter  $\Lambda$  controlling the form factor of the ions.

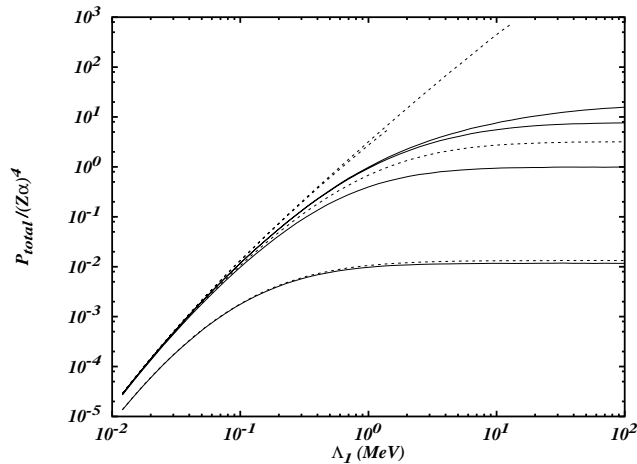


Figure 3.8: A comparison of our calculation (solid) and DEPA (dotted) for  $\gamma = 100$  as a function of  $\Lambda_1$  of one ion.  $\Lambda_2$  of the other ion has been kept fixed at  $\Lambda_2 = 0.1, 1, 10,$  and  $100$  MeV (from bottom to top).

form factor on the total probability. We show  $P_{\text{total}}$  as a function of  $\Lambda_1$ , the parameter controlling the width of one dipole form factor,  $\Lambda_2$  for the other ion has been kept fixed. Here we see again that DEPA massively overestimates the Born calculation, as soon as one, and even more if both  $\Lambda$ 's are larger than the electron mass. We see also that the probability becomes independent of  $\Lambda_1$ , if it is much larger than  $m_e$  and  $\Lambda_2$ . This shows that the production of a pair by a real photon in the field of a nucleus is independent of the size of the nucleus, if the size is much smaller than the Compton wavelength.

### 3.5 The single-differential probabilities

Besides the total probability we have also calculated some of the single-differential probabilities. For this we have used the fact that with a MC integration single-differential distributions can be calculated very easily sorting the individual integration points into bins. Therefore one run of the program can be used to calculate several differential probabilities at once. A disadvantage of this method is that a large number of sample points is needed, if we want to get some accuracy, because the result spans several order of magnitude. Again, as in the previous case, a common factor  $(Z\alpha)^4$  has been extracted from  $P$ .

All calculations were done for CERN SPS, RHIC, and LHC energies, that is, for  $\gamma = 10, 100, 3400$  using both the simple dipole and the double dipole form factor. Generally our results show some difference for the two form factors, but only a very small one, so that our results should represent the real situation well.

Figure 3.9 shows the dependence on the energy of the positron (as the result is symmet-

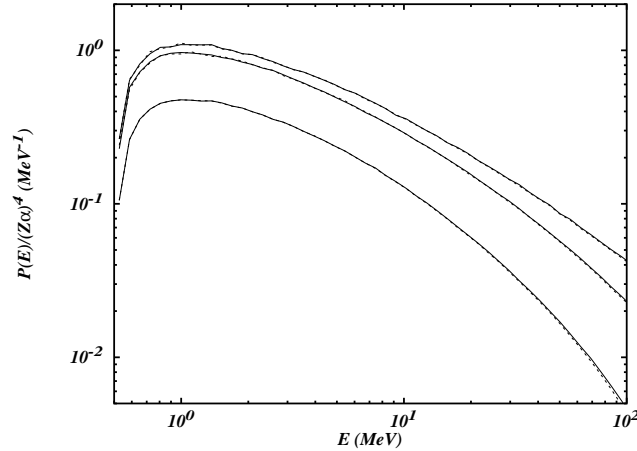


Figure 3.9:  $P(E)/(Z\alpha)^4$  as a function of the energy of the positron. Results for  $\gamma = 10, 100, 3400$  (from bottom to top) are shown; solid lines are the results using the realistic dipole form factor, dotted lines using the realistic double dipole form factor.

ric with respect to electron and positron, this is the same for the electron). The probability has the characteristic peak at low energies and decreases slowly for higher energies.

Figure 3.10 shows the angular distribution, where  $\theta$  is the angle between the momentum  $p_+$  and the beam axis ( $z$  axis). For large values of  $\gamma$  the particles are produced mainly at very small angles.

We also study the distributions related to the total momentum  $P = p_+ + p_-$ . These are the invariant mass  $M = \sqrt{P^2}$ , the rapidity

$$Y = \frac{1}{2} \ln \left( \frac{P_0 + P_z}{P_0 - P_z} \right), \quad (3.42)$$

and the transverse momentum  $P_\perp$ . They are shown in Figures 3.11 ( $P(M)$ ), 3.12 ( $P(Y)$ ), and 3.13 ( $P(P_\perp)$ ). We show  $P(M)$  only for relatively small values of  $M$ . A discussion of the behavior of  $P(M)$  for large invariant mass can be found in the next section.

## 3.6 A comparison with DEPA for large invariant mass

Finally we want to discuss the case where the invariant mass of the two leptons is large. It has been argued that in this case the DEPA approximation, which failed at low invariant mass, should again be applicable. This is based on the assumption that in this case the only relevant momentum scale is the invariant mass, so that one may neglect effects coming from the electron mass.

Figure 3.14 shows a comparison of  $P(M)$  between the DEPA and our calculation. Even though the difference between both is not that bad for large invariant mass, DEPA is off by about a factor of two.

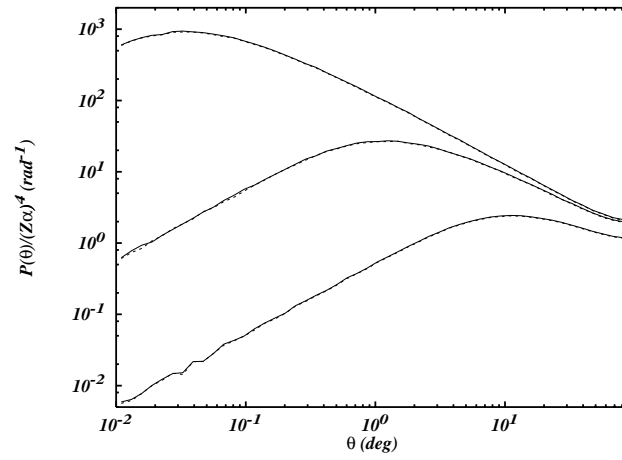


Figure 3.10:  $P(\theta)/(Z\alpha)^4$  as a function of the angle  $\theta$  of  $p_+$  with the z-axis.  $\gamma$  and form factors as in Fig. 3.9.

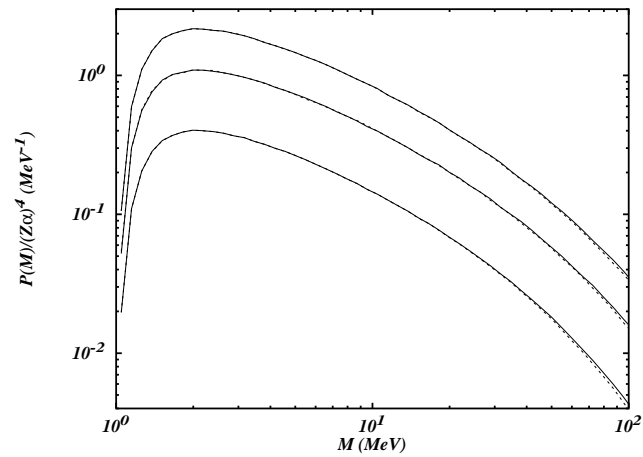


Figure 3.11:  $P(M)/(Z\alpha)^4$  as a function of the invariant mass  $M$  of the pair.  $\gamma$  and form factors as in Fig. 3.9.

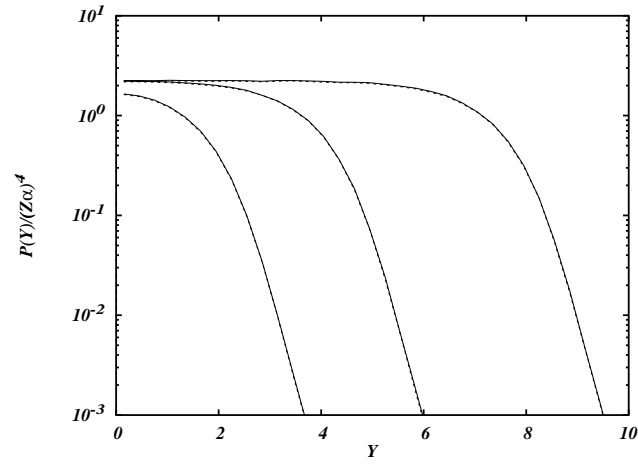


Figure 3.12:  $P(Y)/(Z\alpha)^4$  as a function of the rapidity  $Y$  of the pair.  $\gamma$  and form factors as in Fig. 3.9.

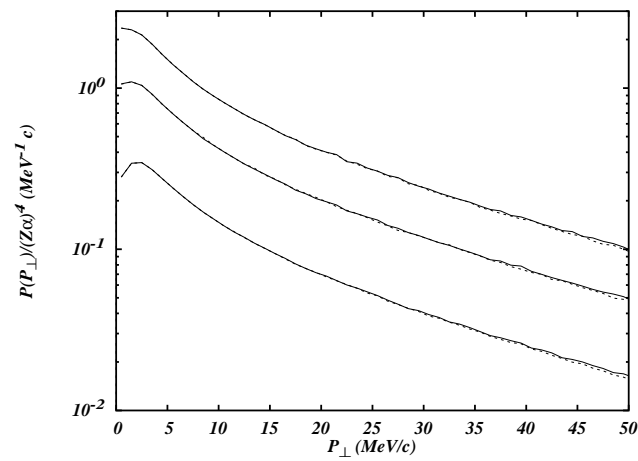


Figure 3.13:  $P(P_{\perp})/(Z\alpha)^4$  as a function of the transverse momentum  $P_{\perp}$  of the pair.  $\gamma$  and form factors as in Fig. 3.9.

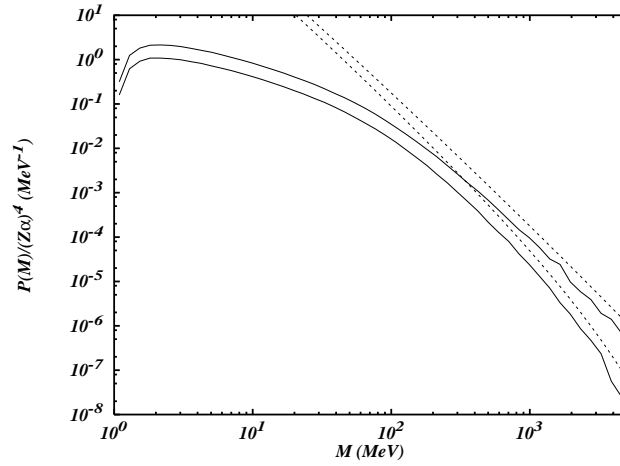


Figure 3.14:  $P(M)/(Z\alpha)^4$  is shown as a function of  $M$  for pairs with large invariant mass  $M$ . Comparison for  $\gamma = 100$  (lower curve) and 3400 (upper curve) of our calculation (solid line) with the DEPA (dotted line) using a realistic dipole form factor in both cases.

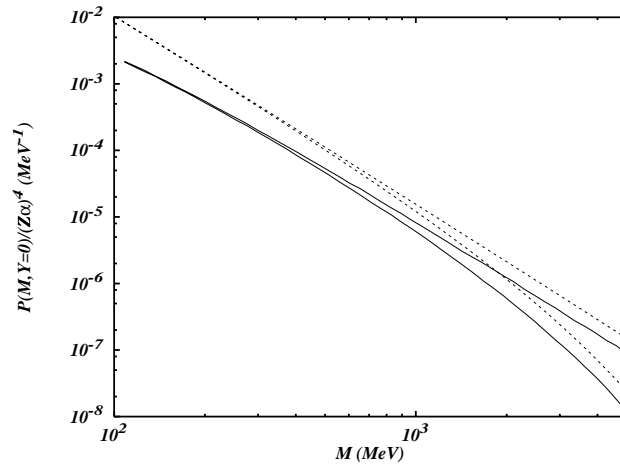


Figure 3.15:  $P(M, Y = 0)/(Z\alpha)^4$  as a function of  $M$ . Comparison for  $\gamma = 100$  (lower curve) and 3400 (upper curve) of our calculation (solid line) with the DEPA (dotted line). Results for a realistic double dipole form factor are shown.

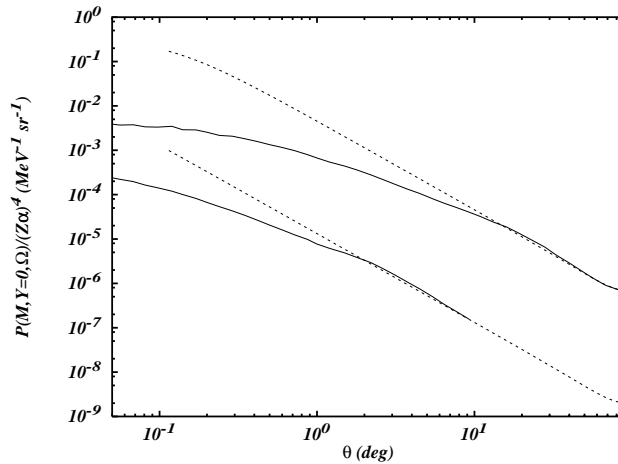


Figure 3.16:  $P(M, Y = 0, \Omega)/(Z\alpha)^4$  as a function of the angle  $\theta$  between  $p_+$  and the  $z$ -axis. Compared are the results of our calculation (solid line) and DEPA (dotted line).  $\gamma = 3400$ ,  $M = 500$  MeV (upper curve), 3500 MeV (lower curve). Results for a realistic double dipole form factor are shown.

The same can be seen in Figure 3.15, where we compare  $P(M, Y)$  for rapidity  $Y = 0$ .

For the calculation of  $P(M, Y = 0)$  we have used the fact that for  $Y = 0$  (which means that  $p_{+z} = -p_{-z}$ ) and with fixed  $M$   $p_{+z}$  and  $p_{-z}$  can be calculated as a function of the transverse momenta  $p_{+\perp}$  and  $p_{-\perp}$  together with their angle  $\phi$ . The remaining three-dimensional integration was done again with the MC integration routine with an error of 1%. For the DEPA calculation  $Y = 0$  and fixed  $M$  means that  $\omega_1$  and  $\omega_2$  are fixed at  $M/2$  and only the integration over  $\rho$  has to be done. As  $\sigma$  is a function of  $M$  alone, we can use formula (3.38) again; see also [67]. We see again that the result of DEPA is too large by a factor of two.

This seems to be in contradiction with the arguments given above. In order to see, where the discrepancy comes from, we calculated also  $P(M, Y, \Omega)$ . For the Born calculation we used again the sorting of  $P$  into bins. For the DEPA calculation the differential cross section for the photon-photon process [2] has been used; see also [68].

We show  $P(M, Y = 0, \Omega)$  in Fig. 3.16 as a function of  $\theta$ , the angle of  $p_+$  with the beam axis. For large angles the DEPA and our calculation agree quite well, but for small angles the DEPA calculation is too high. As one may object that this is an effect of the integration over the transverse momenta in the DEPA, which should smear out the angular distribution, we show in Fig. 3.17  $P(M, Y = 0, \Omega_\Delta)$  as a function of  $\theta_\Delta$ , the angle of  $(p_+ - p_-)$  with the beam axis. For the DEPA, in the form used by us, the two particles are produced with their momenta exactly opposite to each other, so the curve is identical with the previous one (see [67] for a better calculation, where the transverse momentum distribution has been included in the DEPA). But in our calculation we should be able to unfold with this approximately the transverse momentum distribution coming from the

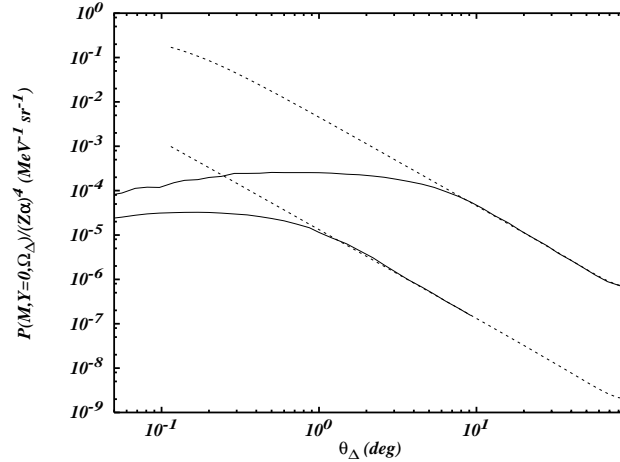


Figure 3.17: Same as Fig. 3.16, but now  $P(M, Y = 0, \Omega_\Delta)/(Z\alpha)^4$  as a function of the angle  $\theta_\Delta$  between  $(p_+ - p_-)$  and the z-axis.

virtual photons. Here again we find good agreement at large angles, but the DEPA is too large at small ones.

The reason for this can be explained as follows: The total cross section for the pair production in lowest order by a photon in the electromagnetic field of a nucleus is given by the Bethe-Heitler formula [69]

$$\sigma = \frac{28}{9} \frac{Z^2 \alpha^3}{m_e^2} \ln \frac{E_\gamma}{m_e}. \quad (3.43)$$

The logarithmic term in this formula is due to pairs, which are produced at very small angles. This behavior is due to a so called “mass singularity” in the matrix element, the fact that the propagator of the internal particle is very large, and even would become singular for  $m_e \rightarrow 0$ . But this behavior is connected to the fact that we are looking at a real photon with  $q^2 = 0$ . In the DEPA or EPA we neglect the dependence of the matrix element on the transverse momentum. But as  $q^2$  is mainly given by  $q_\perp^2$ , this is only justified as long as  $q_\perp$  is smaller than  $m_e$ , whereas the form factor of the ions allows  $q_\perp$  to be as high as 83 MeV. That is, we are not allowed to neglect  $m_e$  compared with  $M$  even for very large  $M$ , because setting  $m_e = 0$  would make our cross section divergent. There are always three momentum scales given by  $M$ ,  $\Lambda$ , and  $m_e$ . The equivalent photon method has to be modified in the region of small angles. This explains why the calculations of  $P(M)$  and  $P(M, Y = 0)$  are too large, as they are integrated over the whole  $\theta$  range. But as this error only shows up in a logarithmic term, the deviation of the DEPA is not that large compared, e.g., with  $P_{\text{total}}$ , where the DEPA overestimates the result by order of magnitude.



# Chapter 4

## Calculations for small impact parameter

In the previous chapter we dealt with impact parameter  $b$  zero only. Even though we argued that this should be a good approximation for very small impact parameter also, there remains the question how the probability decreases for small  $b$  up to several Compton wave length, where we expect then that the equivalent photon approximation can be used. This will be studied in this chapter. Only total probabilities will be discussed, but differential probabilities could be calculated as well using the same technique as described here.

### 4.1 Calculation of the $b$ -dependent probability

The  $b$ -dependent matrix element for this process was already given in the previous chapter. The two processes contributing to it in lowest order were shown in Fig. 3.2. The matrix element was (Eq. (3.3))

$$\begin{aligned}
 M &= -ie^2 \int \frac{d^4 p}{(2\pi)^4} \bar{u}(p_-) \mathcal{A}^{(1)}(p_- - p) \frac{\not{p} + m}{p^2 - m^2} \mathcal{A}^{(2)}(p_+ + p) v(p_+) \\
 &\quad - ie^2 \int \frac{d^4 p}{(2\pi)^4} \bar{u}(p_-) \mathcal{A}^{(2)}(p_- - p) \frac{\not{p} + m}{p^2 - m^2} \mathcal{A}^{(1)}(p_+ + p) v(p_+) \quad (4.1)
 \end{aligned}$$

$$\begin{aligned}
 \hat{M} &= -i \left( \frac{Ze^2}{2\pi} \right)^2 \left[ \not{\epsilon}^{(1)} \int d^4 p \frac{\not{p} + m}{(p_- - p)^2 (p^2 - m^2) (p_+ + p)^2} \not{\epsilon}^{(2)} \right. \\
 &\quad \times \delta((p_- - p)u^{(1)}) \delta((p_+ + p)u^{(2)}) \exp(-ipb) \exp(i(p_- - p_+)b/2) \\
 &\quad + \not{\epsilon}^{(2)} \int d^4 p \frac{\not{p} + m}{(p_- - p)^2 (p^2 - m^2) (p_+ + p)^2} \not{\epsilon}^{(1)} \\
 &\quad \left. \times \delta((p_- - p)u^{(2)}) \delta((p_+ + p)u^{(1)}) \exp(+ipb) \exp(-i(p_- - p_+)b/2) \right]. \quad (4.2)
 \end{aligned}$$

For  $b$  zero we were able to solve the integrals analytically. For arbitrary  $b$  this is not possible any longer, therefore a different method will be used. Also it has the advantage

that with the same calculation a range of impact parameter can be calculated at once.

In a first step we rewrite the matrix element as an integral over the momentum of the first photon  $q_1$ . For this we change the integration variable in the first integral to  $p_- - p = q_1$  and in the second  $p_+ + p = q_1$

$$\begin{aligned}
\hat{M} &= -i \left( \frac{Ze^2}{2\pi} \right)^2 \left[ \int d^4 q_1 \frac{\not{p}^{(1)}(\not{p}_- - \not{q}_1 + m) \not{p}^{(2)}}{q_1^2 (p_+ + p_- - q_1)^2 ((p_- - q_1)^2 - m^2)} \right. \\
&\quad \times \delta(q_1 u^{(1)}) \delta((p_+ + p_- - q_1) u^{(2)}) \exp(-i(p_- - q_1)b + i(p_- - p_+)b/2) \\
&\quad + \int d^4 q_1 \frac{\not{p}^{(2)}(\not{q}_1 - \not{p}_+ + m) \not{p}^{(1)}}{q_1^2 (p_+ + p_- - q_1)^2 ((q_1 - p_+)^2 - m^2)} \\
&\quad \times \delta(q_1 u^{(1)}) \delta((p_+ + p_- - q_1) u^{(2)}) \exp(+i(q_1 - p_+)b - i(p_- - p_+)b/2) \left. \right] \\
&= -i \left( \frac{Ze^2}{2\pi} \right)^2 \int d^4 q_1 \left[ \frac{\not{p}^{(1)}(\not{p}_- - \not{q}_1 + m) \not{p}^{(2)}}{q_1^2 [p_+ + p_- - q_1]^2 [(p_- - q_1)^2 - m^2]} \right. \\
&\quad \left. + \frac{\not{p}^{(2)}(\not{q}_1 - \not{p}_+ + m) \not{p}^{(1)}}{q_1^2 [p_+ + p_- - q_1]^2 [(q_1 - p_+)^2 - m^2]} \right] \\
&\quad \times \delta(q_1 u^{(1)}) \delta((p_+ + p_- - q_1) u^{(2)}) \exp(+iq_1 b) \exp(-i(p_- + p_+)b/2). \quad (4.3)
\end{aligned}$$

Please note that the exponentials of both terms are now of the same form and therefore they can be combined in a single integral with the same dependence on  $b$ . As  $p_+$  and  $p_-$  are fixed values, we can drop the last exponential, as it is only a phase, which drops out, as soon as we square  $M$

$$\begin{aligned}
\hat{M} &= -i \left( \frac{Ze^2}{2\pi} \right)^2 \int d^4 q_1 \frac{1}{q_1^2 [p_+ + p_- - q_1]^2} \\
&\quad \times \left\{ \frac{\not{p}^{(1)}(\not{p}_- - \not{q}_1 + m) \not{p}^{(2)}}{[(p_- - q_1)^2 - m^2]} + \frac{\not{p}^{(2)}(\not{q}_1 - \not{p}_+ + m) \not{p}^{(1)}}{[(q_1 - p_+)^2 - m^2]} \right\} \\
&\quad \times \delta(q_1 u^{(1)}) \delta((p_+ + p_- - q_1) u^{(2)}) \exp(iq_1 b). \quad (4.4)
\end{aligned}$$

As done in the last chapter the two  $\delta$  functions are used in order to reduce the four-dimensional integral to an integral over the transverse components of  $q_1$ . We get

$$q_{10} = \frac{1}{2} [(\epsilon_+ + \epsilon_-) + \beta(p_{+z} + p_{-z})], \quad (4.5a)$$

$$q_{1z} = \frac{1}{2\beta} [(\epsilon_+ + \epsilon_-) + \beta(p_{+z} + p_{-z})] = \frac{1}{\beta} q_{10}, \quad (4.5b)$$

and

$$\begin{aligned}
\hat{M} &= -i \left( \frac{Ze^2}{2\pi} \right)^2 \frac{1}{2\beta} \int d^2 q_{1\perp} \frac{1}{q_1^2 [p_+ + p_- - q_1]^2} \exp(iq_{1\perp} b) \\
&\quad \times \left\{ \frac{\not{p}^{(1)}(\not{p}_- - \not{q}_1 + m) \not{p}^{(2)}}{[(p_- - q_1)^2 - m^2]} + \frac{\not{p}^{(2)}(\not{q}_1 - \not{p}_+ + m) \not{p}^{(1)}}{[(q_1 - p_+)^2 - m^2]} \right\}, \quad (4.6)
\end{aligned}$$

where the factor  $1/(2\beta)$  and the change from  $u$  to  $w$  comes from the evaluation of the  $\delta$  functions as in the previous chapter.

As it makes the numerical calculations more stable, we are splitting again all four-vectors into their longitudinal and transverse parts. For the probability we square  $M$  and sum over the spin indices to get

$$\begin{aligned}
\sum_s |M|^2 &= (Z\alpha)^4 \frac{4}{\beta^2} \text{Tr} \left\{ (\not{p}_- + m) \right. \\
&\quad \times \int d^2 q_{1\perp} \frac{1}{\bar{q}_1^2} \frac{1}{(p_+ + p_- - q_1)^2} \exp(iq_{1\perp} b) \\
&\quad \times \left[ \frac{\psi^{(1)}(\not{p}_- - \not{q}_1 + m) \psi^{(2)}}{((p_- - q_1)^2 - m^2)} + \frac{\psi^{(2)}(\not{q}_1 - \not{p}_+ + m) \psi^{(1)}}{((q_1 - p_+)^2 - m^2)} \right] (\not{p}_+ - m) \\
&\quad \times \int d^2 q'_{1\perp} \frac{1}{\bar{q}'_1{}^2} \frac{1}{(p_+ + p_- - q'_1)^2} \exp(-iq'_{1\perp} b) \\
&\quad \times \left. \left[ \frac{\psi^{(2)}(\not{p}_- - \not{q}'_1 + m) \psi^{(1)}}{((p_- - q'_1)^2 - m^2)} + \frac{\psi^{(1)}(\not{q}'_1 - \not{p}_+ + m) \psi^{(2)}}{((q'_1 - p_+)^2 - m^2)} \right] \right\}. \tag{4.7}
\end{aligned}$$

We change the integration variable  $q'_1$  to the difference of both momenta  $\Delta q_1 = q'_1 - q_1$  and get

$$\begin{aligned}
\sum_s |M|^2 &= (Z\alpha)^4 \frac{4}{\beta^2} \int d^2 \Delta q_1 d^2 q_1 [N_0 N_1 N_3 N_4]^{-1} \exp(i\Delta \vec{q}_1 \vec{b}) \\
&\quad \times \text{Tr} \left\{ (\not{p}_- + m) \left[ N_{2D}^{-1} \psi^{(1)}(\not{p}_- - \not{q}_1 + m) \psi^{(2)} + N_{2X}^{-1} \psi^{(2)}(\not{q}_1 - \not{p}_+ + m) \psi^{(1)} \right] \right. \\
&\quad \times (\not{p}_+ - m) \left. \left[ N_{5D}^{-1} \psi^{(2)}(\not{p}_- - \not{q}'_1 + m) \psi^{(1)} + N_{5X}^{-1} \psi^{(1)}(\not{q}'_1 - \not{p}_+ + m) \psi^{(2)} \right] \right\} \tag{4.8}
\end{aligned}$$

with

$$\begin{aligned}
N_0 &= -q_1^2 = \bar{q}_{1\perp}^2 + m_0^2, \\
m_0^2 &= -q_{1l}^2, \tag{4.9a}
\end{aligned}$$

$$\begin{aligned}
N_1 &= -(q_1^2 - (p_+ + p_-)^2) = [\vec{q}_{1\perp} + \vec{k}_1]^2 + m_1^2, \\
\vec{k}_1 &= -\vec{p}_{+\perp} - \vec{p}_{-\perp}, \\
m_1^2 &= -(q_{1l} - p_{+l} - p_{-l})^2, \tag{4.9b}
\end{aligned}$$

$$\begin{aligned}
N_{2D} &= -(q_1 - p_-)^2 + m^2 = (\vec{q}_{1\perp} + \vec{k}_{2D})^2 + m_{2D}^2, \\
\vec{k}_{2D} &= -\vec{p}_{-\perp}, \\
m_{2D}^2 &= m^2 - (q_{1l} - p_{-l})^2, \tag{4.9c}
\end{aligned}$$

$$\begin{aligned}
N_{2X} &= -(q_1 - p_+)^2 + m^2 = (\vec{q}_{1\perp} + \vec{k}_{2X})^2 + m_{2X}^2, \\
\vec{k}_{2X} &= -\vec{p}_{+\perp}, \\
m_{2X}^2 &= m^2 - (q_{1l} - p_{+l})^2, \tag{4.9d}
\end{aligned}$$

$$N_3 = -(q_1 + \Delta q_1)^2 = (\vec{q}_{1\perp} + \vec{k}_3)^2 + m_3^2,$$

$$\begin{aligned}\vec{k}_3 &= \Delta\vec{q}_1, \\ m_3^2 &= m_0^2,\end{aligned}\tag{4.9e}$$

$$\begin{aligned}N_4 &= -[q_1 + (\Delta q_1 - p_+ - p_-)]^2 = (\vec{q}_{1\perp} + \vec{k}_4)^2 + m_4^2, \\ \vec{k}_4 &= \Delta\vec{q}_1 - \vec{p}_{+\perp} - \vec{p}_{-\perp}, \\ m_4^2 &= m_1^2,\end{aligned}\tag{4.9f}$$

$$\begin{aligned}N_{5D} &= -[q_1 + (\Delta q_1 - p_-)]^2 + m^2 = (\vec{q}_{1\perp} + \vec{k}_{5D})^2 + m_{5D}^2, \\ \vec{k}_{5D} &= \Delta\vec{q}_1 - \vec{p}_{-\perp}, \\ m_{5D}^2 &= m_{2D}^2,\end{aligned}\tag{4.9g}$$

$$\begin{aligned}N_{5X} &= -[q_1 + (\Delta q_1 - p_+)]^2 + m^2 = (\vec{q}_{1\perp} + \vec{k}_{5X})^2 + m_{5X}^2, \\ \vec{k}_{5X} &= \Delta\vec{q}_1 - \vec{p}_{+\perp}, \\ m_{5X}^2 &= m_{2X}^2.\end{aligned}\tag{4.9h}$$

The  $b$  dependence of this expression is only due to the exponential in combination with  $\Delta q_1$ . Therefore we get for the differential probability

$$P(p_+, p_-, b) = \int d^2\Delta q_1 \tilde{P}(p_+, p_-, \Delta q_1) \exp(i\Delta\vec{q}_1 \vec{b}),\tag{4.10}$$

where we have introduced the Fourier transform of the differential probability

$$\begin{aligned}\tilde{P}(p_+, p_-, \Delta q_1) &= (Z\alpha)^4 \frac{4}{\beta^2} \int d^2q_1 [N_0 N_1 N_3 N_4]^{-1} \\ &\times \text{Tr} \left\{ (\not{p}_- + m) \left[ N_{2D}^{-1} \psi^{(1)}(\not{p}_- - \not{q}_1 + m) \psi^{(2)} + N_{2X}^{-1} \psi^{(2)}(\not{q}_1 - \not{p}_+ + m) \psi^{(1)} \right] \right. \\ &\left. \times (\not{p}_+ - m) \left[ N_{5D}^{-1} \psi^{(2)}(\not{p}_- - \not{q}'_1 + m) \psi^{(1)} + N_{5X}^{-1} \psi^{(1)}(\not{q}'_1 - \not{p}_+ + m) \psi^{(2)} \right] \right\}.\end{aligned}\tag{4.11}$$

For the total probability we have to integrate over  $p_+$  and  $p_-$ . As this integration can be exchanged with the integration over  $\Delta q_1$ , we get

$$P_{\text{total}}(b) = \int d^2\Delta q_1 \tilde{P}_{\text{total}}(\Delta q_1) \exp(i\Delta\vec{q}_1 \vec{b})\tag{4.12}$$

with

$$\tilde{P}_{\text{total}}(\Delta q_1) = \int \frac{d^3p_-}{(2\pi)^3 2\epsilon_-} \frac{d^3p_+}{(2\pi)^3 2\epsilon_+} \tilde{P}(p_+, p_-, \Delta q_1).\tag{4.13}$$

Because of the integration over  $p_+$  and  $p_-$   $P_{\text{total}}(\Delta q_1)$  is invariant under a rotation in the transverse plane and therefore a function of  $|\Delta q_1|$  alone. Therefore we can integrate over the angular part of the integral and get  $P_{\text{total}}(b)$  as a Bessel transform of the form

$$P_{\text{total}}(b) = 2\pi \int d\Delta q_1 \Delta q_1 \tilde{P}_{\text{total}}(\Delta q_1) J_0(|\Delta q_1| |b|),\tag{4.14}$$

For the calculation of  $P_{\text{total}}(\Delta q_1)$  we reduce first the trace with the help of the algebraic calculation program FORM [62]. From this we get a sum of scalar products of longitudinal and transverse vectors. The integration over  $q_1$  consists of integrals that are again standard scalar or tensor Feynman integrals in two dimensions but now with six terms in the denominator

$$\int \frac{d^2 q_1 \{1, q_i, q_i q_j\}}{N_0 N_1 N_2 N_3 N_4 N_5}. \quad (4.15)$$

These integrals can again be solved analytically, as shown in Appendix A.5. As all  $q_i$  in the numerator appear in scalar products together with some transverse vectors, the calculation of the tensor integrals is greatly simplified. An explicit inspection of the integrals shows that only the following terms occur in the numerator of the integrals:  $(p_+ q_1)$ ,  $(p_- q_1)$ ,  $(\Delta q_1 q_1)$ ,  $(p_+ q_1)(p_- q_1)$ , each of them together with all four possible combination of  $D$  and  $X$  for  $N_2$  and  $N_5$ .

As the  $k_i$ 's of the propagators are either  $p_+$ ,  $p_-$  or  $\Delta q_1$  or can be written as simple linear combinations of them, we can use the usual trick to express the scalar products in terms of the propagators

$$2q_1 k_i = N_i - N_0 \pm r_i \quad (4.16)$$

(see Appendix A.5 for details). This then leads to scalar Feynman integrals with six or fewer terms in the denominator. The only difficulty is then to choose the right linear combination of the  $k_i$ 's, so that the  $N_i$  is always present in the denominator. For the tensor integral with  $(p_+ q_1)(p_- q_1)$  we can use the fact that the scalar products with  $p_+$  and  $p_-$  can be rewritten in terms of  $N_0$ ,  $N_1$ , and  $N_2$  but also in terms of  $N_3$ ,  $N_4$ , and  $N_5$ . Because of this all tensor integrals can be written in terms of four-, five- and six-term integrals.

One disadvantage of this method to calculate the integrals by reducing them to lower order integrals is the fact that our method needs all propagators to be different. This is not the case for  $\Delta q_1 = 0$  and also for  $\Delta q_1 \rightarrow \infty$ . Therefore we expect to get numerical instabilities for very small and very large values of  $\Delta q_1$ . Fortunately for the calculation of  $P(b)$  we need  $\Delta q_1 \tilde{P}_{\text{total}}(\Delta q_1)$  with vanishes at small and large values of  $\Delta q_1$ , so that these numerical problems are not relevant for us. This is different in the calculation of the total cross section and will be discussed there.

The integration over  $p_+$  and  $p_-$  was done again with the MC integration routine within an error of less than 1%. One might think that doing the first integration analytically is unnecessary and that an integration over all variables by a MC method is much easier. The advantage of calculating the integrals this way is that the integrand for the later integrations over  $p_+$  and  $p_-$  is much smoother and is therefore better suited for a Monte Carlo integration.

The inclusion of a dipole form factor is now straightforward using the same trick as before. As we have four form factors now, this gives a total of sixteen integrals, which have to be calculated. As  $\tilde{P}_{\text{total}}(\Delta q_1)$  is symmetric with respect to the change of the integration variable from  $q_1$  to  $q'_1$  or  $q_2$ , the total number of integrals, which have to be calculated, can be reduced to seven. Calculations with a double dipole form factor have not been done, as

we expect to have 81 integrals then. Even though we could reduce the number of integrals again with the help of some symmetries, the numerical calculations would take very long. The numerical stability decreases also with the inclusion of the form factor, as we have to calculate differences of integrals, which differ by a small value only.

Finally we want to show that  $\tilde{P}_{\text{total}}(\Delta q_1)$  can also be used for a calculation of the total cross section  $\sigma_{\text{total}}$  for this process. The total cross section is given by the integration of the probability over all impact parameter. Using for the probability Eq. (4.12) we get

$$\begin{aligned}
 \sigma_{\text{total}} &= \int d^2b P(b) \\
 &= \int d^2b d^2\Delta q_1 \tilde{P}_{\text{total}}(\Delta q_1) \exp(i\Delta\vec{q}_1\vec{b}) \\
 &= (2\pi)^2 \int d^2\Delta q_1 \delta(\Delta\vec{q}_1) \tilde{P}_{\text{total}}(\Delta q_1) \\
 &= (2\pi)^2 \tilde{P}_{\text{total}}(0),
 \end{aligned} \tag{4.17}$$

that is,  $\sigma$  is directly connected with the value of  $\tilde{P}_{\text{total}}$  at  $\Delta q_1$  zero. As we have already mentioned above, our method to calculate the integrals can not be used in this case, as some of the propagators are identical then and our reduction scheme fails. On the other hand we can extrapolate to the limit  $\Delta q_1 \rightarrow 0$  and use this value in order to calculate the cross section. It is possible also to calculate  $\tilde{P}_{\text{total}}(0)$  analytically, if one modifies the reduction scheme. This possibility has been studied by us, but has not been used at the moment.

## 4.2 Results for the total probability $P_{\text{total}}(b)$

Using the method described above we have calculated values of  $\tilde{P}_{\text{total}}$  for some  $\Delta q_1$ . This values were then used in a spline interpolation in order to calculate the Bessel transform. For the choice of the appropriate points of  $\Delta q_1$  and also for the interpolation polynom we have used  $\ln(\Delta q_1)$  instead of  $\Delta q_1$ , as it is more appropriate in our case.

In Fig. 4.1 and 4.2 we show  $\Delta q_1 \tilde{P}_{\text{total}}(\Delta q_1)$  with and without a dipole form factor for  $\gamma = 10$  and  $\gamma = 100$ . The curve increases up to a maximum, which is at about  $m_e$ , then it decreases slowly. The difference between the calculations with and without a form factor is only visible at very large values of  $\Delta q_1$  of about  $\Lambda$ . From this we conclude already that the  $b$  dependent probability for large values of  $b$ , where only very small values of  $\Delta q_1$  contribute, should be identical in both cases.

If one looks at the decrease of the curve for large  $\Delta q_1$ , one sees that the result for a point charge decreases only as  $\Delta q_1^{-1}$ . As we have to integrate over the whole  $\Delta q_1$  range in order to get  $P(0)$ , this means that the total probability for a point charge diverges at  $b \rightarrow 0$ . We can determine even the exact form of this divergence. For small values of  $b$  only the contribution of large  $\Delta q_1$  is relevant. If we approximate the function there by

$$\Delta q_1 \tilde{P}_{\text{total}}(\Delta q_1) \approx C \frac{\Delta q_1}{\Delta q_1^2 + k^2}, \tag{4.18}$$

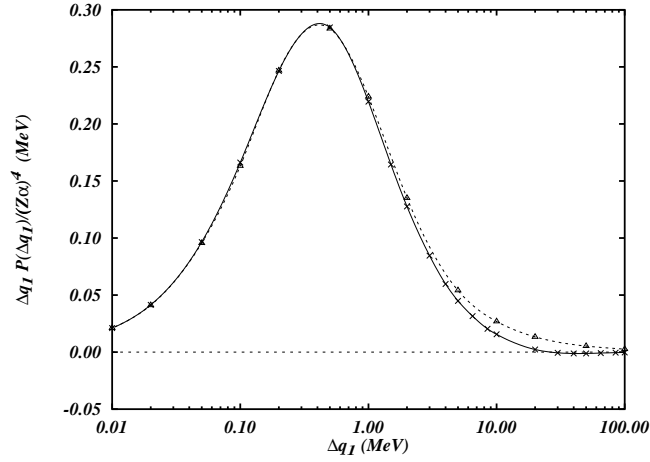


Figure 4.1:  $\Delta q_1 P(\Delta q_1)$  as a function of  $\Delta q_1$ . Shown are the results for  $\gamma = 10$ . The points are the calculated values, the lines the results of a spline interpolation. The solid line shows the result for a calculation with a realistic dipole form factor, the dashed line the result for a point charge distribution.

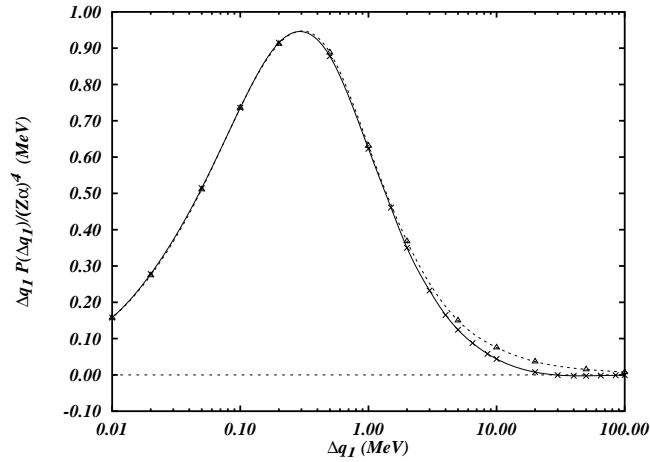


Figure 4.2:  $\Delta q_1 P(\Delta q_1)$  as a function of  $\Delta q_1$  for  $\gamma = 100$ . Same notation as in Fig. 4.1.

we can do the Bessel transformation analytically [70] in order to get

$$P_{\text{total}}(b) \approx 2\pi CK_0(bk). \quad (4.19)$$

As the Bessel function  $K_0(z)$  diverges with  $-\ln(z)$  for small  $z$ , we finally get

$$P_{\text{total}}(b) \sim -\ln(b) \quad (b \rightarrow 0). \quad (4.20)$$

With a form factor the curve decreases much faster, so that  $P(b)$  remains finite for  $b = 0$ .

Doing now the Bessel transformation explicitly we get  $P(b)$  as shown in Fig. 4.3 and 4.4. First we note that we get the same results for  $b$  zero, as already found in the previous chapter. Second we see, as already mentioned earlier, that the results with and without a form factor agree for impact parameter  $b$  much larger than the nuclear radius. We see also that the result for a point charge diverges logarithmically with  $b$ , whereas with a form factor  $P(b)$  remains at about the same size from  $b = 0$  to  $b \approx 2R$ . The reduced total probability even increases slightly there. That this is a real effect and not due to the numerical errors in the Bessel transformation can be understood easily, as  $\tilde{P}_{\text{total}}(\Delta q_1)$  changes its sign for large values of  $\Delta q_1$ . The reason for this may be due to the choice of the form factor. As our form factor corresponds to a Yukawa charge distribution, the charge is concentrated mainly at small distances, so that with a more realistic charge distribution this increase may be absent. But in order to really proof this, calculations with a realistic form factor would be necessary. But as this increase is only of the order of one percent, our results are good at least within this accuracy.

Unfortunately it is difficult to give a good error estimate for  $P(b)$ , as the error due to the interpolation can not be estimated easily. Based on the error of the individual calculated points we estimate it to be of the order of one percent. Its accuracy decreases for larger values of  $b$  because of the oscillating behavior of the Bessel function.

Using again the Poisson distribution for the  $N$ -pair probabilities we get the results as shown in Fig. 4.5 for  $\gamma = 100$  and Au–Au collisions. Shown are the  $N$ -pair probabilities for up to four pairs and also the sum of all  $N$ -pair probabilities, which is given by  $1 - P(b, 0)$ .

In Fig. 4.6 we compare our result with the EPA approximation (Eq. 7.3.10 of [16]). We see that EPA is too high for impact parameter about the size of the Compton wavelength  $\lambda_c$ , but we find agreement between both for large values of  $b$ . Therefore the use of EPA seems to be justified but only for values of  $b$  much larger than the Compton wavelength.

Finally we want to calculate also the total cross section  $\sigma_{\text{total}}$ , for which we only need  $\tilde{P}_{\text{total}}(0)$ . This calculation is in principle identical to the one done by Bottcher and Strayer [11], with the difference that they did all integrals by a MC method. Therefore we can compare our results with them. Also shown are the results of Bertulani and Baur based on EPA [16].

Unfortunately, as described above, our methods for calculating the integrals can not be used for  $\Delta q_1 = 0$ . Therefore we made an extrapolation of our results for very small  $\Delta q_1$ . This extrapolation was limited by the numerical instabilities of the calculation. The value of  $\tilde{P}_{\text{total}}(0)$  was estimated using a linear interpolation of the last two calculated points as an upper boundary together with the last point itself as a lower boundary. We used then



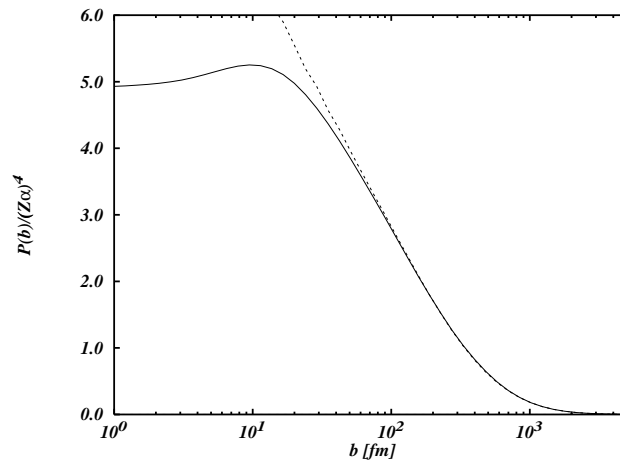


Figure 4.3: The  $b$  dependent reduced probability  $P_{\text{total}}(b)$  for  $\gamma = 10$  as a function of  $b$  for impact parameters up to five Compton wavelengths. The solid line is the result for a calculation with a realistic dipole form factor, the dashed line the result for a point charge distribution.

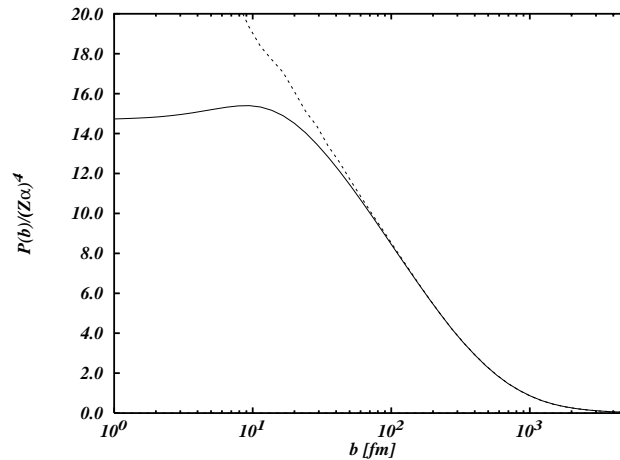


Figure 4.4: The  $b$  dependent reduced probability  $P_{\text{total}}(b)$  for  $\gamma = 100$  as a function of  $b$  for impact parameters up to five Compton wavelengths. Same notation as in Fig. 4.3.

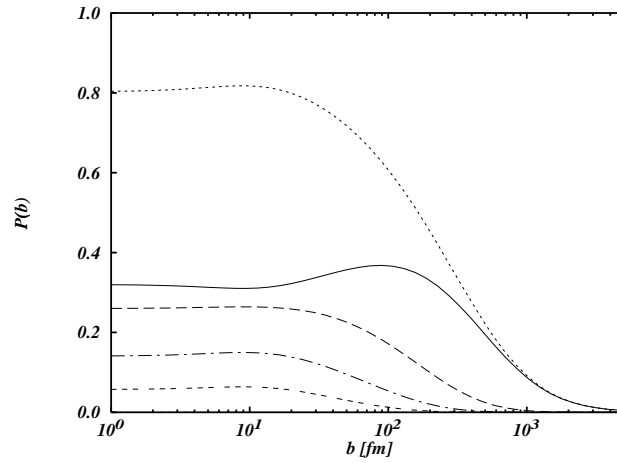


Figure 4.5: The  $b$  dependent  $N$ -pair probabilities for  $\gamma = 100$  and Au ions based on the Poisson distribution. Shown are the results for one pair (solid line), two pairs (dashed line), three pairs (dashed-dotted line), and four pairs (three-dash line) together with the sum of all pair production probabilities (dotted line) given by  $1 - P(b, 0)$ .

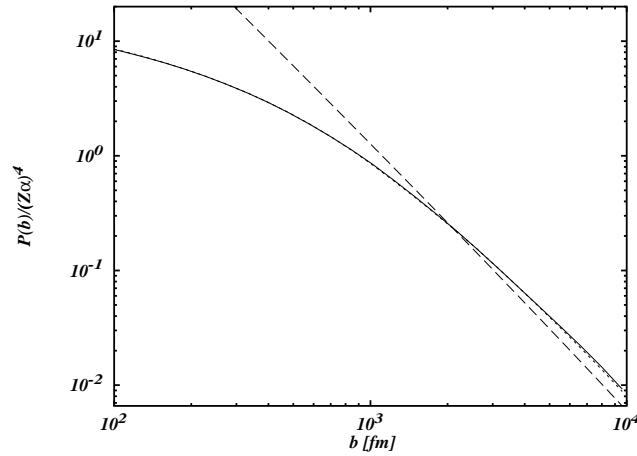


Figure 4.6: Comparison of the  $b$  dependent probability  $P_{\text{total}}(b)$  for  $\gamma = 100$  and large values of  $b$  with the result of EPA. The solid and the dotted line are the result of our calculation with and without a form factor, the dashed line the results of EPA [16].

$\gamma$	$\sigma_{\text{total}}/(Z\alpha)^4$ (kbarn)	$\sigma_{\text{BS}}/(Z\alpha)^4$ (kbarn)	$\sigma_{\text{BB}}/(Z\alpha)^4$ (kbarn)
10	$32.6 \pm 0.8$	31	37
100	$290 \pm 15$	270	340

Table 4.1: Results of the calculation of the total cross section  $\sigma_{\text{total}}$  for different values of  $\gamma$ . A comparison is made with the results of Bottcher and Strayer  $\sigma_{\text{BS}}$  [11] and of Bertulani and Baur  $\sigma_{\text{BB}}$  [16].

the mean value of both as an estimate for  $\tilde{P}_{\text{total}}(0)$  and the difference of both point together with the error of the last two points itself as an estimate of the error. A comparison of our results with the results of Bottcher and Strayer and Bertulani and Baur is given in Table 4.1. Unfortunately the results of Bottcher and Strayer had to be extracted from the diagrams shown in [11], as the approximation formula given by them is not able to reproduce these results, and are therefore not very accurate. We find good agreement between all three calculations, where the results of Bertulani and Baur are higher than the two others, which is a well known property of the EPA at low values of  $\gamma$ .

As already mentioned earlier a calculation with better accuracy is possible by modifying the reduction scheme for the integrals.



# Chapter 5

## Multiple particle corrections to the one-pair creation

Having calculated  $P(b)$  in lowest order, we now come back to the higher-order processes, especially to the multiple-particle corrections already discussed in Sec. 2.4 (see also Fig. 2.5). In this chapter we are going to use the general form of the  $S$  operator in second-order Magnus theory derived in Sec. 2.5 for the reduced one-pair creation probability. Again we will suppress the spin indices in this chapter assuming that it has been incorporated into the momenta.

### 5.1 One-pair creation in second-order Magnus theory

The  $S$  operator given in Eq. (2.81) was derived for an arbitrary external field. We are now specializing to the case of pair production in heavy-ion collisions. In this case there are some kinematical restrictions, so that some of the terms in  $S$  can be dropped. Especially there is no pair creation or pair annihilation in first-order Magnus theory and we can replace the principal value integrals in the pair creation and annihilation term in the second order by ordinary integrals, as the intermediate state is not allowed to be on-shell in this case.

As we want to concentrate on the multiple-particle effects we will neglect also all Coulomb scattering terms. It is generally assumed that these terms do change the differential probabilities, but are only of minor importance for the total probabilities. Also their influence seems to become smaller for higher energies. Therefore we will neglect all terms of the form  $: b^+ b :$  and  $: d d^+ :$ . Also the vacuum terms will be dropped, as we are only interested in the calculation of the reduced amplitude, where vacuum corrections do not appear. The  $S$  operator with these approximations is (see Eq. (A.12) for the definition of  $d\tilde{p}$ )

$$S = \exp \left\{ -ie^2 \int d\tilde{p}_1 d\tilde{p}_2 \frac{dp}{(2\pi)^4} \right.$$

$$\begin{aligned} & \times \left[ b^+(p_1)d^+(p_2) \bar{u}(p_1) \not{A}(p_1 - p) \frac{\not{p} + m}{p^2 - m^2} \not{A}(p + p_2)v(p_2) \right. \\ & \left. + d(p_1)b(p_2) \bar{v}(p_1) \not{A}(-p_1 - p) \frac{\not{p} + m}{p^2 - m^2} \not{A}(p - p_2)u(p_2) \right] \}. \end{aligned} \quad (5.1)$$

The integrals over  $p$  in this expression are just the pair creation and pair annihilation amplitude in second-order Born approximation as discussed in Chap. 3. We define the pair creation and annihilation potential  $V$  and  $V^*$  as

$$V(p_1, p_2) = e^2 \int \frac{d^4p}{(2\pi)^4} \bar{u}(p_1) \not{A}(p_1 - p) \frac{\not{p} + m}{p^2 - m^2} \not{A}(p + p_2)v(p_2) \quad (5.2a)$$

$$V^*(p_2, p_1) = e^2 \int \frac{d^4p}{(2\pi)^4} \bar{v}(p_1) \not{A}(-p_1 - p) \frac{\not{p} + m}{p^2 - m^2} \not{A}(p - p_2)u(p_2) \quad (5.2b)$$

(where  $V^*$  is just the complex conjugate of  $V$ ) in order to write  $S$  as:

$$S = \exp \left\{ -i \int d\tilde{p} d\tilde{q} \left[ b^+(p)d^+(q)V(p, q) + d(q)b(p)V^*(p, q) \right] \right\}. \quad (5.3)$$

The matrix element defined in Eq. (3.3) is connected with the potential  $V$  through

$$M(p, q) = -iV(p, q). \quad (5.4)$$

For the reduced one-pair creation amplitude we have to calculate

$$\langle f | S | i \rangle = \langle 0 | d(q_f)b(p_f)S | 0 \rangle. \quad (5.5)$$

We are now expanding the exponential in  $S$  in order to get the different contributions to the one pair creation. In lowest order we expect to get back the second-order Born result. We get

$$\langle f | S^{(1)} | i \rangle = -i \int d\tilde{p} d\tilde{q} V(p, q) \langle 0 | d(q_f)b(p_f)b^+(p)d^+(q) | 0 \rangle \quad (5.6)$$

$$= -i\gamma(p_f)\gamma(q_f)V(p_f, q_f) \quad (5.7)$$

$$= M(p_f, q_f)\gamma(p_f)\gamma(q_f), \quad (5.8)$$

where we have used  $\gamma(p)$  as defined in Eq. (A.13).

The differential probability in first order therefore is

$$P(p_f, q_f) = |M(p_f, q_f)|^2 \gamma^2(p_f)\gamma^2(q_f) \quad (5.9)$$

and the total probability is given by

$$P_{\text{total}} = \int |M(p_f, q_f)|^2 d\Gamma(p_f)d\Gamma(q_f), \quad (5.10)$$

where  $d\Gamma(p)$  is the Lorentz invariant phase space as defined in Eq. (A.14). This is indeed the Born result.

As the vacuum expectation values, we get from higher orders, vanish, if the number of creation and annihilation operators is not equal for each kind of particles, we see easily that only odd orders in the expansion of  $S$  contribute. The next order is therefore the third one, where we get

$$\begin{aligned} \langle f | S^{(3)} | i \rangle &= \frac{i}{3!} \int d\tilde{p}_1 d\tilde{p}_2 d\tilde{p}_3 d\tilde{q}_1 d\tilde{q}_2 d\tilde{q}_3 \\ &\times \left[ V(p_1, q_1) V^*(p_2, q_2) V(p_3, q_3) \langle 0 | d(q_f) b(p_f) b^+(p_1) d^+(q_1) d(q_2) b(p_2) b^+(p_3) d^+(q_3) | 0 \rangle \right. \\ &\left. + V^*(p_1, q_1) V(p_2, q_2) V(p_3, q_3) \langle 0 | d(q_f) b(p_f) d(q_1) b(p_1) b^+(p_2) d^+(q_2) b^+(p_3) d^+(q_3) | 0 \rangle \right]. \end{aligned} \quad (5.11)$$

Here we have used the fact that only two of the eight possible combinations do not vanish trivially. Again the vacuum expectation value can be calculated using the anticommutation relations of the particle operators. The first expectation value is

$$\begin{aligned} \langle 0 | d(q_f) b(p_f) b^+(p_1) d^+(q_1) d(q_2) b(p_2) b^+(p_3) d^+(q_3) | 0 \rangle &= \\ \delta(p_f - p_1) \delta(p_2 - p_3) \delta(q_f - q_1) \delta(q_2 - q_3) & \end{aligned} \quad (5.12)$$

and the second one

$$\begin{aligned} \langle 0 | d(q_f) b(p_f) d(q_1) b(p_1) b^+(p_2) d^+(q_2) b^+(p_3) d^+(q_3) | 0 \rangle &= \\ \delta(p_1 - p_2) \delta(q_1 - q_2) \delta(p_f - p_3) \delta(q_f - q_3) & \\ - \delta(p_1 - p_2) \delta(p_f - p_3) \delta(q_f - q_2) \delta(q_1 - q_3) & \\ - \delta(p_f - p_2) \delta(p_1 - p_3) \delta(q_1 - q_2) \delta(q_f - q_3) & \\ + \delta(p_f - p_2) \delta(p_1 - p_3) \delta(q_f - q_2) \delta(q_1 - q_3). & \end{aligned} \quad (5.13)$$

Terms of the form  $\delta(p_2 - p_3) \delta(q_2 - q_3)$  describe closed fermion loops, and we drop them in the calculation of the reduced amplitude. Therefore only two terms remain. In third order we get

$$\langle f | S^{(3)} | i \rangle = -i \frac{2}{3!} \gamma(p_f) \gamma(q_f) \int d\Gamma(p_1) d\Gamma(q_1) V(p_f, q_1) V^*(p_1, q_1) V(p_1, q_f). \quad (5.14)$$

Combining both results we get up to third order

$$\langle f | S^{(1+3)} | i \rangle = \gamma(p_f) \gamma(q_f) \left[ M(p_f, q_f) + \frac{1}{3} \int d\Gamma(p_1) d\Gamma(q_1) M(p_f, q_1) M^*(p_1, q_1) M(p_1, q_f) \right]. \quad (5.15)$$

The interpretation of this higher-order process is straightforward. If we keep in mind that  $M(p, q)$  is the amplitude for the production of a pair and  $M^*(p, q)$  the amplitude for the annihilation of a pair, we get the Feynman diagram as shown in Fig. 5.1. These are just those higher-order processes, we already discussed before in Sec. 2.4 (see Fig. 2.5). Two pairs are created and then one of the electrons annihilates with the other positron, so

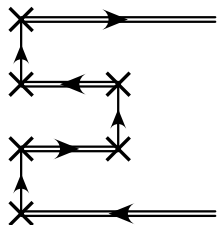


Figure 5.1: *Third order correction to the one-pair creation process in second-order Magnus theory; compare with Fig. 2.5. Double lines mean that the particles are on shell.*

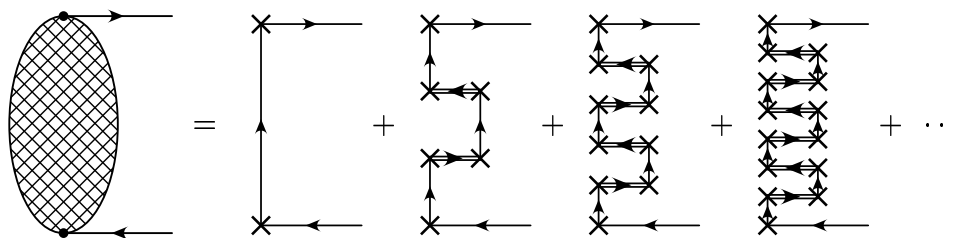


Figure 5.2: *General form of the expansion of the reduced one-pair creation amplitude in second-order Magnus theory. Double lines mean that the particles are on shell. The coefficients appearing in front of each term have been neglected.*



that finally only one electron and one positron remain. The Magnus theory restricts these intermediate particles to the mass shell, so that we only need the on-shell  $M$ , whereas they may be off-shell in the general case.

Using the same technique higher orders can also be calculated. The explicit calculation of the fifth and seventh order gives (see also Fig. 5.2)

$$\begin{aligned} \langle f | S^{(5)} | i \rangle &= \frac{16}{5!} \gamma(p_f) \gamma(q_f) \int d\Gamma(p_1) d\Gamma(q_1) d\Gamma(p_2) d\Gamma(q_2) \\ &\quad \times M(p_f, q_1) M^*(p_1, q_1) M(p_1, q_2) M^*(p_2, q_2) M(p_2, q_f) \end{aligned} \quad (5.16a)$$

$$\begin{aligned} \langle f | S^{(7)} | i \rangle &= \frac{272}{7!} \gamma(p_f) \gamma(q_f) \int d\Gamma(p_1) d\Gamma(q_1) d\Gamma(p_2) d\Gamma(q_2) d\Gamma(p_3) d\Gamma(q_3) \\ &\quad \times M(p_f, q_1) M^*(p_1, q_1) M(p_1, q_2) M^*(p_2, q_2) M(p_2, q_3) M^*(p_3, q_3) M(p_3, q_f), \end{aligned} \quad (5.16b)$$

where in the calculation of the vacuum expectation values also more complicated fermion loops occur, which have to be neglected. The following properties are remarkable, as they are true for all higher orders: First all contributions coming from the same order are of the same type and can therefore be summed. Second all amplitudes have the same sign, that is, they are all added coherently. Therefore they increase all the reduced total probability, no cancellation or reduction occurs. This same sign can also be understood from the connection of the higher-order processes with the vacuum corrections. Vacuum loops contribute with a negative sign to the amplitude (see Sec. 2.2 and [59]). As our diagrams are connected with a vacuum diagram by the permutation of some lines, it is clear that it has to have the same sign as the lowest-order diagram.

For higher orders the number of terms occurring in the reduction of the vacuum expectation values can no longer be calculated explicitly, as these get rather large and the number of diagrams increases rapidly. However we show in App. A.4 how the total number of processes can be calculated using combinatorial arguments and a recursive formula.

Finally we calculate the lowest-order correction to the reduced total probability. Squaring the pair production amplitude up to third order (Eq. (5.15)) we get

$$P^{(1+3)}(p_f, q_f) = \left| \langle f | S^{(1+3)} | i \rangle \right|^2 \quad (5.17)$$

$$\begin{aligned} &= \left[ M^*(p_f, q_f) + \frac{1}{3} \int d\Gamma(p) d\Gamma(q) M^*(p_f, q) M(p, q) M^*(p, q_f) \right] \\ &\quad \times \left[ M(p_f, q_f) + \frac{1}{3} \int d\Gamma(p') d\Gamma(q') M(p_f, q') M^*(p', q') M(p', q_f) \right] \\ &\quad \times \gamma^2(p_f) \gamma^2(q_f) \end{aligned} \quad (5.18)$$

$$\begin{aligned} &= \left\{ |M(p_f, q_f)|^2 + \frac{1}{3} \left[ \int d\Gamma(p) d\Gamma(q) M(p_f, q_f) M^*(p_f, q) M(p, q) M^*(p, q_f) \right. \right. \\ &\quad \left. \left. + M^*(p_f, q_f) M(p_f, q) M^*(p, q) M(p, q_f) \right] + \dots \right\} \gamma^2(p_f) \gamma^2(q_f) \end{aligned} \quad (5.19)$$

$$= \left\{ |M(p_f, q_f)|^2 + \frac{2}{3} \int d\Gamma(p) d\Gamma(q) \right.$$

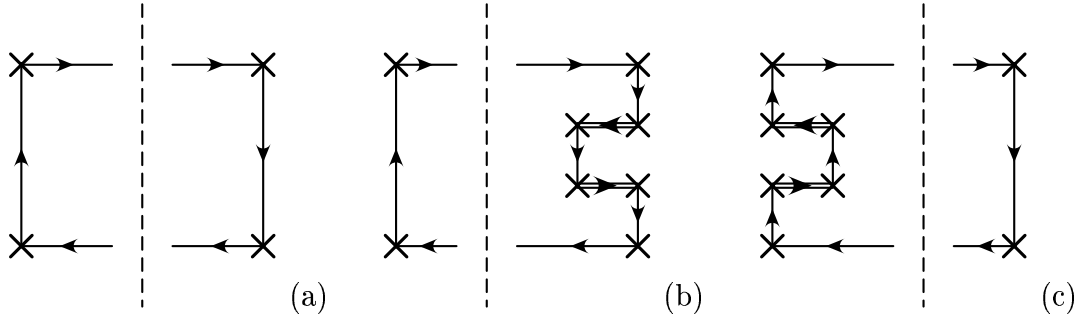


Figure 5.3: Lowest order (a) and the first two correction terms (b and c) to the reduced one-pair creation probability.

$$\times \text{Re} [M(p_f, q_f)M^*(p_f, q)M(p, q)M^*(p, q_f)] + \dots \} \gamma^2(p_f)\gamma^2(q_f). \quad (5.20)$$

Integrating over  $p_f$  and  $q_f$  we get the total probability (Fig. 5.3)

$$P_{\text{total}} = \int d\Gamma(p_f)d\Gamma(q_f)|M(p_f, q_f)|^2 + \frac{2}{3} \int d\Gamma(p_f)d\Gamma(q_f)d\Gamma(p)d\Gamma(q) \times \text{Re} [M(p_f, q_f)M^*(p_f, q)M(p, q)M^*(p, q_f)] \quad (5.21)$$

$$=: P^{(B)} + P^{(M)}. \quad (5.22)$$

This result is easily generalized. The general series is of the form

$$P_{\text{total}} = \int d\Gamma(p_1)d\Gamma(q_1)|M(p_1, q_1)|^2 + d_3 \int d\Gamma(p_1)d\Gamma(q_1)d\Gamma(p_2)d\Gamma(q_2)\text{Re} [M(p_1, q_1)M^*(p_1, q_2)M(p_2, q_2)M^*(p_2, q_1)] + \dots + d_{2l-1} \int d\Gamma(p_1) \dots d\Gamma(q_l)\text{Re} [\underbrace{M(p_1, q_1)M^*(p_1, q_2) \dots M(p_l, q_l)M^*(p_l, q_1)}_{l \times}] + \dots \quad (5.23)$$

The coefficients  $d_n$  are again calculated in App. A.4. They can be derived easily from the coefficients  $c_n$  of the amplitudes.

## 5.2 Calculation for impact parameter zero

For the calculation of the lowest-order multiple-particle correction to the one-pair creation probability we make use of the analytic form of the matrix element for impact parameter  $b$  zero, found in Chap. 3. The Feynman diagrams contributing to the process in lowest-order Born approximation were shown in Fig. 3.2. We will use this result for  $M$  in Eq. (5.22). The

usual way to calculate expressions of this kind is to rewrite the spin summation as a trace over gamma matrices. But as each of the  $M$  consists of two diagrams, we finally get a total of sixteen different traces, which all give large expressions, which are not manageable by an algebraic calculation program and therefore can not be used for numerical calculations. Therefore we prefer to calculate  $M$  directly and to do the spin summation numerically.

Several methods have been proposed in the literature, how to calculate amplitudes directly instead of their squares [71, 72, 73]. We use the method described by Fearing and Silbar [74]. It consists of multiplying and dividing  $M$  with  $\bar{v}(q)u(p)$  in order to get (see Eq. (A.7b))

$$\begin{aligned}
M &= \bar{u}(p)\hat{M}v(q) \\
&= \frac{1}{\bar{v}(q)u(p)}\text{Tr}\left\{v(q)\bar{v}(q)u(p)\bar{u}(p)\hat{M}\right\} \\
&= \frac{1}{\bar{v}(q)u(p)}\text{Tr}\left\{(\not{q}-m)\frac{1}{2}(1+\gamma_5\lambda_q\not{s}_q)(\not{p}+m)\frac{1}{2}(1+\gamma_5\lambda_p\not{s}_p)\hat{M}\right\} \\
&= \frac{1}{4S(p,q)}\text{Tr}\left\{(\not{q}-m)(1+\gamma_5\lambda_q\not{s}_q+\gamma_5\lambda_p\not{s}_p-\lambda_p\lambda_q\not{s}_q\not{s}_p)(\not{p}+m)\hat{M}\right\}, \quad (5.24)
\end{aligned}$$

where  $s_p$ ,  $s_q$  are the spinvectors of the electron and the positron, and  $\lambda_p$ ,  $\lambda_q$  are the eigenvalues of the spinors with respect to the spinvector, that is, they have values of  $\pm 1$ .  $S(p, q)$  is a complex number, which has been calculated using an explicit form for the spinors for the standard form of the gamma matrices. In order to make the numerical calculations easier we have used polarisation vectors  $s_p$  and  $s_q$ , which are longitudinal vectors:

$$s_p = \frac{1}{\sqrt{p_0^2 - p_z^2}}(p_z, 0, 0, p_0) \quad (5.25)$$

and similar for  $s_q$ . The calculation of the trace has been done with the help of the algebraic calculation program FORM [62] (Note that the definition of  $\gamma_5$  used in this program differs by a factor of  $i$  from the one used by us). All sixteen different spin combinations have been calculated and summed. The final expression has to be real, which has been used to test the program (As the final expression can be expressed as a trace, which does not contain any  $\gamma_5$  matrices, it must be equivalent to an expression containing only real numbers and real scalar products, therefore it has to be real). The integration over four particles gives a 12-dimensional integral, of which one angular integration is trivial. It was calculated using the same MC method as before (VEGAS [65, 66]). Together with the total probability we have calculated also single differential probabilities by sorting the points into appropriate bins. The error of the total probability is always less than 1%. An explicit error estimate is given for all the differential probabilities. As our calculation is symmetric with respect to all four momenta and all four electron–positron combinations, this error has been calculated from the standard deviation of the four results.

Finally we want to point out that the expression in Eq. (5.22) can be interpreted also in a different way: If we calculate the reduced total two-pair creation probability exactly

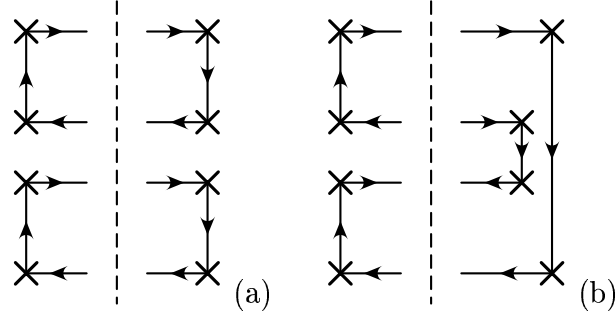


Figure 5.4: The two Feynman diagrams contributing to the two-pair creation in lowest order: The direct term (a) and the exchange term (b).

in lowest order according to the previous chapters, we get

$$P_{\text{total}}^{(2)} = \frac{1}{(2!)^2} \int d\Gamma(p_1)d\Gamma(p_2)d\Gamma(q_1)d\Gamma(q_2) [M^*(p_1, q_1)M^*(p_2, q_2) - M^*(p_1, q_2)M^*(p_2, q_1)] \times [M(p_1, q_1)M(p_2, q_2) - M(p_1, q_2)M(p_2, q_1)] \quad (5.26)$$

$$= \frac{1}{2} \int d\Gamma(p_1)d\Gamma(p_2)d\Gamma(q_1)d\Gamma(q_2) \left\{ |M(p_1, q_1)|^2 |M(p_1, q_1)|^2 - \text{Re} [M^*(p_1, q_1)M(p_2, q_1)M^*(p_2, q_2)M(p_1, q_2)] \right\} \quad (5.27)$$

$$= P_{\text{total}}^{(D)} - P_{\text{total}}^{(X)}. \quad (5.28)$$

The first term is the direct part, which is used in order to get the Poisson distribution, whereas the second term is the exchange part, which we neglect in the Poisson distribution (see also Fig. 5.4). Comparing the second expression with that in Eq. (5.22) we see that they are identical. Comparing Fig. 5.4 with Fig. 5.3 we see that we only have to change the interpretation of the diagram by cutting it at a different point. Therefore the result of the calculation for the total probability can also be used to test, if the neglect of the exchange term in order to get the Poisson distribution is justified.

### 5.3 Results for impact parameter $b$ zero

Figure 5.5 shows the results of our calculations for the reduced probability as a function of  $\gamma$ . In all our diagrams, we set  $Z\alpha = 1$ , as this is a common factor in all results. Also shown is the result for the corresponding probability of the lowest-order calculation. In order to test the dependence on the form factor the calculations have been done for the dipole form factor and the double dipole form factor. Both agree within the error interval, therefore we show only the results for the double dipole form factor here. We see that the correction is similar in size as the lowest-order result for large values of  $\gamma$ . Using realistic values for  $Z\alpha$  its importance is reduced, as the higher-order correction has to be

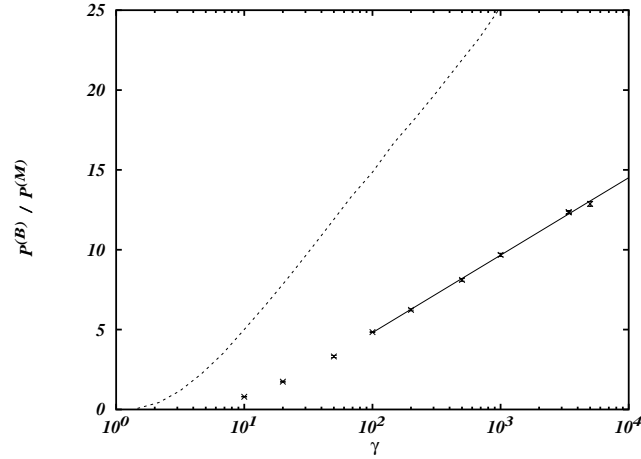


Figure 5.5: Comparison of the correction to the reduced one-pair creation probability with the lowest-order result as a function of  $\gamma$ .  $Z\alpha$  is set to 1. The points are the results of the calculation of the multiple-particle corrections, the solid line a fitted  $\ln \gamma$  dependence. The dotted line is the result of the lowest-order Born approximation.

	$\gamma$	Ion	$P^{(B)}$	$P^{(M)}$	
SPS	10	Pb	0.63	0.013	2.1 %
RHIC	100	Au	1.6	0.059	3.7 %
LHC	3400	Pb	3.9	0.21	5.3 %
LHC	3400	U	6.1	0.49	8.1 %

Table 5.1: Comparison of the contribution of the multiple-particle correction  $P^{(M)}$  to the reduced probability with the lowest order Born result  $P^{(B)}$  (see Eq. (5.22)).

multiplied by  $(Z\alpha)^8$ , the lowest-order result by  $(Z\alpha)^4$ . In Table 5.1 we give predictions for the contribution of the higher-order correction to the reduced total probability. For  $\gamma$  and  $Z$  we have used again typical values for relativistic heavy-ion colliders. The higher-order correction increases the reduced probability to up to about 5–10%. Therefore they should be observable in principal. Using this increased reduced total probability in the Poisson distribution we get the total  $N$ -pair probabilities as shown in Figs. 5.6 and 5.7. Based on this calculation we expect that higher-order corrections (5th order and more) are again only of about 5–10% of the third-order results and are therefore corrections of less than 1% to the total probability.

Also shown are a number of single differential probabilities, which are compared with the lowest-order results also. We show them here for  $\gamma = 10, 100, \text{ and } 3400$ . They are shown as a function of the energy  $P(E)$  (Fig. 5.9), of the angle of the momentum of one particle with the beam axis  $P(\theta)$  (Fig. 5.10), of the transverse momentum of one particle

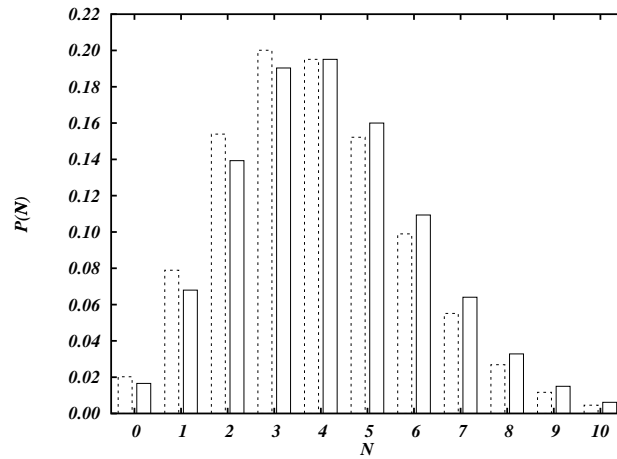


Figure 5.6: Total probabilities for the total  $N$ -pair production for  $\gamma = 3400$  and  $Pb$  ions based on the Poisson distribution. Dotted bars are the results of the lowest-order calculation, solid bars those with the inclusion of the multiple-particle processes.

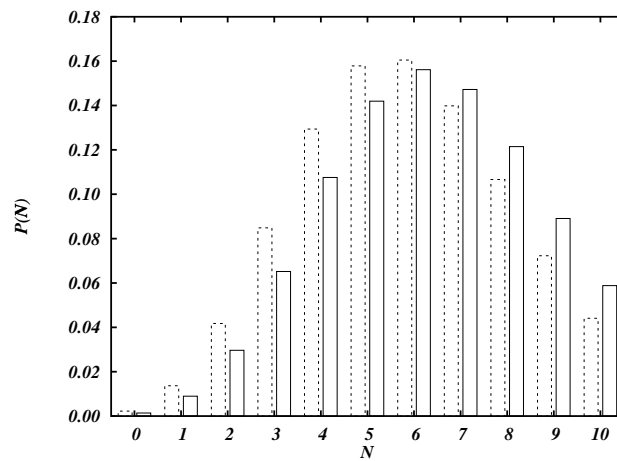


Figure 5.7: Total probabilities for the total  $N$ -pair production for  $\gamma = 3400$  and  $U$  ions. Same notation as in Fig. 5.6.

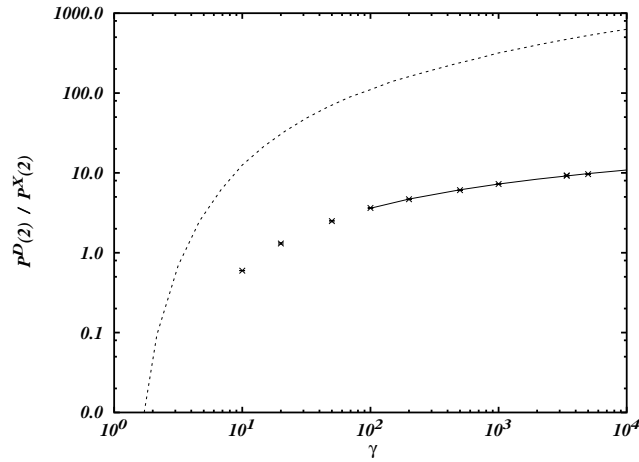


Figure 5.8: Comparison of the contributions of the direct process  $P^{(D)}$  (dotted line) and the exchange process  $P^{(X)}$  (solid line and data points) to the reduced two-pair creation process.  $Z\alpha$  is set to 1.

$P(p_{\perp})$  (Fig. 5.11), of the invariant mass  $P(M)$  (Fig. 5.12), the rapidity  $P(Y)$  (Fig. 5.13), and the transverse momentum of the pair  $P(P_{\perp})$  (Fig. 5.14). In all of these diagrams the single differential probability of the correction follows more or less the lowest-order result.

In Fig. 5.8 we compare both terms contributing to the total two-pair production probability. Here the first and the second diagrams of Fig. 5.4 are multiplied by the same factor  $(Z\alpha)^8$ , therefore the ratio of both curves gives directly the contribution of the exchange term to the first term, which is used in the Poisson distribution alone. We see that the exchange diagram contributes only with about 1% to the reduced total probability. Also its importance gets smaller for larger values of  $\gamma$ , therefore the use of the Poisson distribution seems to be justified. This could be different, of course, if one looks at differential probabilities in some region of the phase space.

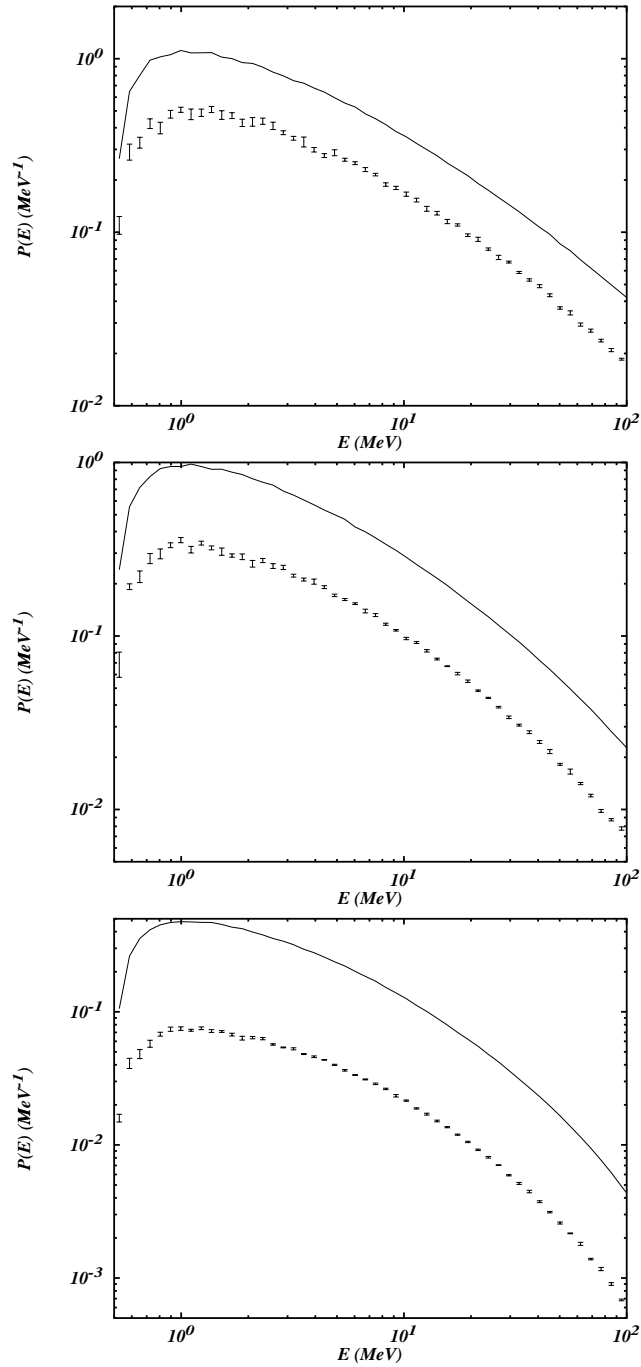


Figure 5.9: Comparison of the differential probability  $P(E)$  for  $\gamma = 3400$  (top),  $\gamma = 100$  (middle), and  $\gamma = 10$  (bottom). Data points are the results of the calculation of the multiple-particle correction, the solid line results of the lowest-order Born calculation.  $Z\alpha$  is set to 1.



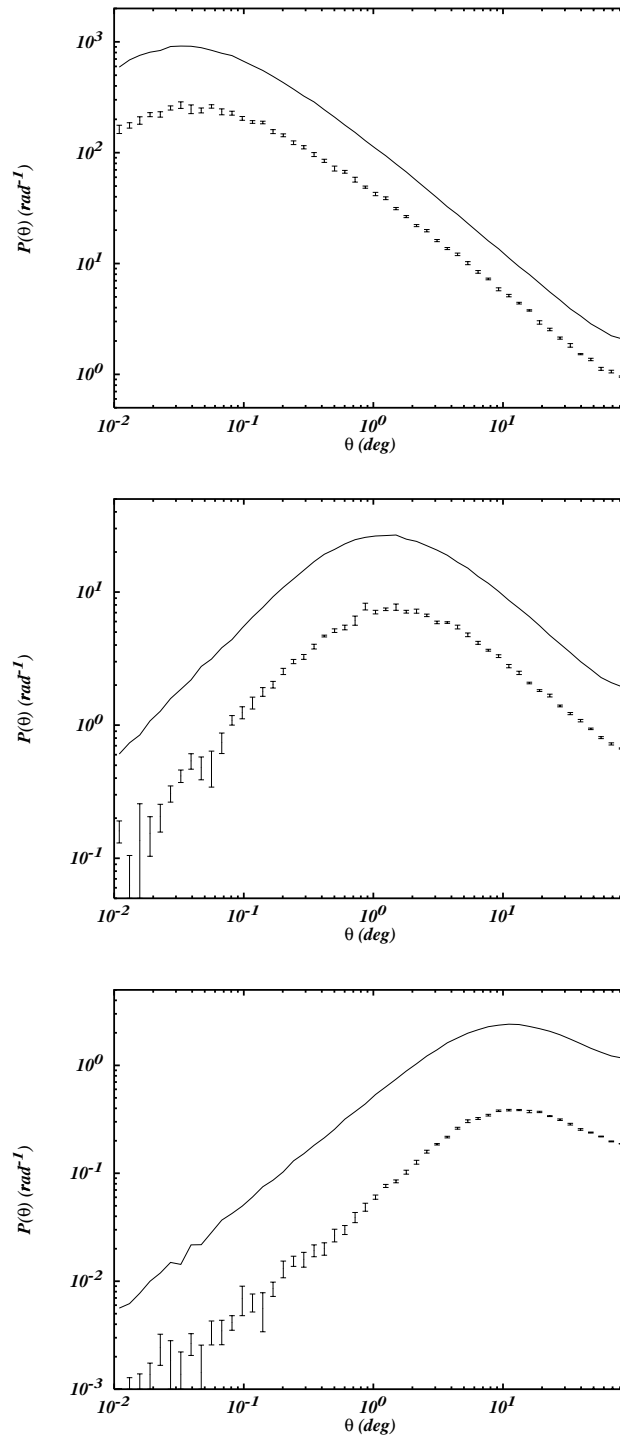


Figure 5.10: Comparison of the differential probability  $P(\theta)$  for  $\gamma = 3400$  (top),  $\gamma = 100$  (middle), and  $\gamma = 10$  (bottom). Definitions are the same as in Fig. 5.9.

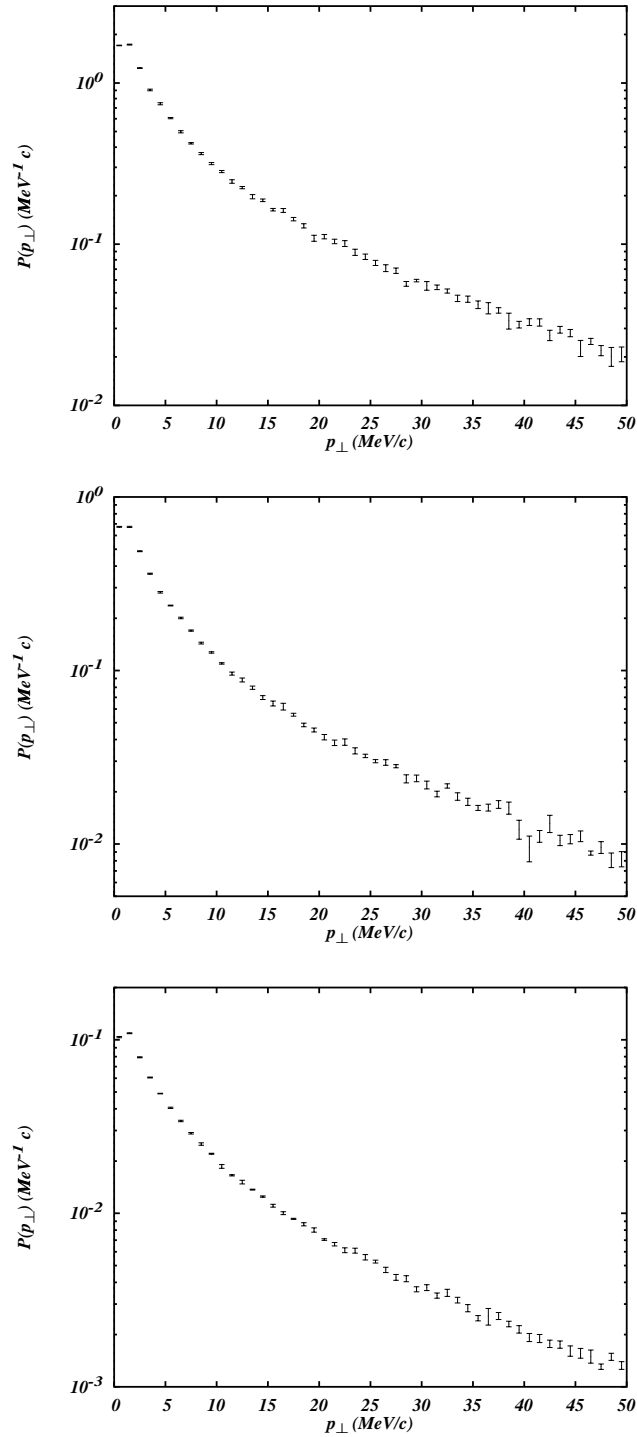


Figure 5.11: Results of the differential probability  $P(p_{\perp})$  for  $\gamma = 3400$  (top),  $\gamma = 100$  (middle), and  $\gamma = 10$  (bottom). Definitions are the same as in Fig. 5.9. No comparison with the lowest order is made.

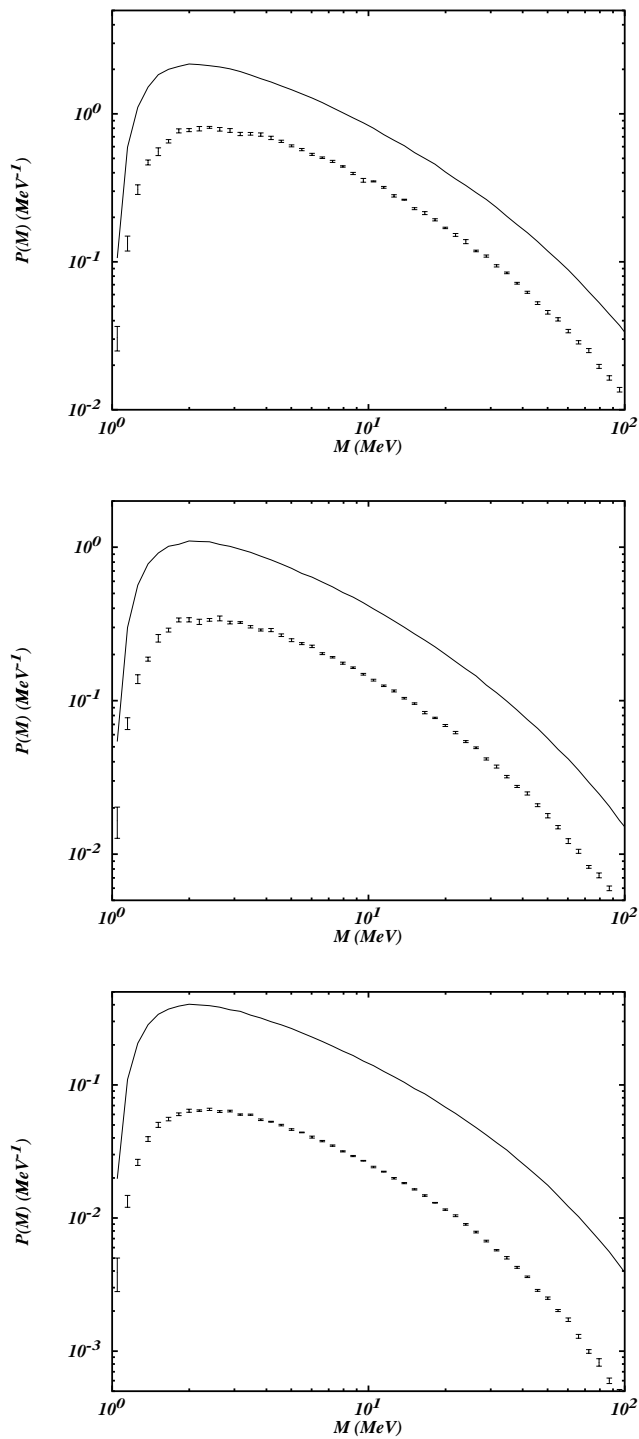


Figure 5.12: Comparison of the differential probability  $P(M)$  for  $\gamma = 3400$  (top),  $\gamma = 100$  (middle), and  $\gamma = 10$  (bottom). Definitions are the same as in Fig. 5.9.

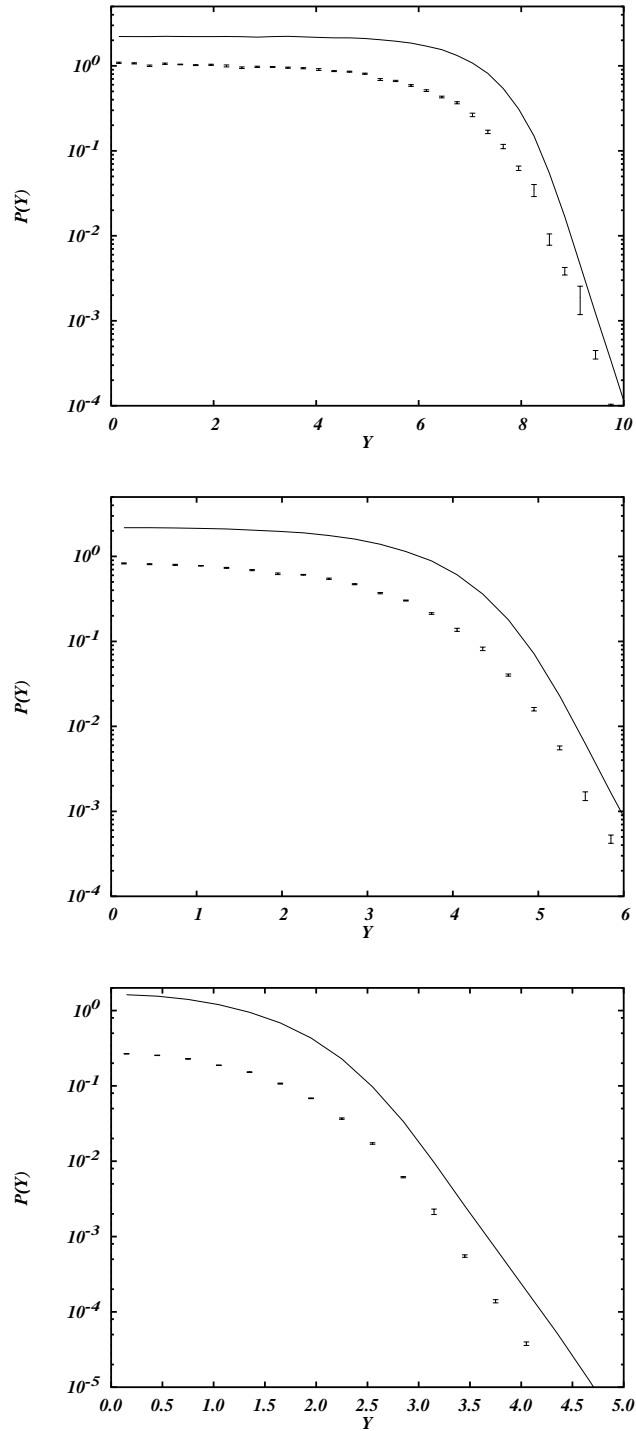


Figure 5.13: Comparison of the differential probability  $P(Y)$  for  $\gamma = 3400$  (top),  $\gamma = 100$  (middle), and  $\gamma = 10$  (bottom). Definitions are the same as in Fig. 5.9.

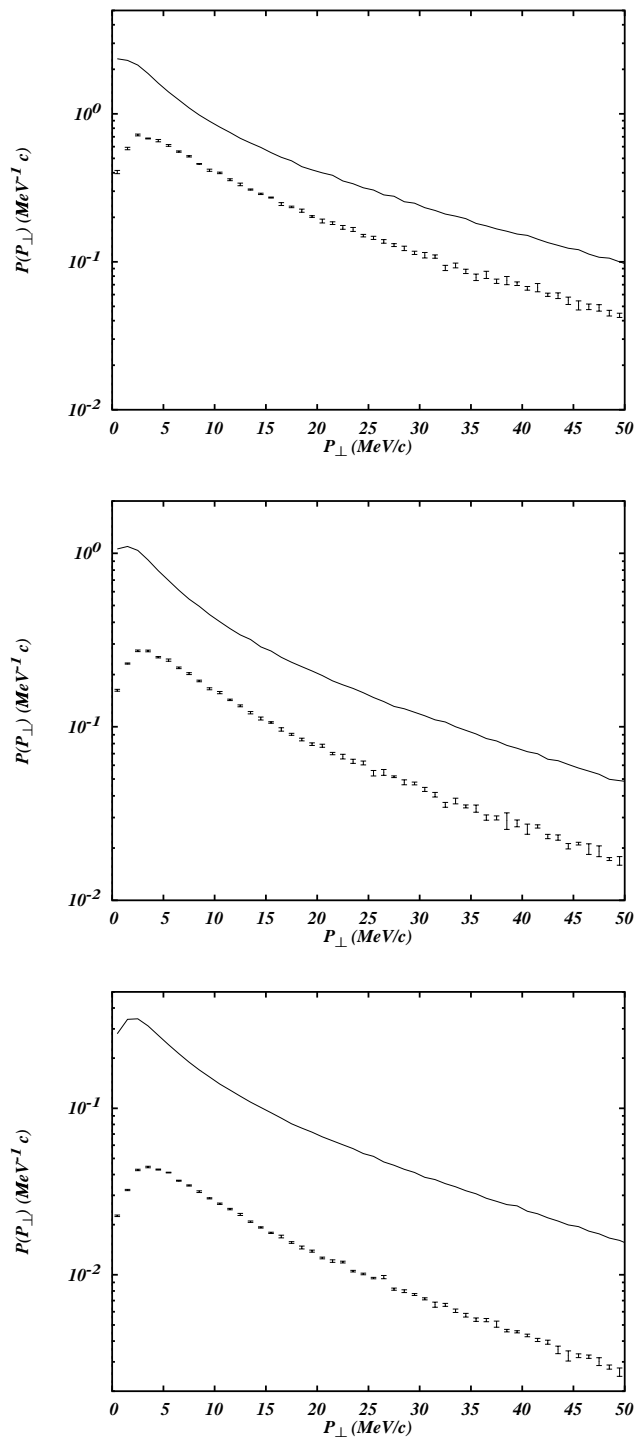


Figure 5.14: Comparison of the differential probability  $P(P_{\perp})$  for  $\gamma = 3400$  (top),  $\gamma = 100$  (middle), and  $\gamma = 10$  (bottom). Definitions are the same as in Fig. 5.9.



# Chapter 6

## Conclusions and Outlook

*“We have seen that the cross-section for pair creation by a fast charged particle increases at least as  $\log^2 E_0$  . . . Theoretically, when  $E_0 \rightarrow \infty$ , it becomes infinitely large. This is clearly impossible . . . The indefinite increase also contradicts the elementary fact that all probabilities are normalized to unity and therefore the probability of the final state cannot increase indefinitely. The reason for this failure must be sought in the application of perturbation theory. In particular it is to be expected that the damping effects will eventually limit the cross-section. However, the question is academic because the energy where this becomes effective is so high (owing to the logarithmic increase) that the correction need not be considered.”*

W. Heitler, *The Quantum Theory of Radiation*, 1954, p.265f

### 6.1 Conclusions

We have studied various aspects of the electron-positron pair creation in relativistic heavy-ion collisions. First we looked at the general theory of pair creation in an external field using several different approaches. The main result of all these models was the fact that the  $N$ -pair creation amplitude can be reduced to an antisymmetrised product of  $N$  reduced one-pair creation amplitudes and the vacuum amplitude. The many particle aspect is only present in the antisymmetrisation of these amplitudes in the final state. If one neglects all exchange terms and therefore neglects in principle the Pauli principle in the final state, one gets a simple Poisson distribution for the total probabilities. Contrary to other models, we had not to restrict the processes to a subclass only in order to get this result. Especially all Coulomb rescattering and multiple-particle effects can be included.

In order to calculate arbitrary higher-order processes the only amplitudes that are really needed are the reduced one-pair creation amplitude and the vacuum amplitude. If we use the approximate Poisson distribution, things are even easier. Now we only need the reduced one-pair creation probability.

Using perturbation theory we have been able to find explicit forms for the reduced one-pair creation amplitude, which is identical to the normal perturbation expansion of

the one-pair creation amplitude and neglecting all vacuum processes, that is, neglecting all diagrams with disconnected parts, and for the vacuum amplitude, which was found to be the sum over all possible closed fermion loops. Both amplitudes are therefore accessible through perturbation theory. None of them was found to be of a principal nonperturbative character.

Comparing the Feynman interpretation of the pair creation with the Dirac sea picture we found that the Feynman picture leads to much simpler formulae and also to a much easier interpretation of the processes. In the Dirac sea picture we found that in order to include higher-order corrections we had to go from the single particle to the many particle theory, whereas the inclusion of these higher-order processes was without any problems in the Feynman picture. One of the big advantages compared with the Dirac sea picture was the fact that the individual processes are really separated in the Feynman picture, whereas in the Dirac sea picture they can not be separated that easily. We found that in the calculation of the higher-order amplitudes the Pauli principle is neglected for the intermediate particles (according to the rules of the Feynman diagrams), as the effects coming from this neglect are compensated by the inclusion of the vacuum processes.

Comparing our models with those found earlier we found that all three models are essentially “quasi boson” models because of the restrictions on the processes, which are included. Our investigations suggest that there are higher-order processes, which can not be described in the quasi boson models, as they are multiple-particle effects. But as the quasi bosonic treatment is not necessary for the Poisson distribution, the inclusion of these multiple-particle corrections is easy, as one only has to include them in the calculation of the reduced one-pair creation probability.

Finally we have derived the general form of the  $S$  operator in second-order Magnus theory. As this is an expansion in the interaction time it is a good approximation in this case. The result was found to be of a simple form and the interpretation of the individual terms was easy.

Starting with Chapter 3 we looked at explicit calculations of the  $b$  dependent probability. The reduced probability was calculated in lowest order (second order) first for impact parameter  $b$  zero, where an analytic form for the matrix element was found, and then also for arbitrary small  $b$ . Differential probabilities have been calculated also for impact parameter  $b$  zero. A comparison with EPA and DEPA showed that these approximations fail at small  $b$ . The reason for this was found to be the neglect of the dependence of the matrix element from the momentum of the intermediate fermion. A comparison between DEPA and the exact calculation for large invariant masses showed that both also disagree there at small angle  $\theta$ . DEPA was therefore too large also for large invariant masses. The reason for this was found to be due to the mass singularity in the photo cross section.

The influence of the extended charge distribution on the  $b$  dependent probability was studied with the help of some simple form factors. It was found that the form factor changes the total probability considerably for small  $b$  especially for values of the size of the nuclear radius, where the probability was found to reach a constant value for  $b \rightarrow 0$  and for an extended charge distribution, whereas it diverges logarithmically for a point charge. The calculation for  $b$  zero are therefore a good approximation for very close collisions, that



is, for collisions with an impact parameter of the size of the nuclear radius.

In Chap. 5 we looked at the higher-order corrections to the reduced one-pair creation. We found the explicit form of these corrections, where we neglected the Coulomb rescattering terms and used second-order Magnus theory. The lowest of these multiple-particle corrections was calculated and found to increase the reduced total probability to about 5–10%. Differential probabilities were calculated also and it was found that they follow the lowest-order results more or less. Comparing the exact form of the two-pair creation probability with the Poisson distribution we found that the deviation from the Poisson distribution is rather small of the size of 1%, so that the use of the Poisson distribution seems to be justified.

## 6.2 Outlook

We hope that this work has thrown some light on the higher-order processes of electron-positron pair creation in heavy-ion collisions. The theoretical results indicate that for the calculation of all higher-order processes only the reduced one-pair creation probability is really necessary. The second-order Magnus theory, which was used here without the Coulomb rescattering terms and for the calculation of a single process only, could be a good starting point for an extension of the present calculation, especially as all processes appearing in the exponential (see Eq. (2.81) and also Fig. 2.8) could be calculated analytical in principle. Even though we think that the Coulomb rescattering will only be of minor importance for the total probability for very large values of  $\gamma$ , a detailed calculation is useful especially for the differential probabilities. Also there have been some indications in the recent past, that Coulomb scattering may increase the total probability for smaller values of  $\gamma$  [28], so that this area should be studied in more detail.

Our calculation have shown also that  $b$  dependent probabilities can be calculated reliably. In order to study the higher-order process it is necessary to look at small impact parameter. The experimental challenge now consists of finding a way how the impact parameter can be measured or at least how one can tag collisions with small impact parameter. The deflection angle of the ions could be used in principle for this, even though it is very small and therefore may not be observable. It has also been proposed to look at the electron-positron pair creation together with other reactions, which mainly occur at small impact parameter. For example, one might look at pair creation together with the production of a muon pair [75] or with the emission of a neutron from the heavy ions [76].

As indicated in the calculations of the  $b$  dependent probability, our calculations can also be used in order to look at the total cross section along the line of Botcher and Strayer [11]. Besides the calculation of the electron-positron pairs it might be interesting to look also at the muon pair production, which has been proposed for the measurement of the beam luminosity at LHC [77]. For this it might be necessary also to use a more realistic form factor in the calculation.

If multiple-particle creation becomes accessible in experiments, more detailed calculations of the two-pair production may be necessary, especially for the differential probab-

ities, where the exchange term may now be important.

Also the electron-positron pair production is only one of a variety of electromagnetic processes, which are of interest. The calculation of the cross section for the pair creation with capture is important for the design of the heavy-ion colliders, as it is one of the processes, which limits the life time of the beam. The calculation of muon pair production has already been mentioned. It has the advantage, that the calculations are in principle identical to the electron-positron case. Other particles may be produced and studied also in electromagnetic collisions, as already mentioned in the introduction. Especially the production of light mesons may be interesting there, as they are produced in large quantities in these collisions.

Electromagnetic processes are surely not the reason why relativistic heavy-ion colliders are planned and built. But they can provide us with informations, which are to some extend complementary to the central collisions. Measurements are much cleaner because of the smaller multiplicities and therefore allow much more detailed investigations of the individual processes.

But especially the electron-positron pair creation allows one to study QED with strong fields. The fact, that higher-order processes are important there, has already been noted early, as can be seen from the quote of W. Heitler above. But whereas the measurement of these effects was not possible at that time, relativistic heavy-ion collisions allow us to study quantum electrodynamic with strong external fields from a new point of view.

# Chapter 7

## Appendix

### A.1 Conventions and notations

In this appendix we discuss the conventions and notations used throughout this work. We use natural units with  $\hbar = c = 1$ . The metric tensor is

$$g^{\mu\nu} = \begin{pmatrix} 1 & 0 & 0 & 0 \\ 0 & -1 & 0 & 0 \\ 0 & 0 & -1 & 0 \\ 0 & 0 & 0 & -1 \end{pmatrix}. \quad (\text{A.1})$$

For the Dirac equation we use the standard form of the gamma matrices

$$\gamma^0 = \begin{pmatrix} \mathbf{1} & \mathbf{0} \\ \mathbf{0} & -\mathbf{1} \end{pmatrix}, \quad \gamma^i = \begin{pmatrix} \mathbf{0} & \sigma^i \\ -\sigma^i & \mathbf{0} \end{pmatrix}, \quad (\text{A.2})$$

and also for  $\gamma_5$ :

$$\gamma_5 = i\gamma^0\gamma^1\gamma^2\gamma^3 = \begin{pmatrix} \mathbf{0} & \mathbf{1} \\ \mathbf{1} & \mathbf{0} \end{pmatrix}. \quad (\text{A.3})$$

The solutions of the free Dirac equation

$$(\not{p} - m)\Psi = 0 \quad (\text{A.4})$$

(with the usual definition of the Feynman dagger  $\not{p} = \gamma_i p^i$ ) are

$$\Psi(x, s) = u(p, s) \exp(-ipx), \quad (\text{A.5a})$$

$$\Psi(x, s) = v(p, s) \exp(+ipx). \quad (\text{A.5b})$$

The Dirac spinors  $u(p, s)$  and  $v(p, s)$  are normalized to

$$\bar{u}_r(p)u_s(p) = 2m\delta_{rs}, \quad \bar{v}_r(p)v_s(p) = -2m\delta_{rs}. \quad (\text{A.6})$$

(This normalization differs from the one used by other authors, for example[78, 79], by a factor  $2m$  leading to expressions with differ by the same factor.) They have the properties:

$$u(p, s)\bar{u}(p, s) = (\not{p} + m)\frac{1 + \gamma_5 \not{s}}{2}, \quad (\text{A.7a})$$

$$v(p, s)\bar{v}(p, s) = (\not{p} - m)\frac{1 + \gamma_5 \not{s}}{2}, \quad (\text{A.7b})$$

and also the spin sums

$$\sum_s u(p, s)\bar{u}(p, s) = (\not{p} + m), \quad (\text{A.8a})$$

$$\sum_s v(p, s)\bar{v}(p, s) = (\not{p} - m). \quad (\text{A.8b})$$

$s$  denotes the eigenvalues of the spin. The corresponding spin vector  $s^\mu$  is defined by the two properties

$$s^2 = -1, \quad sp = 0, \quad (\text{A.9})$$

which can be verified easily in the rest frame. For the calculations in Chap. 5 we need the explicit form of the longitudinal spin vector, i.e., with only zero and z component. One sees easily that for an arbitrary momentum  $p$  it is given by

$$s_p = \frac{1}{\sqrt{p_0^2 - p_z^2}}(p_z, 0, 0, p_0). \quad (\text{A.10})$$

The decomposition of the field operator into the free solutions is given by

$$\Psi(x) = \sum_s \int d\tilde{p} \left[ b(p, s)u(p, s) \exp(-ipx) + d^+(p, s)v(p, s) \exp(ipx) \right], \quad (\text{A.11a})$$

$$\bar{\Psi}(x) = \sum_s \int d\tilde{p} \left[ b^+(p, s)\bar{u}(p, s) \exp(ipx) + d(p, s)\bar{v}(p, s) \exp(-ipx) \right], \quad (\text{A.11b})$$

where we have defined  $d\tilde{p}$  as

$$d\tilde{p} := \frac{d^3p}{(2\pi)^{3/2}(2p_0)^{1/2}}. \quad (\text{A.12})$$

We define also the factor of  $d\tilde{p}$  as

$$\gamma(p) = \frac{1}{(2\pi)^{3/2}(2p_0)^{1/2}}. \quad (\text{A.13})$$

The Lorentz-invariant phase space is given by

$$d\Gamma(p) := \frac{d^3p}{(2\pi)^3 2p_0}. \quad (\text{A.14})$$

Following the decomposition of the field into the free solutions, we define the four-dimensional Fourier transformation as

$$f(x^\mu) = \int \frac{d^4 p}{(2\pi)^4} \hat{f}(p^\mu) \exp(-ip^\nu x_\nu), \quad (\text{A.15a})$$

$$\hat{f}(p^\mu) = \int d^4 x f(x^\mu) \exp(ip^\nu x_\nu), \quad (\text{A.15b})$$

Since we write the wave equation of the electromagnetic potential as

$$\square A^\mu(x) = j^\mu(x) \quad (\text{A.16})$$

the fine structure constant has to be defined as  $\alpha := e^2/(4\pi)$ .

## A.2 Connection between particle operators

In Chap. 2 we made use of the connection between the particle creation and annihilation operators for  $t \rightarrow \pm\infty$  in the interaction picture. We are going to derive this connection here first in the Heisenberg picture and then transform it back into the interaction picture (see also, for example, [35, 53, 56, 80]).

As described in the introduction we assume that the system changes only under the influence of the external field and also vanishes asymptotically, so that we have the free system then.

Let us start in the Heisenberg picture. In this picture the states are time independent and so are the creation and annihilation operators. The field operator can be decomposed in two different ways similar to Eq. (A.11) corresponding to the two different asymptotic systems:

$$\Psi(x) = \sum_{i>0} \phi_i^{IN}(x) b_i^{IN} + \sum_{j<0} \phi_j^{IN} d_j^{IN+} \quad (\text{A.17a})$$

$$\Psi(x) = \sum_{i>0} \phi_i^{OUT}(x) b_i^{OUT} + \sum_{j<0} \phi_j^{OUT} d_j^{OUT+} \quad (\text{A.17b})$$

and similar for  $\bar{\Psi}$ . Here the  $\phi^{IN}$ 's are the wave functions of the system going over to the free solutions for  $t \rightarrow -\infty$  and similar for the  $\phi^{OUT}$ 's for  $t \rightarrow \infty$ .  $i > 0$  means that we only sum over the states of the positive continuum,  $j < 0$  only over the states of the negative continuum.

The (time-independent) creation and annihilation operators  $b^{IN}$ ,  $d^{IN}$ , etc., are therefore the particle creation and annihilation operators of the initial system and similar for  $OUT$  and the final system. The general  $N$ -particle initial state is given by

$$|i\rangle = b_{k_1}^{IN+} \dots b_{k_m}^{IN+} d_{l_1}^{IN+} \dots d_{l_n}^{IN+} |0, IN\rangle. \quad (\text{A.18})$$

Here the  $IN$  vacuum state is defined as the state that is annihilated by all  $IN$  annihilation operators. The same is also defined for the  $OUT$  system, where  $|0, IN\rangle$  and  $|0, OUT\rangle$  normally do not coincide.

The matrix element for an arbitrary process from  $i$  to  $f$  is given by

$$\langle f, OUT | i, IN \rangle \quad (\text{A.19})$$

( $OUT$  and  $IN$  have been written explicitly in order to emphasize the difference of both).

As the  $\phi^{IN}$  and also the  $\phi^{OUT}$  form orthonormal systems, we can find a relation between them and therefore also between the  $IN$  and  $OUT$  particle operators. Forming the scalar product of  $\Psi$  with  $\phi_p^{OUT}$ , we get

$$b_p^{OUT} = \sum_{i>0} a_{pi} b_i^{IN} + \sum_{j<0} a_{pj} d_j^{IN+} \quad (\text{A.20a})$$

$$d_q^{OUT+} = \sum_{i>0} a_{qi} b_i^{IN} + \sum_{j<0} a_{qj} d_j^{IN+}, \quad (\text{A.20b})$$

where we have defined the matrix  $a_{pi}$  as

$$a_{pi} = \left( \phi_p^{OUT}, \phi_i^{IN} \right) \quad (\text{A.21})$$

with  $p$  and  $i$  any state of the positive or negative continuum.

Forming the scalar product with  $\phi_p^{IN}$  and using also the conjugate forms we get the relation between all eight particle operators:

$$b_p^{OUT} = \sum_{i>0} a_{pi} b_i^{IN} + \sum_{j<0} a_{pj} d_j^{IN+}, \quad (\text{A.22a})$$

$$d_q^{OUT} = \sum_{i>0} a_{qi}^* b_i^{IN+} + \sum_{j<0} a_{qj}^* d_j^{IN}, \quad (\text{A.22b})$$

$$b_p^{OUT+} = \sum_{i>0} a_{pi}^* b_i^{IN+} + \sum_{j<0} a_{pj}^* d_j^{IN}, \quad (\text{A.22c})$$

$$d_q^{OUT+} = \sum_{i>0} a_{qi} b_i^{IN} + \sum_{j<0} a_{qj} d_j^{IN+}, \quad (\text{A.22d})$$

$$b_p^{IN} = \sum_{i>0} a_{ip}^* b_i^{OUT} + \sum_{j<0} a_{jp}^* d_j^{OUT+}, \quad (\text{A.22e})$$

$$d_q^{IN} = \sum_{i>0} a_{ip} b_i^{OUT+} + \sum_{j<0} a_{jp} d_j^{OUT}, \quad (\text{A.22f})$$

$$b_p^{IN+} = \sum_{i>0} a_{ip} b_i^{OUT+} + \sum_{j<0} a_{jp} d_j^{OUT}, \quad (\text{A.22g})$$

$$d_q^{IN+} = \sum_{i>0} a_{iq}^* b_i^{OUT} + \sum_{j<0} a_{jq}^* d_j^{OUT+}. \quad (\text{A.22h})$$

Now we transform this relation into the interaction picture. In this picture the creation and annihilation operators of the free system are time independent, whereas our Heisenberg

particle operators will be time dependent. As the interaction vanishes for  $t \rightarrow \pm\infty$  they reach an asymptotic value, which coincides with those of the free system. Generally the connection between an operator in the Heisenberg picture and the interaction picture is given by

$$O_H(t) = U^{-1}(t) O_I(t) U(t), \quad (\text{A.23})$$

where  $U(t)$  is the time development operator given in our case by

$$U(t) = \mathcal{T} \exp \left[ -i \int_{-\infty}^t H_I(t) dt \right]. \quad (\text{A.24})$$

As the  $S$  operator corresponds to  $U(\infty)$  and  $U(-\infty) = 1$ , we find for the creation and annihilation operators in the corresponding limes

$$b_p^{OUT} = U^{-1}(\infty) b_p(\infty) U(\infty) = S^{-1} b_p S \quad (\text{A.25a})$$

$$b_p^{IN} = U^{-1}(-\infty) b_p(-\infty) U(-\infty) = b_p \quad (\text{A.25b})$$

and the same relation is also true for all other  $OUT$  and  $IN$  creation and annihilation operators. We have no longer written  $IN$  and  $OUT$  indices on the right side, as we know, that the operators go over to the creation and annihilation operators of the free system in the corresponding asymptotic cases. Using this in Eq. (A.22) we get the corresponding relation in the interaction picture.

$$b_p S = \sum_{i>0} a_{pi} S b_i + \sum_{j<0} a_{pj} S d_j^+, \quad (\text{A.26a})$$

$$d_q S = \sum_{i>0} a_{qi}^* S b_i^+ + \sum_{j<0} a_{qj}^* S d_j, \quad (\text{A.26b})$$

$$b_p^+ S = \sum_{i>0} a_{pi}^* S b_i^+ + \sum_{j<0} a_{pj}^* S d_j, \quad (\text{A.26c})$$

$$d_q^+ S = \sum_{i>0} a_{qi} S b_i + \sum_{j<0} a_{qj} S d_j^+, \quad (\text{A.26d})$$

$$S b_p = \sum_{i>0} a_{ip}^* b_i S + \sum_{j<0} a_{jp}^* d_j^+ S, \quad (\text{A.26e})$$

$$S d_q = \sum_{i>0} a_{ip} b_i^+ S + \sum_{j<0} a_{jp} d_j S, \quad (\text{A.26f})$$

$$S b_p^+ = \sum_{i>0} a_{ip} b_i^+ S + \sum_{j<0} a_{jp} d_j S, \quad (\text{A.26g})$$

$$S d_q^+ = \sum_{i>0} a_{iq}^* b_i S + \sum_{j<0} a_{jq}^* d_j^+ S. \quad (\text{A.26h})$$

These are the relations, that we need in Sec. 2.3. They are of a retarded type and therefore correspond to the Dirac sea interpretation, as they connect the final state of electrons and positrons with those of the initial states of electrons and positrons.

Following Feynman we want to translate these relations into a connection of the particle operators with different boundary conditions. For this we start, for example, with

Eq. (A.26a):

$$b_p S = \sum_{i>0} a_{pi} S b_i + \sum_{j<0} a_{pj} S d_j^+. \quad (\text{A.27})$$

In the Stückelberg-Feynman interpretation the positron is a particle moving backward in time, therefore the positron creation operator in this equation should be seen as an outgoing line and therefore should not appear at the right side. In order to eliminate this part of the equation we subtract from this equation a linear combination of Eq. (A.26d) of the form

$$\sum_{q<0} g_{pq} d_q^+ S = \sum_{i>0, q<0} g_{pq} a_{qi} S b_i + \sum_{j<0, q<0} g_{pq} a_{qj} S d_j^+. \quad (\text{A.28})$$

As we want that the term with  $S d_j^+$  vanishes, we define  $g_{pq}$  so that the contributions of both cancel:

$$\sum_{q<0} g_{pq} a_{qj} = a_{pj}. \quad (\text{A.29})$$

Formally this can be solved for  $g_{pq}$  by using  $a^I$ , the inverse of  $a$ , defined by

$$\sum_{j<0} a_{qj} a_{jl}^I = \delta_{ql}, \quad (\text{A.30})$$

where we have used the index  $I$  instead of the normal  $-1$  in order to emphasize that the inverse is defined through a summation over the negative continuum only, whereas  $a^{-1}$  is the inverse of the full matrix  $a$  defined in the negative and positive continuum.

$g_{pq}$  is then given by

$$g_{pq} = \sum_{j<0} a_{pj} a_{jq}^I. \quad (\text{A.31})$$

Subtracting now the second equation from the first one we get

$$b_p S - \sum_{q<0} g_{pq} d_q^+ S = \sum_{i>0} \left( a_{pi} - \sum_{q<0} g_{pq} a_{qi} \right) S b_i \quad (\text{A.32})$$

and therefore

$$b_p S = \sum_{i>0} \left( a_{pi} - \sum_{q<0} g_{pq} a_{qi} \right) S b_i + \sum_{q<0} g_{pq} d_q^+ S \quad (\text{A.33})$$

$$=: \sum_{i>0} s_{pi}^{++} S b_i + \sum_{j<0} s_{pj}^{+-} d_j^+ S. \quad (\text{A.34})$$

This is the relation we need in Sec. 2.1. It gives the final electron states through the initial electron states and the final positron states and therefore corresponds to the Feynman boundary conditions.



### A.3 Vacuum expectation values and singular functions

In principal the connection between the vacuum expectation values of the time-ordered and anti-time-ordered product with the singular functions is straightforward. But as the notation of these together with those of the propagators is different in nearly all textbooks and as the anti-time-ordered product is rather uncommon, we will give here a short derivation of this connection especially for the difference of the time-ordered and anti-time-ordered product (Eq. (2.75)).

We will derive first the three-dimensional momentum form of the products and then compare these results with the ones we obtain from the corresponding form of the singular functions by integration with respect to the time coordinate.

The field operator and its conjugate are given by (Eq. (A.11))

$$\Psi(x) = \sum_s \int d\tilde{p} \left[ b(p, s) u(p, s) \exp(-ipx) + d^+(p, s) v(p, s) \exp(ipx) \right], \quad (\text{A.35a})$$

$$\bar{\Psi}(x) = \sum_s \int d\tilde{p} \left[ b^+(p, s) \bar{u}(p, s) \exp(ipx) + d(p, s) \bar{v}(p, s) \exp(-ipx) \right], \quad (\text{A.35b})$$

where the operators  $b$  and  $d$  obey the usual anticommutation relations

$$\{b(p, s), b^+(p', s')\} = \{d(p, s), d^+(p', s')\} = \delta_{ss'} \delta(\vec{p} - \vec{p}'). \quad (\text{A.36})$$

For the definition of  $d\tilde{p}$  see Eq. (A.12). For the simple vacuum expectation values without any ordering we get

$$\begin{aligned} \langle 0 | \Psi(x) \bar{\Psi}(x') | 0 \rangle &= \\ & \sum_{s, s'} \int d\tilde{p} d\tilde{p}' \langle 0 | \left[ b(p, s) u(p, s) \exp(-ipx) + d^+(p, s) v(p, s) \exp(ipx) \right] \\ & \times \left[ b^+(p', s') \bar{u}(p', s') \exp(ip'x') + d(p', s') \bar{v}(p', s') \exp(-ip'x') \right] | 0 \rangle. \end{aligned} \quad (\text{A.37})$$

As  $d|0\rangle = 0$  and  $\langle 0|d^+ = 0$  this reduces to

$$\begin{aligned} \langle 0 | \Psi(x) \bar{\Psi}(x') | 0 \rangle &= \\ & \sum_{s, s'} \int d\tilde{p} d\tilde{p}' \langle 0 | b(p, s) b^+(p', s') | 0 \rangle u(p, s) \bar{u}(p', s') \exp(-ipx + ip'x'). \end{aligned} \quad (\text{A.38})$$

Using  $\langle 0 | b(p, s) b^+(p', s') | 0 \rangle = \delta_{ss'} \delta(\vec{p} - \vec{p}')$  and  $\sum_s u(p, s) \bar{u}(p, s) = (\not{p} + m)$  this finally gives

$$\langle 0 | \Psi(x) \bar{\Psi}(x') | 0 \rangle = \int d\Gamma(p) (\not{p} + m) \exp(-ip(x - x')). \quad (\text{A.39})$$

The other simple vacuum expectation value, which we need, gives

$$\langle 0 | \bar{\Psi}(x') \Psi(x) | 0 \rangle = \sum_{s, s'} \int d\tilde{p} d\tilde{p}'$$

$$\begin{aligned}
& \times \langle 0 | \left[ b^+(p', s') \bar{u}(p', s') \exp(ip'x') + d(p', s') \bar{v}(p', s') \exp(-ip'x') \right] \\
& \times \left[ b(p, s) u(p, s) \exp(-ipx) + d^+(p, s) v(p, s) \exp(ipx) \right] | 0 \rangle \\
& = \sum_{s, s'} \int d\tilde{p} d\tilde{p}' \\
& \quad \times \langle 0 | d(p', s') d^+(p, s) | 0 \rangle v(p, s) \bar{v}(p', s') \exp(-ip'x') \exp(ipx) \\
& = \sum_s \int d\Gamma(p) v(p, s) \bar{v}(p, s) \exp(ip(x - x')) \\
& = \int d\Gamma(p) (\not{p} - m) \exp(ip(x - x')). \tag{A.40}
\end{aligned}$$

From these we can directly derive the ordered vacuum expectation values with the help of the step function  $\Theta$ :

$$\mathcal{T}\Psi(x)\bar{\Psi}(x') = \Theta(t - t')\Psi(x)\bar{\Psi}(x') - \Theta(t' - t)\bar{\Psi}(x')\Psi(x) \tag{A.41}$$

and therefore the vacuum expectation value is:

$$\begin{aligned}
\langle 0 | \mathcal{T}\Psi(x)\bar{\Psi}(x') | 0 \rangle & = \Theta(t - t') \langle 0 | \Psi(x)\bar{\Psi}(x') | 0 \rangle \\
& \quad - \Theta(t' - t) \langle 0 | \bar{\Psi}(x')\Psi(x) | 0 \rangle \tag{A.42}
\end{aligned}$$

$$\begin{aligned}
& = \Theta(t - t') \int d\Gamma(p) (\not{p} + m) \exp(-ip(x - x')) \\
& \quad - \Theta(t' - t) \int d\Gamma(p) (\not{p} - m) \exp(ip(x - x')) \tag{A.43}
\end{aligned}$$

and similar for  $\mathcal{A}$ . For  $\mathcal{D} = \mathcal{T} - \mathcal{A}$ , we get

$$\begin{aligned}
\langle 0 | \mathcal{D}\Psi(x)\bar{\Psi}(x') | 0 \rangle & = \epsilon(t - t') \left[ \int d\Gamma(p) (\not{p} + m) \exp(-ip(x - x')) \right. \\
& \quad \left. + \int d\Gamma(p) (\not{p} - m) \exp(ip(x - x')) \right]. \tag{A.44}
\end{aligned}$$

For the sum of  $\mathcal{T}$  and  $\mathcal{A}$ , which we need in the calculation of the vacuum diagrams, we get

$$\begin{aligned}
\langle 0 | (\mathcal{T} + \mathcal{A})\Psi(x)\bar{\Psi}(x') | 0 \rangle & = \int d\Gamma(p) (\not{p} + m) \exp(-ip(x - x')) \\
& \quad - \int d\Gamma(p) (\not{p} - m) \exp(ip(x - x')). \tag{A.45}
\end{aligned}$$

We derive now the corresponding forms of the singular functions by integrating over the zero component of the four-momentum. Please note that the zero component in these formulae can be positive or negative unless stated otherwise, contrary to  $p_0$  in the previous formulae, which was always the physical energy and therefore positive. Our notation follows in principal the one used by Bjorken and Drell [78, 79].

The first singular function is the Feynman propagator, defined as

$$S_F(x - x') := \int \frac{d^4p}{(2\pi)^4} \frac{\not{p} + m}{p^2 - m^2 + i\epsilon} \exp(-ip(x - x')). \tag{A.46}$$

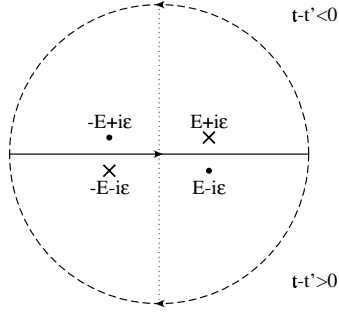


Figure A.1: Poles of the singular functions and the integration paths in the complex  $p_0$  plane. The dots are the poles of  $S_F$ , the crosses the poles of  $S_A$ .

For the integration we need the zero points of the denominator, which are at

$$p_0 = \pm \sqrt{\vec{p}^2 + m^2 - i\epsilon} \approx \pm \left( \sqrt{\vec{p}^2 + m^2} - i\epsilon \right) =: \pm(E - i\epsilon), \quad (\text{A.47})$$

where  $E$  is defined as the “physical energy”  $\sqrt{\vec{p}^2 + m^2} > 0$ . The denominator can therefore be written as

$$p^2 - m^2 + i\epsilon = (p_0 - E + i\epsilon)(p_0 + E - i\epsilon) \quad (\text{A.48})$$

giving

$$S_F(x - x') = \int \frac{d^3p}{(2\pi)^3} \exp(i\vec{p}(\vec{x} - \vec{x}')) \int \frac{dp_0}{(2\pi)} \frac{(\not{p} + m)}{(p_0 - E + i\epsilon)(p_0 + E - i\epsilon)} \exp(-ip_0(t - t')). \quad (\text{A.49})$$

As usual we close the integration path in the lower plane for  $(t - t') > 0$  and in the upper plane for  $(t - t') < 0$  (see Fig. A.1). We get then from the corresponding residui

$$\begin{aligned} S_F &= \int \frac{d^3p}{(2\pi)^3} \exp(i\vec{p}(\vec{x} - \vec{x}')) \frac{-2\pi i}{2\pi} \frac{(\not{p} + m)}{2(E - i\epsilon)} \exp[-i(E - i\epsilon)(t - t')] \quad (t - t' > 0) \\ &= \int \frac{d^3p}{(2\pi)^3} \exp(i\vec{p}(\vec{x} - \vec{x}')) \frac{2\pi i}{2\pi} \frac{(\not{p} + m)}{-2(E - i\epsilon)} \exp[i(E - i\epsilon)(t - t')] \quad (t - t' < 0). \end{aligned} \quad (\text{A.50})$$

Changing the integration variable in the second expression from  $\vec{p}$  to  $-\vec{p}$  and combining both expressions, we get (where  $p_0$  is now the physical energy  $> 0$ )

$$\begin{aligned} S_F(x - x') &= \Theta(t - t')(-i) \int d\Gamma(p)(\not{p} + m) \exp(-ip(x - x')) \\ &\quad + \Theta(t' - t)(+i) \int d\Gamma(p)(\not{p} - m) \exp(ip(x - x')), \end{aligned} \quad (\text{A.51})$$

which is identical to the result of [79].

The same can be done for the propagator  $S_A$  (sometimes called the anti Feynman propagator), which differs from the Feynman propagator by a different sign in front of the  $i\epsilon$  term:

$$S_A(x - x') := \int \frac{d^4 p}{(2\pi)^4} \frac{\not{p} + m}{p^2 - m^2 - i\epsilon} \exp(-ip(x - x')). \quad (\text{A.52})$$

The zero points of the denominator are now at

$$p_0 = \pm(E + i\epsilon) \quad (\text{A.53})$$

giving

$$S_A(x - x') = \int \frac{d^3 p}{(2\pi)^3} \exp(i\vec{p}(\vec{x} - \vec{x}')) \int \frac{dp_0}{2\pi} \frac{(\not{p} + m)}{(p_0 - E - i\epsilon)(p_0 + E + i\epsilon)} \exp(-ip_0(t - t')). \quad (\text{A.54})$$

Closing again the integration paths in the lower or upper plane and calculating the residui (see Fig. A.1) we get

$$\begin{aligned} S_A &= \int \frac{d^3 p}{(2\pi)^3} \exp(i\vec{p}(\vec{x} - \vec{x}')) (-i) \frac{(\not{p} + m)}{-2E} \exp(iE(t - t')) \quad (t - t' > 0) \\ &= \int \frac{d^3 p}{(2\pi)^3} \exp(i\vec{p}(\vec{x} - \vec{x}')) i \frac{(\not{p} + m)}{2E} \exp(-iE(t - t')) \quad (t - t' < 0). \end{aligned} \quad (\text{A.55})$$

Changing the integration variable again in the first expression to  $\vec{p} \leftrightarrow -\vec{p}$  and combining both results we finally get (where  $p_0$  is now the physical energy)

$$\begin{aligned} S_A(x - x') &= \Theta(t - t') (-i) \int d\Gamma(p) (\not{p} - m) \exp(ip(x - x')) \\ &\quad + \Theta(t' - t) (+i) \int d\Gamma(p) (\not{p} + m) \exp(-ip(x - x')). \end{aligned} \quad (\text{A.56})$$

Comparing the results (A.51) and (A.56) with (A.43) we get the final result

$$\begin{aligned} \langle 0 | \mathcal{T} \Psi(x) \bar{\Psi}(x') | 0 \rangle &= i S_F(x - x') \\ &= i \int \frac{d^4 p}{(2\pi)^4} \frac{\not{p} + m}{p^2 - m^2 + i\epsilon} \exp(-ip(x - x')), \end{aligned} \quad (\text{A.57})$$

$$\begin{aligned} \langle 0 | \mathcal{A} \Psi(x) \bar{\Psi}(x') | 0 \rangle &= -i S_A(x - x') \\ &= -i \int \frac{d^4 p}{(2\pi)^4} \frac{\not{p} + m}{p^2 - m^2 - i\epsilon} \exp(-ip(x - x')). \end{aligned} \quad (\text{A.58})$$

and also for  $\mathcal{D}$

$$\begin{aligned} \langle 0 | \mathcal{D} \Psi(x) \bar{\Psi}(x') | 0 \rangle &= i [S_F(x - x') + S_A(x - x')] \\ &= 2i \int \frac{d^4 p}{(2\pi)^4} (\not{p} + m) \frac{\text{P.P.}}{p^2 - m^2} \exp(-ip(x - x')). \end{aligned} \quad (\text{A.59})$$

where P.P. denotes the principal part of the integral, and we have used the fact that

$$\frac{1}{\alpha + i\epsilon} = \frac{\text{P.P.}}{\alpha} - i\pi\delta(\alpha), \quad \frac{1}{\alpha - i\epsilon} = \frac{\text{P.P.}}{\alpha} + i\pi\delta(\alpha). \quad (\text{A.60})$$

Similar we get for  $\mathcal{T} + \mathcal{A}$

$$\begin{aligned} \langle 0 | (\mathcal{T} + \mathcal{A}) \Psi(x) \bar{\Psi}(x') | 0 \rangle &= i [S_F(x - x') - S_A(x - x')] \\ &= \int \frac{d^4 p}{(2\pi)^4} (\not{p} + m) (2\pi) \delta(p^2 - m^2) \exp(-ip(x - x')). \end{aligned} \quad (\text{A.61})$$

In the calculation of the vacuum diagrams, where this vacuum expectation value is needed, we prefer to use the form of Eq. (A.45) instead of this one, as it is easier interpreted as the propagation of the on-shell electrons and positrons.

## A.4 Coefficients in Magnus theory

As shown in section 5.1 all higher-order processes in the Magnus theory without Coulomb rescattering terms are of the same type. The number of terms in each order is given by the reduction of the vacuum expectation values. The explicit reduction is not useful because the complexity of the expressions increases quickly. Therefore we show here how these can be calculated more easily.

This is a combinatorial problem, which can be formulated in the following way: In  $N$ th order we have  $N$  interaction points, each of which either corresponds to a pair creation or pair annihilation process. In terms of the fermion lines this means that a line entering one point from the left also leaves it to the left and the same from the right. We need the total number of paths through these  $N$  points using the above condition, where the line initially enters from the right and finally leaves to the right. As we look only at reduced amplitudes, no closed loops are allowed.

Let us find a recursive formula for the number of paths: We define  $A(n, i)$  as the number of distinct paths for  $i$  fermion lines (coming from and leaving to the right) going through  $n$  interaction points. If we add now another interaction point to the right, there are two possibilities: If it is a pair creation process, the number of lines is increased by one. If we have a pair annihilation process, we have to connect it with one outgoing and one ingoing line, therefore reducing their number by one. For this we have to choose one of the  $i$  outgoing lines and one of the ingoing lines, where we have to be careful not to make a closed loop; therefore only  $i - 1$  of them are allowed. This means that there are  $i(i - 1)$  possible combinations. This gives us the recursion relation

$$A(n + 1, i) = A(n, i - 1) + i(i + 1)A(n, i + 1), \quad (\text{A.62})$$

together with the boundary conditions

$$A(1, 1) = 1 \quad (\text{A.63a})$$

$n$	# Diags.	$c_n$	$d_n$
1	$1.0000 \times 10^0$	1.0000000000	1.0000000000
3	$2.0000 \times 10^0$	0.3333333333	0.6666666667
5	$1.6000 \times 10^1$	0.1333333333	0.3777777778
7	$2.7200 \times 10^2$	0.0539682540	0.1968253968
9	$7.9360 \times 10^3$	0.0218694885	0.0974955908
11	$3.5379 \times 10^5$	0.0088632355	0.0466976645
13	$2.2368 \times 10^7$	0.0035921280	0.0218375158
15	$1.9038 \times 10^9$	0.0014558344	0.0100304665
17	$2.0987 \times 10^{11}$	0.0005900274	0.0045434532
19	$2.9089 \times 10^{13}$	0.0002391291	0.0020352230
21	$4.9515 \times 10^{15}$	0.0000969154	0.0009034014
23	$1.0154 \times 10^{18}$	0.0000392783	0.0003979726
25	$2.4692 \times 10^{20}$	0.0000159189	0.0001741956

Table A.1: *The number of diagrams and the coefficients  $c_n$  and  $d_n$  appearing in Magnus theory for different orders  $n$ .*

$$A(1, i) = 0 \quad \text{for } i > 1 \quad (\text{A.63b})$$

$$A(n, 0) = 0 \quad \text{for all } n. \quad (\text{A.63c})$$

With this recursion relation we can calculate  $A(n, 1)$  for all  $n$ . This is just the number of diagrams that we were looking for. Dividing it by  $n!$  gives the coefficient  $c_n$  in the expansion of the amplitude. These coefficients are given in Table A.1. For the coefficients in the reduced total probability we have to multiply  $c_l$  and  $c_{n+1-l}$  and sum over all  $l \in 0 \dots n$ . These are the coefficients  $d_n$  of Eq. (5.23). They are also given in Table A.1.

## A.5 Two dimensional Feynman integrals

### A.5.1 Notation

The general scalar Feynman integral is the integral of the form

$$\int \frac{d^2q}{N_0 N_1 N_2 \dots}, \quad (\text{A.64})$$

where the propagators in the denominator are defined as

$$N_0 = q^2 + m_0^2, \quad N_i = (q + k_i)^2 + m_i^2. \quad (\text{A.65})$$

Besides these scalar integrals we will need also tensor integrals, where we have terms with  $q_i$  in the numerator. The simplest of these tensor integrals is

$$\int \frac{d^2 q q_i}{N_0 N_1 N_2 \dots}. \quad (\text{A.66})$$

For this integral we will give an analytic form in the case of the three-term integral. For the higher-term integrals we use the fact that the  $q_i$ 's in the numerator always appear in a scalar product with some  $k_i$  in our calculation. These integrals can then be calculated easier as the general ones.

All integrals, we need, can be calculated analytically in our case, as the  $k_i$ 's and  $m_i$ 's are all real. The only integral, that we have to solve explicitly, is the two-term integral. All higher-term integrals and also the tensor integrals can be reduced then to this one. This will be done as follows: First we show how the three-term integral can be reduced to a sum of three two-term integrals. Then we show how the simplest tensor integral with three terms can be reduced to the scalar three-term integral and three two-term integrals. Finally we show how all  $N$ -term integrals with  $N > 4$  can be reduced to a sum of four  $(N - 1)$ -term integrals. The formulae used here are a specialization of the general results of van Neerven and Vermaseren for arbitrary dimensions to two dimensions [81]. As the expression in two dimensions are sometimes easier and more compact, we give them here.

### A.5.2 The two-term integral

This is the integral of the form

$$I_2(k_1, m_0^2, m_1^2) := \int \frac{d^2 q}{N_0 N_1} = \int d^2 q \left\{ [q^2 + m_0^2] [(q + k_1)^2 + m_1^2] \right\}^{-1}. \quad (\text{A.67})$$

Introducing standard Feynman parameters we find

$$I_2 = \int_0^1 dx \int d^2 q \left\{ [q^2 + m_0^2] x + [(q + k_1)^2 + m_1^2] (1 - x) \right\}^{-2}. \quad (\text{A.68})$$

Rearranging the term in brackets the integral is

$$\begin{aligned} I_2 &= \int_0^1 dx \int d^2 q \left\{ [q + k_1(1 - x)]^2 + k_1^2 x(1 - x) + m_0^2 x + m_1^2(1 - x) \right\}^{-2} \\ &= \pi \int_0^1 dx \left[ k_1^2 x(1 - x) + m_0^2 x + m_1^2(1 - x) \right]^{-1}. \end{aligned} \quad (\text{A.69})$$

The evaluation of the last integral is straightforward and we get in a numerical stable form

$$I_2(k_1, m_0^2, m_1^2) = \pi \ln \left[ \frac{(k_1^2 + m_0^2 + m_1^2 + s)^2}{4m_0^2 m_1^2} \right] / \left[ (m_0^2 - m_1^2)^2 + k_1^2 (k_1^2 + 2m_0^2 + 2m_1^2) \right]^{1/2} \quad (\text{A.70})$$

with

$$s := \left[ (k_1^2 + m_1^2 + m_0^2)^2 - 4m_0^2 m_1^2 \right]^{1/2}. \quad (\text{A.71})$$

Note that the final result depends only on the values of  $k_1^2$ ,  $m_0^2$  and  $m_1^2$ .

### A.5.3 The three-term integral

This is the integral

$$\begin{aligned} I_3^S(k_1, k_2, m_0^2, m_1^2, m_2^2) &:= \int \frac{d^2q}{N_0 N_1 N_2} \\ &= \int d^2q \left\{ [q^2 + m_0^2] [(q + k_1)^2 + m_1^2] [(q + k_2)^2 + m_2^2] \right\}^{-1}. \end{aligned} \quad (\text{A.72})$$

In principal an analytic form can be found directly by doing the integration over two auxiliary variables using the trick described by t'Hooft and Veltman [82]. This calculation is rather tedious and it is easier to use the formula by van Neerven and Vermaseren [81] for the reduction of an  $(N + 1)$ -term integral in  $N$  dimensions into  $(N + 1)$   $N$ -term integrals. We will derive this formula in the following for two dimensions.

We will need the fact that the integral

$$\int \frac{d^2q \epsilon^{k_1 q}}{N_0 N_1} = 0 \quad (\text{A.73})$$

vanishes. We use the Schoonship notation here, that is, we write

$$\epsilon^{k_1 q} := \epsilon^{ij} k_{1i} q_j. \quad (\text{A.74})$$

The vanishing of this integral can be understood easily as the tensor integral has to be proportional to  $k_1$ , the only vector in this formula:

$$\int \frac{d^2q q_i}{N_0 N_1} = k_{1i} I \quad (\text{A.75})$$

and the contraction vanishes then.

The reductions of the integrals are all based on the Schouten identity, which in two dimensions is

$$\epsilon^{k_1 k_2} q_i = \epsilon^{i k_2} (k_1 q) + \epsilon^{k_1 i} (k_2 q) =: v_{1i} (k_1 q) + v_{2i} (k_2 q). \quad (\text{A.76})$$

The Schouten identity describes the decomposition of an arbitrary vector in two dimensions in terms of the basis  $v_1, v_2$ , which are normal vectors to  $k_2$  and  $k_1$ .

We define also the contraction of two vectors  $k_i$  and  $k_j$  as

$$a_{ij} := \epsilon^{k_i k_j}. \quad (\text{A.77})$$

Multiplying the Schouten identity with  $q$  gives

$$a_{12} q^2 = (v_1 q)(k_1 q) + (v_2 q)(k_2 q). \quad (\text{A.78})$$

Let us now express  $q^2$  and  $k_i q$  through the propagators:

$$q^2 = N_0 - m_0^2 \quad (\text{A.79a})$$

$$\begin{aligned} 2qk_i &= N_i - q^2 - k_i^2 - m_i^2 \\ &= N_i - N_0 + m_0^2 - k_i^2 - m_i^2 \\ &=: N_i - N_0 - r_i \end{aligned} \quad (\text{A.79b})$$



with  $r_i := m_i^2 - m_0^2 + k_i^2$ . We get

$$2a_{12}(N_0 - m_0^2) - (v_1 q)(N_1 - N_0 - r_1) - (v_2 q)(N_2 - N_0 - r_2) = 0, \quad (\text{A.80})$$

that is,

$$\int d^2 q \frac{2a_{12}(N_0 - m_0^2) - (v_1 q)(N_1 - N_0 - r_1) - (v_2 q)(N_2 - N_0 - r_2)}{N_0 N_1 N_2} = 0. \quad (\text{A.81})$$

As the integral

$$\int d^2 q \frac{\epsilon^{k_1 q}}{N_0 N_1} = \int d^2 q \frac{v_2 q}{N_0 N_1} = 0 \quad (\text{A.82})$$

vanishes (see Eq. (A.73)), and similar for  $v_1$ , we get

$$\int d^2 q \frac{2a_{12}(N_0 - m_0^2) + (v_1 q)(N_0 + r_1) + (v_2 q)(N_0 + r_2)}{N_0 N_1 N_2} = 0. \quad (\text{A.83})$$

Let us also rewrite the integral

$$\int d^2 q \frac{(v_1 q + v_2 q)N_0}{N_0 N_1 N_2} = \int d^2 q \frac{\epsilon^{q k_2} + \epsilon^{k_1 q}}{N_1 N_2}. \quad (\text{A.84})$$

Changing the integration variable to  $K = q + k_1$  and therefore  $N_1 = K^2 + m_1^2$  we get

$$\begin{aligned} \int d^2 K \frac{\epsilon^{(K-k_1)k_2} + \epsilon^{k_1(K-k_1)}}{N_1 N_2} &= \int d^2 K \frac{\epsilon^{K(k_2-k_1)} - \epsilon^{k_1 k_2}}{[K^2 + m_1^2][(K + k_2 - k_1)^2 + m_2^2]} \\ &= -a_{12} \int d^2 q \frac{1}{N_1 N_2}, \end{aligned} \quad (\text{A.85})$$

as the integral over the first contraction vanishes (see Eq. (A.73)). Therefore we have

$$\int d^2 q \frac{2a_{12}(N_0 - m_0^2) + r_1 v_1 q + r_2 v_2 q - a_{12} N_0}{N_0 N_1 N_2} = 0. \quad (\text{A.86})$$

We multiply the whole expression with  $a_{12}$

$$\int d^2 q \frac{-2m_0^2 a_{12}^2 + N_0 a_{12}^2 + r_1 a_{12} v_1 q + r_2 a_{12} v_2 q}{N_0 N_1 N_2} = 0. \quad (\text{A.87})$$

Now the Schouten identity is used again to rewrite

$$a_{12}(v_i q) = (q k_1)(v_1 v_i) + (q k_2)(v_2 v_i). \quad (\text{A.88})$$

Using the explicit forms of  $v_1$  and  $v_2$  we get

$$a_{12}(v_1 q) = (q k_1)k_2^2 - (q k_2)(k_1 k_2), \quad (\text{A.89a})$$

$$a_{12}(v_2 q) = (q k_2)k_1^2 - (q k_1)(k_1 k_2), \quad (\text{A.89b})$$

and therefore

$$\int d^2q \left\{ -2m_0^2 a_{12}^2 + N_0 a_{12}^2 + r_1 [(qk_1)k_2^2 - (qk_2)(k_1k_2)] + r_1 [(qk_2)k_1^2 - (qk_1)(k_1k_2)] \right\} / (N_0 N_1 N_2) = 0. \quad (\text{A.90})$$

Expressing  $qk_1$  and  $qk_2$  again with the help of the propagators we get the final result

$$\begin{aligned} \int \frac{d^2q}{N_0 N_1 N_2} [4m_0^2 a_{12}^2 + (r_1 k_2 - r_2 k_1)^2] = \\ [2a_{12}^2 + (r_1 + r_2)k_1 k_2 - r_1 k_2^2 - r_2 k_1^2] \int \frac{d^2q}{N_1 N_2} \\ + [r_1 k_2^2 - r_2 k_1 k_2] \int \frac{d^2q}{N_0 N_2} + [r_2 k_1^2 - r_1 k_1 k_2] \int \frac{d^2q}{N_0 N_1}. \end{aligned} \quad (\text{A.91})$$

This gives the reduction of the three-term integral in terms of three two-term integrals.

### A.5.4 The three-term tensor integral

For the calculation of  $M$  for  $b$  zero we need also the three-term integral with one momentum in the numerator. Generally all tensor integrals can be reduced to the scalar integrals. Here we use the method, which is described, for example, in t'Hooft and Veltman [82].

The standard form of the integral is

$$I_3^i(k_1, k_2, m_0^2, m_1^2, m_2^2) = \int d^2q \frac{q^i}{N_0 N_1 N_2}. \quad (\text{A.92})$$

As  $k_1$  and  $k_2$  are the only variables in the integral with a vector character, the integral can be split into

$$I_3^i = k_1^i I_3^1 + k_2^i I_3^2. \quad (\text{A.93})$$

In order to find expressions for  $I_3^1$  and  $I_3^2$  we multiply with  $k_1$  and  $k_2$  and solve for  $I_3^1$  and  $I_3^2$ :

$$I_3^1 = [k_1^2 k_2^2 - (k_1 k_2)^2]^{-1} [k_2^2 (k_1 I_3) - k_1 k_2 (k_2 I_3)], \quad (\text{A.94a})$$

$$I_3^2 = [k_1^2 k_2^2 - (k_1 k_2)^2]^{-1} [-k_1 k_2 (k_1 I_3) + k_1^2 (k_2 I_3)]. \quad (\text{A.94b})$$

Expressing now  $qk_1$  again with the help of the propagators  $qk_1 = 1/2 (N_1 - N_0 - r_1)$ , and similarly for  $qk_2$ , we get

$$\begin{aligned} (k_1 I_3) &= \int d^2q \frac{k_1 q}{N_0 N_1 N_2} \\ &= \frac{1}{2} I_2(k_2, m_0^2, m_1^2) - \frac{1}{2} I_2(k_2 - k_1, m_1^2, m_2^2) - \frac{1}{2} r_1 I_3^S(k_1, k_2, m_0^2, m_1^2, m_2^2) \end{aligned} \quad (\text{A.95})$$

and similarly for  $k_2 I_3$ . We find finally for  $I_3^1$  and  $I_3^2$

$$I_3^1 = \left[ 2 \left( k_1^2 k_2^2 - (k_1 k_2)^2 \right) \right]^{-1} \left[ \left( k_1 k_2 - k_2^2 \right) I_2(k_2 - k_1, m_1^2, m_2^2) + k_2^2 I_2(k_2, m_0^2, m_2^2) \right. \\ \left. - k_1 k_2 I_2(k_1, m_0^2, m_1^2) + \left( r_2 k_1 k_2 - r_1 k_2^2 \right) I_3^S(k_1, k_2, m_0^2, m_1^2, m_2^2) \right], \quad (\text{A.96a})$$

$$I_3^2 = \left[ 2 \left( k_1^2 k_2^2 - (k_1 k_2)^2 \right) \right]^{-1} \left[ \left( k_1 k_2 - k_1^2 \right) I_2(k_2 - k_1, m_1^2, m_2^2) + k_1^2 I_2(k_1, m_0^2, m_1^2) \right. \\ \left. - k_1 k_2 I_2(k_2, m_0^2, m_2^2) + \left( r_1 k_1 k_2 - r_2 k_1^2 \right) I_3^S(k_1, k_2, m_0^2, m_1^2, m_2^2) \right]. \quad (\text{A.96b})$$

### A.5.5 The higher-term integrals

The difficulty with the reduction of the scalar three-term integral was the fact that only two external vectors are available. With four- and higher-term integrals this reduction is easier, as we have at least three external momenta available. Let us start again with the Schouten identity for  $q$ :

$$a_{12} q_i = v_{1i}(q k_1) + v_{2i}(q k_2). \quad (\text{A.97})$$

Multiplying now with  $k_3$  we get as symmetric form for the  $k_i$ :

$$a_{12}(q k_3) + a_{23}(q k_1) + a_{31}(q k_2) = 0 \quad (\text{A.98})$$

(see also the definition of the  $a_{ij}$  in Eq. (A.77)). We can again express the scalar products in terms of the propagators

$$a_{12}(N_3 - N_0 - r_3) + a_{23}(N_1 - N_0 - r_1) + a_{31}(N_2 - N_0 - r_2) = 0. \quad (\text{A.99})$$

Dividing by  $N_0 N_1 N_2 N_3 \cdots$  and integrating over  $d^2 q$  we get after sorting the different terms

$$\int \frac{d^2 q}{N_0 N_1 N_2 N_3 \cdots} (a_{12} r_3 + a_{23} r_1 + a_{31} r_2) = - (a_{12} + a_{23} + a_{31}) \int \frac{d^2 q}{N_1 N_2 N_3 \cdots} \\ + a_{12} \int \frac{d^2 q}{N_0 N_1 N_2 \cdots} + a_{23} \int \frac{d^2 q}{N_0 N_2 N_3 \cdots} + a_{31} \int \frac{d^2 q}{N_0 N_1 N_3 \cdots}. \quad (\text{A.100})$$

This reduction formula has been used recursively for the calculation of the integrals up to six terms. The  $a_{ij}$  were calculated using

$$a_{ij} = k_i k_j \sin(\phi_j - \phi_i) \quad (\text{A.101})$$

in terms of radial coordinates.

As described in section 4.1 the reduction of the higher-term tensor integrals was simplified because of the fact that they only appear in scalar products with some  $k_i$ . In this case

the reduction is straightforward, as we can use directly the formula to rewrite the scalar products in terms of the propagators:

$$\int \frac{d^2q(k_1q)}{N_0N_1N_2N_3\cdots} = \frac{1}{2} \int \frac{d^2q}{N_0N_2N_3\cdots} - \frac{1}{2} \int \frac{d^2q}{N_1N_2N_3\cdots} - \frac{r_1}{2} \int \frac{d^2q}{N_0N_1N_2N_3\cdots} \quad (\text{A.102})$$

and similar for all other  $k_i$ .

### A.5.6 Testing the formulae

The numerical calculation of the integrals has been tested with the help of the following properties: First the symmetry of the formulae with respect to the exchange of the  $N_i$ 's has been tested. Second a test can be done based on the following mathematical property [82]:

Starting from

$$\frac{1}{[q^2 + m_0^2][(q + k_1)^2 + m_1^2]}, \quad (\text{A.103})$$

we multiply numerator and denominator with

$$\begin{aligned} & (1 - \alpha)[q^2 + m_0^2] + \alpha[(q + k_1)^2 + m_1^2] \\ &= (q + \alpha k_1)^2 + \alpha m_1^2 + (1 - \alpha)m_0^2 + \alpha(1 - \alpha)k_1^2 \\ &=: (q + K)^2 + M^2, \end{aligned} \quad (\text{A.104})$$

where  $\alpha$  is an arbitrary real parameter. With this we find

$$\begin{aligned} & \frac{1}{[q^2 + m_0^2][(q + k_1)^2 + m_1^2]} \\ &= \frac{1 - \alpha}{[(q + k_1)^2 + m_1^2][(q + K)^2 + M^2]} + \frac{\alpha}{[q^2 + m_0^2][(q + K)^2 + M^2]}. \end{aligned} \quad (\text{A.105})$$

This gives an identity between three integrals with different parameters, which can be verified.

## A.6 Discussion of the form factors

Normally a Gaussian form factor or that of a homogeneous charged sphere are used for heavy ions. They are given by (note that in our metric  $q^2 < 0$ ):

$$F_{\text{Gauss}}(q^2) = \exp\left(-\frac{|q^2|}{2Q_0^2}\right), \quad (\text{A.106})$$

$$F_{\text{h.c.s.}}(q^2) = \frac{3j_1(\sqrt{|q^2|R_0})}{\sqrt{|q^2|R_0}}, \quad (\text{A.107})$$

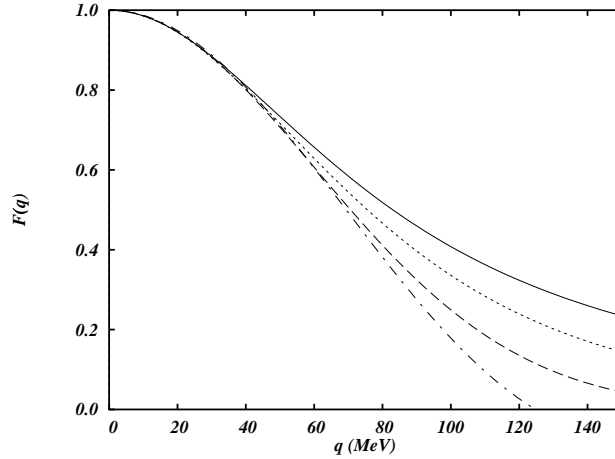


Figure A.2: A comparison of different form factors. The dashed line is the Gauss form factor, the dashed-dotted line the form factor of a homogeneously charged sphere. The solid line is the simple dipole form factor, the dotted line the double dipole form factor with parameter  $c_1 = 10$ .

with parameters  $Q_0 = 60$  MeV and  $R_0 = 1.2$  fm  $A^{1/3} \approx 7$  fm.

We are using here two different form factors, which have the advantage that our matrix element can be expressed analytically with them. One is the dipole form factor

$$F_{\text{dipole}}(q^2) = \frac{\Lambda^2}{\Lambda^2 - q^2}, \quad (\text{A.108})$$

which is the form factor of a Yukawa charge distribution

$$\rho(r) = \frac{\Lambda^2}{4\pi} \frac{\exp(-\Lambda r)}{r}. \quad (\text{A.109})$$

$\Lambda$  has been determined so that the root mean square of the electric radius is equal to the experimental value

$$\sqrt{\langle r^2 \rangle} = \sqrt{\frac{6}{\Lambda^2}} = 1 \text{ fm } A^{1/3}, \quad (\text{A.110})$$

giving a  $\Lambda$  of about 83 MeV. This value has been used throughout the calculations, even though it varies slightly with  $A$ , for example, for Pb to Au.

A comparison of the different form factors can be found in Fig. A.2. The disadvantage of the dipole form factor is that it decreases too slowly and overestimates the real value, if  $q$  is larger than about 50 MeV. To see if our result depends on the exact form of the form factor, we use a second one, which has a better behavior for large  $q$ . It is a linear combination of two dipole form factors:

$$F_{\text{double}}(q^2) = c_1 \frac{\Lambda_1^2}{\Lambda_1^2 - q^2} + c_2 \frac{\Lambda_2^2}{\Lambda_2^2 - q^2}. \quad (\text{A.111})$$

Therefore we call it a “double dipole form factor.” With  $F(0) = 1$  we have  $c_1 + c_2 = 1$ . The behavior of this form factor for large values of  $|q|$  is

$$F(q^2) \sim \frac{\Lambda_1^2 \Lambda_2^2 - (c_1 \Lambda_1^2 + c_2 \Lambda_2^2) q^2}{q^4}. \quad (\text{A.112})$$

For that the form factor vanishes faster than  $1/q^2$ , the coefficient in front of  $q^2$  has to be zero, therefore  $\Lambda_2^2$  has to be chosen as

$$\Lambda_2^2 = -\frac{c_1}{c_2} \Lambda_1^2. \quad (\text{A.113})$$

As we do not want to have a singularity in the form factor, we have to choose  $\Lambda_2^2 > 0$ , that is,  $c_1 > 1$ . Finally we want that  $\langle r^2 \rangle$  is again the same as the experimental one. As the density corresponding to this form factor is a sum of two Yukawa charge densities,  $\langle r^2 \rangle$  is

$$\langle r^2 \rangle = 6 \left( \frac{c_1}{\Lambda_1^2} + \frac{c_2}{\Lambda_2^2} \right). \quad (\text{A.114})$$

Therefore

$$\Lambda_1^2 = \frac{6}{\langle r^2 \rangle} \left( 2 - \frac{1}{c_1} \right), \quad (\text{A.115})$$

and  $c_1$  is the only parameter, which can be varied. For  $c_1 = 1$  we have the normal dipole form factor; for  $c_1 \rightarrow \infty$  it decreases faster than it. In Fig. A.2 we have plotted  $F_{\text{double}}(q)$  for  $c_1 = 10$ , a value that we have used also throughout the calculations, because the cancellations between the two dipole terms are not too large.

The reason why these form factors can be treated analytically is due to the fact that with the dipole form factor, we can write

$$\frac{F_{\text{dipole}}(q^2)}{q^2} = \frac{1}{q^2} \frac{\Lambda^2}{\Lambda^2 - q^2} = \frac{1}{q^2} + \frac{1}{\Lambda^2 - q^2}, \quad (\text{A.116})$$

having a term of the form  $1/(q^2 + m^2)$  again. Therefore our momentum integrals can be written as sums and differences of the standard Feynman integrals.

# Bibliography

- [1] L.D. Landau and E.M. Lifshitz, Phys. Z. Sowjet. **6**, 244 (1934).
- [2] A.I. Achieser and W.B. Berestezki, *Quanten-Elektrodynamik* (B.G. Teubner Verlag, Leipzig, 1962).
- [3] G. Racah, Nuovo Cimento **14**, 93 (1937).
- [4] H.J. Bhabha, Proc. R. Soc. (London) **A152**, 559 (1935).
- [5] K.F. Weizsäcker, Z. Phys. **88**, 612 (1934).
- [6] E.J. Williams, Phys. Rev. **45**, 729 (1934).
- [7] E. Fermi, Z. Phys. **29**, 315 (1924).
- [8] W. Heitler, *The quantum theory of radiation* (Oxford, 1954).
- [9] V.M. Budnev, I.F. Ginzburg, G.V. Meledin, and V.G. Serbo, Phys. Rep. **15**, 181 (1975).
- [10] H. Terazawa, Rev. Mod. Phys. **45**, 615 (1973).
- [11] C. Bottcher and M.R. Strayer, Phys. Rev. **D39**, 1330 (1989).
- [12] P.B. Eby, Phys. Rev. **A39**, 2374 (1989).
- [13] P.B. Eby, Phys. Rev. **A43**, 2258 (1991).
- [14] U. Becker, N. Grün, W. Scheid, and G. Soff, Phys. Rev. Lett. **56**, 2016 (1986).
- [15] U. Becker, N. Grün, and W. Scheid J. Phys. **B19**, 1347 (1986).
- [16] C.A. Bertulani and G. Baur, Phys. Rep. **163**, 299 (1988).
- [17] F. Decker, Phys. Rev. **A44**, 2883 (1991).
- [18] F. Decker and J. Eichler, Phys. Rev. **A45**, 3343 (1992).
- [19] D.C. Ionescu and J. Eichler, Phys. Rev. **A48**, 1176 (1993).

- [20] C. Bottcher and M.R. Strayer, *Ann. Phys.* **175**, 64 (1987).
- [21] J.C. Wells, V.E. Oberacker, A.S. Umar, C. Bottcher, M.R. Strayer, J.-S. Wu, and G. Plunien, *Phys. Rev.* **A45**, 6296 (1992).
- [22] J. Thiel, A. Bunker, K. Momberger, N. Grün, and W. Scheid, *Phys. Rev.* **A46**, 2607 (1992).
- [23] K. Rumrich, G. Soff, and W. Greiner, *Phys. Rev.* **A47**, 215 (1993).
- [24] K. Momberger, N. Grün, and W. Scheid, *Z. Phys.* **D18**, 133 (1991).
- [25] A.J. Baltz, M.J. Rhoades-Brown, and J. Weneser, *Phys. Rev.* **A44**, 5569 (1991).
- [26] A.J. Baltz, M.J. Rhoades-Brown, and J. Weneser, *Phys. Rev.* **A47**, 3444 (1993).
- [27] A.J. Baltz, M.J. Rhoades-Brown, and J. Weneser, *Phys. Rev.* **A48**, 2002 (1993).
- [28] J. Thiel, Ph.D. thesis, Universität Giessen, 1993 (unpublished).
- [29] T. Lippert, J. Thiel, N. Grün, and W. Scheid, *Int. J. Mod. Phys.* **6A**, 5249 (1991).
- [30] J. Weinbrenner, N. Grün, and W. Scheid, DPG (HK) Mainz, 1993 (unpublished).
- [31] J. Eichler, *Phys. Rep.* **193**, 165 (1990).
- [32] M. Fatyga, M.J. Rhoades-Brown, and M.J. Tannenbaum, Brookhaven National Laboratory report No. BNL 52247, 1990 (unpublished).
- [33] G. Baur, *Phys. Rev.* **A42**, 5736 (1990).
- [34] M.J. Rhoades-Brown and J. Weneser, *Phys. Rev.* **A44**, 330 (1991).
- [35] C. Best, W. Greiner, and G. Soff, *Phys. Rev.* **A46**, 261 (1992).
- [36] C. Best, Diplomarbeit, Universität Frankfurt, GSI-92-09 1992 (unpublished).
- [37] D.C. Ionescu, Hahn-Meitner-Institut preprint No. HMI 1993/P1-Ion 2, 1993 (submitted to *Phys. Rev. D*).
- [38] C.R. Vane, S. Datz, P.F. Dittner, H.F. Krause, C. Bottcher, M. Strayer, R. Schuch, H. Gao, and R. Hutton, *Phys. Rev. Lett.* **69**, 1911 (1992).
- [39] A. Belkacem, H. Gould, B. Feinberg, R. Bossingham, and W.E. Meyerhoff, *Phys. Rev. Lett.* **71**, 1514 (1993).
- [40] 12. Arbeitsbericht Arbeitsgruppe Energiereiche Atomare Stösse, EAS-12, 1991 (unpublished).



- [41] N. Baron, Ph.D. thesis, Universität Bonn, Forschungszentrum Jülich report No. Jül-2846, 1993 (unpublished).
- [42] M. Vidović, M. Greiner, Ch. Best, and G. Soff, Phys. Rev. **C47**, 2308 (1993).
- [43] M. Drees, J. Ellis, and D. Zeppenfeld, Phys. Lett. **B223**, 454 (1989).
- [44] E. Papageorgiu, Phys. Rev. **D40**, 92 (1989).
- [45] R.N. Cahn and J.D. Jackson, Phys. Rev. **D42**, 3690 (1990).
- [46] J.N. Norbury, Phys. Rev. **D42**, 3696 (1990).
- [47] B. Müller and A.J. Schramm, Phys. Rev. **D42**, 3699 (1990).
- [48] M. Greiner, M. Vidović, and G. Soff, Phys. Rev. **C47**, 2288 (1993).
- [49] M. Grabiak, B. Müller, W. Greiner, G. Soff, and P. Koch, J. Phys. **G15**, L25 (1989).
- [50] J. Rau, B. Müller, W. Greiner, and G. Soff, J. Phys. **G16**, 211 (1990).
- [51] L.D. Almeida, A.A. Natale, S.F. Novaes, and O.J.P. Éboli, Phys. Rev. **D44**, 118 (1991).
- [52] J.D. Jackson, *Klassische Elektrodynamik* (Walter de Gruyter, 1983).
- [53] R. P. Feynman, Phys. Rev. **76**, 749 (1949).
- [54] J. Schwinger, Phys. Rev. **93**, 615 (1954).
- [55] C. Itzykson and J.-B. Zuber, *Quantum Field Theory* (McGraw-Hill, 1980).
- [56] I. Białynicki-Birula and Z. Białynicki-Birula, *Quantum Electrodynamics* (Pergamon, 1975).
- [57] S.S. Schweber, *An Introduction to Relativistic Quantum Field Theory* (Row, Peterson, 1961).
- [58] N.N. Bogoliubov and D.V. Shirkov, *Quantum Fields* (Benjamin/Cummings, 1983).
- [59] R.P. Feynman, *Quantum Electrodynamics* (W.A. Benjamin, 1961).
- [60] I. Białynicki-Birula, B. Mielnik, and J. Plebański, Ann. Phys. (NY) **51**, 187 (1969).
- [61] P. Pechukas and J.C. Light, J. Chem. Phys. **44**, 3897 (1966).
- [62] FORM is an algebraical calculation program by J.A.M. Vermaseren, the free version 1.0 can be found, e.g., at FTP.NIKHEF.NL.
- [63] G. Baur and L.G. Ferreira Filho, Phys. Lett. **B254**, 30 (1991).

- [64] G. Baur, Z. Phys. **C54**, 419 (1992).
- [65] G.P. Lepage, J. Comp. Phys. **27**, 192 (1978).
- [66] G.P. Lepage, Cornell laboratory for nuclear sciences report No. CLNS-80/447, 1980 (unpublished).
- [67] G. Baur and N. Baron, Nucl. Phys. **A561**, 629 (1993).
- [68] N. Baron and G. Baur, Z. Phys. **C60**, 95 (1993).
- [69] H. Bethe and W. Heitler, Proc. R. Soc. (London) **146**, 83 (1934).
- [70] I.S. Gradshteyn and I.M. Ryzhik, *Tables of series, products and integrals, Vol. 2* (Harry Deutsch, 1981).
- [71] J.D. Bjorken and M.C. Chen, Phys. Rev. **154**, 1335 (1967).
- [72] R. Kleiss and W.J. Stirling, Nucl. Phys. **B262**, 235 (1985).
- [73] E. Yehudai, Stanford Linear Accelerator Report No. SLAC-PUB-92/256-T 1992 (submitted to Phys. Rev. D).
- [74] H. W. Fearing and R. R. Silbar, Phys. Rev. **D6**, 471 (1972).
- [75] M. Fatyga and B. Moskowitz, Brookhaven National Laboratory report No. BNL 52262, 1990 (unpublished).
- [76] M. Fatyga, (private communication).
- [77] D. Brandt, K. Eggert, and A. Morsch, CERN report No. CERN AT/94-05(DI), CERN SL/94-04(AP), 1994 (unpublished).
- [78] J.D. Bjorken and S.D. Drell, *Relativistische Quantenmechanik* (BI Bd. 98, 1966).
- [79] J.D. Bjorken and S.D. Drell, *Relativistische Quantenfeldtheorie* (BI Bd. 101, 1967).
- [80] W. Greiner, B. Müller, and J. Rafelski, *Quantum Electrodynamics of Strong Fields* (Springer, 1985).
- [81] W.L. van Neerven and J.A.M. Vermaseren, Phys. Lett. **B137**, 241 (1984).
- [82] G. t'Hooft and M. Veltman, Nucl. Phys. **B153**, 265 (1979).

## Curriculum Vitae

- 18. Sep. 1965 Geboren in Hamburg als Sohn des Dr. Hermann Hencken und der Karin Hencken geb. Dünkel
- 1971 – 1975 Besuch der Grundschule in Lörrach–Brombach
- 1975 – 1984 Besuch des mathematisch-naturwissenschaftlichen Hans-Thoma–Gymnasiums in Lörrach
- Mai 1984 Abitur
- 1985 – 1991 Studium an der Universität Basel in den Fächern Physik, Mathematik und Chemie
- Oktober 1987 Vordiplomprüfung
- 1989 – 1990 Diplomarbeit über „Untersuchungen zu relativistischen Gleichungen für Spin 0 Teilchen“ unter der Anleitung von Prof. Dr. Dirk Trautmann
- April 1990 Diplomprüfung in theoretischer Physik
- 1990 – 1994 Doktorarbeit über „elektromagnetische Produktion von Elektron-Positron-Paaren bei relativistischen Schwerionenstößen“ unter der Anleitung von Prof. Dr. Gerhard Baur und Prof. Dr. Dirk Trautmann.

Meine Ausbildung verdanke ich den folgenden Dozentinnen und Dozenten: Prof. Dr. N. A Campo, Prof. K. Alder, Prof. Dr. G. Backenstoss, Prof. Dr. C. Bandle, Prof. Dr. E. Baumgartner, Prof. Dr. G. Baur, Prof. Dr. H. Burkhardt, PD Dr. H. Christen, Prof. Dr. W. Czaja, Prof. Dr. J. Fünfschilling, PD Dr. U. Götz, Prof. Dr. H. Güntherodt, Prof. Dr. H. Huber, Prof. Dr. H. Kraft, Prof. Dr. G.-R. Plattner, Prof. Dr. H. Rudin, Prof. Dr. B. Scarpellini, Prof. Dr. P. Schiess, PD Dr. T. Schucan, Prof. Dr. I. Sick, Prof. Dr. H. Sigel, Prof. Dr. P. Talkner, Prof. Dr. L. Tauscher, Prof. Dr. H. Thomas, Prof. Dr. D. Trautmann, Prof. Dr. Ch. Ullrich, Prof. Dr. R. Wagner, Prof. Dr. J. Wirz, Prof. Dr. I. Zschokke, Prof. Dr. A.D. Zuberbühler.

## Dank

Mein Dank gilt all denen, die durch Ihre Unterstützung diese Arbeit ermöglicht haben. Dies gilt vor allem natürlich für Gerhard Baur und Dirk Trautmann, die diese Arbeit angeregt haben und sie mit ihrem Wissen und mit zahllosen Diskussionen begleitet und gefördert haben. Aber auch allen anderen Mitarbeitern hier am Institut möchte ich für die vielen Diskussionen und Anregungen danken, vor allem meinen Zimmerkollegen Thomas Heim und Torsten Strunz aber auch Daniel Wirz, Rick Brandenburg und Boris Blankleider.

Mein besonderer Dank gilt natürlich auch meiner zukünftigen Frau Franziska für die viele Geduld, die sie manchmal mit mir haben mußte, der Mannschaft der “Kaffeerunde 1.20” und natürlich Wolfgang Löffler und Thilo Enderle.